國家同步輻射研究中心
National Synchrotron Radiation Research Center

Overview of Synchrotron Radiation

Cheiron School 2008, SPring-8

Keng Liang

September 29, 2008

Light Source: Sun

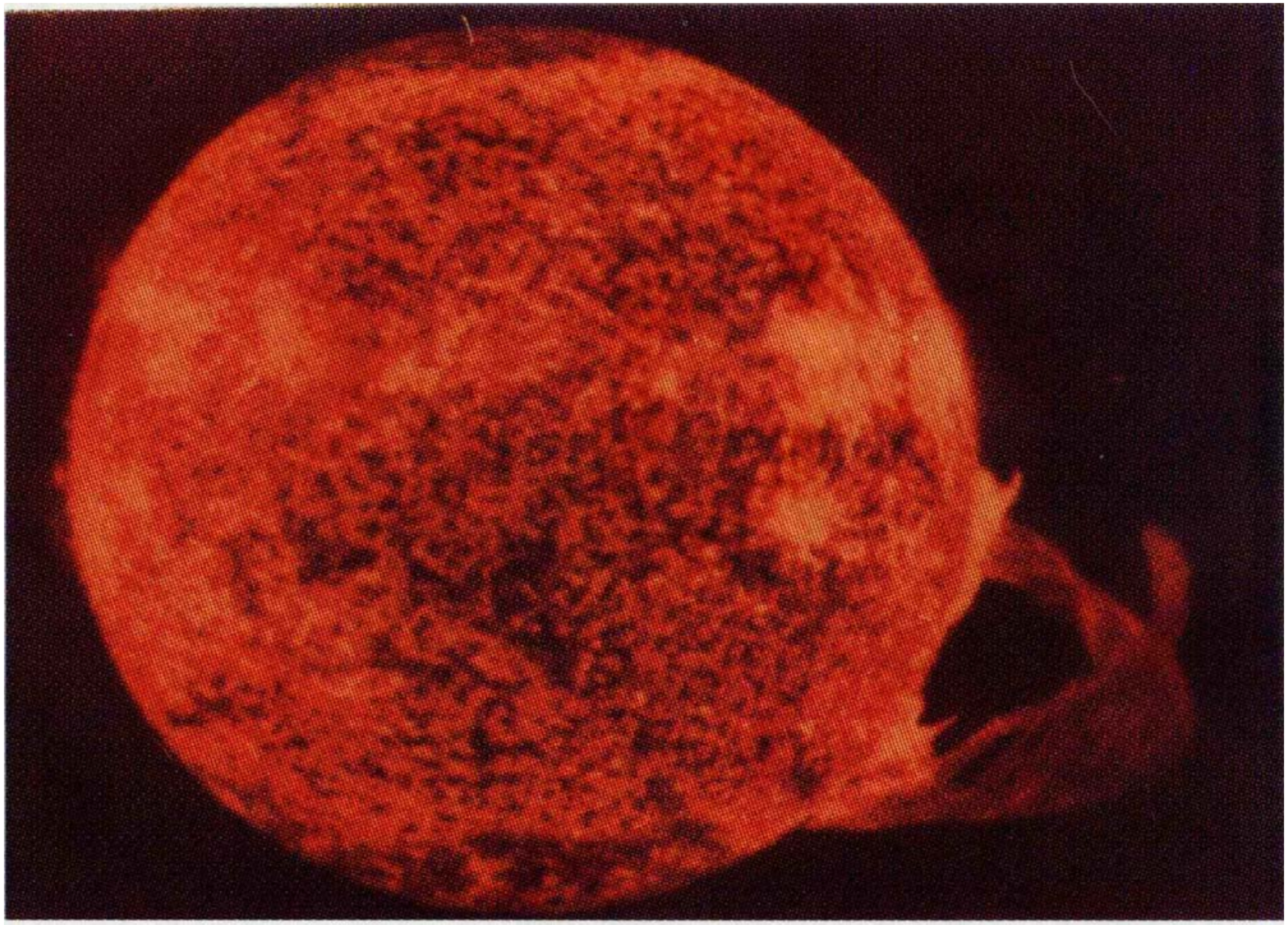

The Sun appears to have been active for 4.6 billion years and has enough fuel to go on for another five billion years or so.

Light: wave or particle

Isaac Newton, 1642-1727

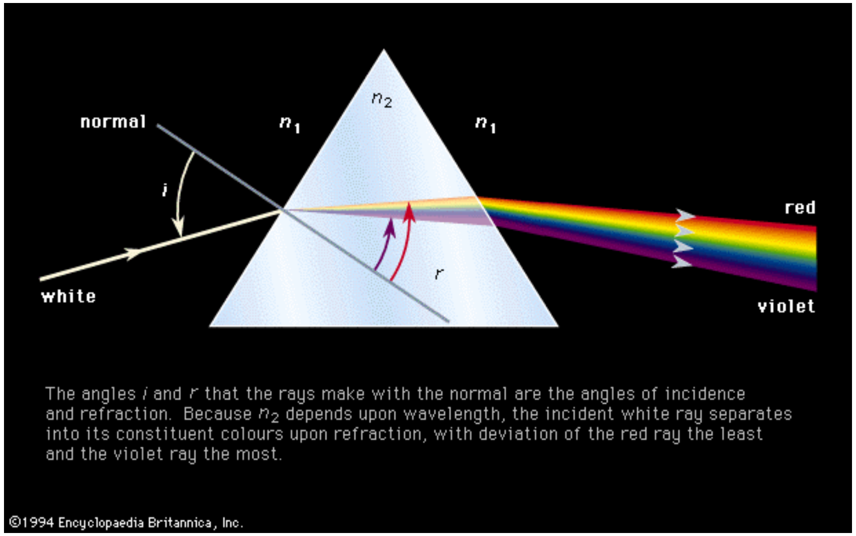

+ The prism: Energy Analyzer (energy resolution)

+ The eye: Detector (sensitivity)

+ Wave: described by wave length, phase, amplitude
+ Matter: optical index of reflection

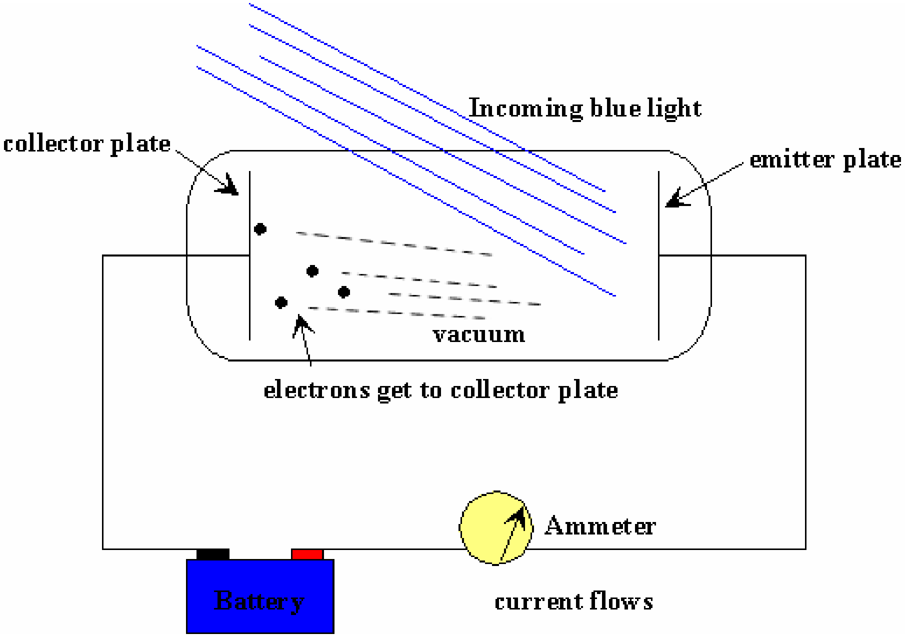

- $e/m = 1.76*10^8$ c/g

J.J.Thomson was awarded the 1906 Nobel Prize in Physics for the discovery of the electron and his work on the conduction of electricity in gases.

Year 1895

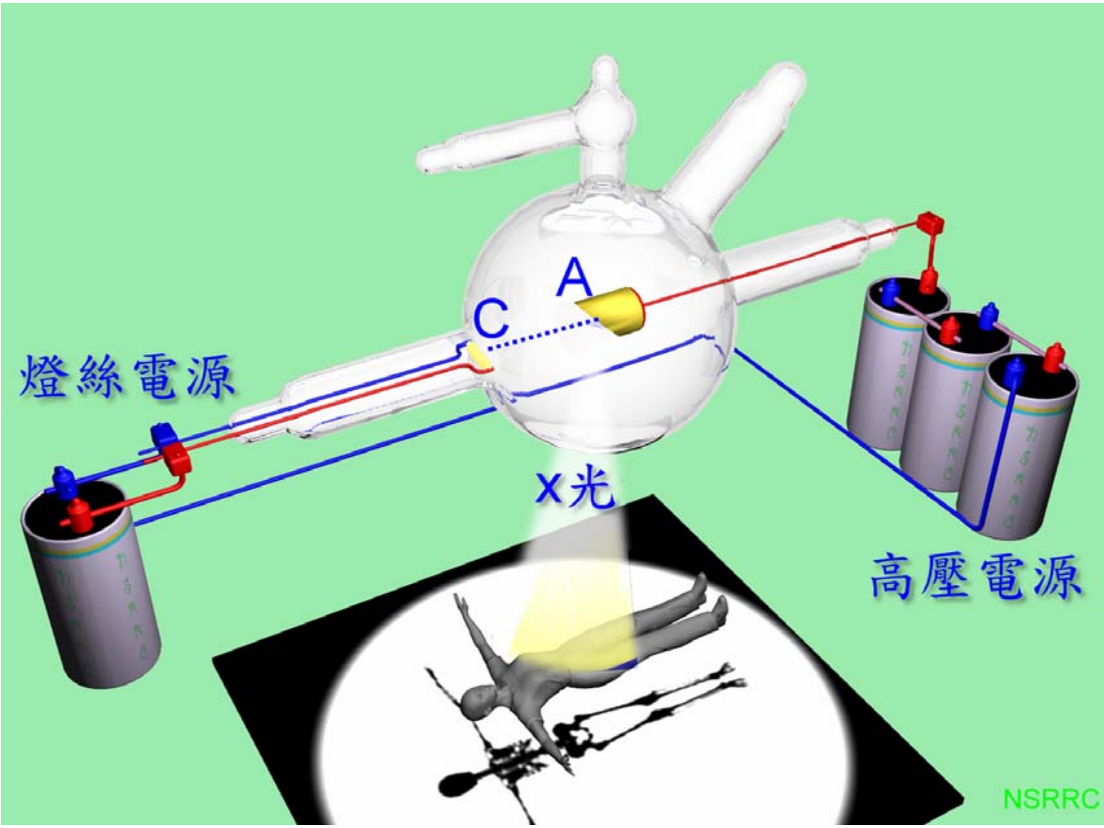

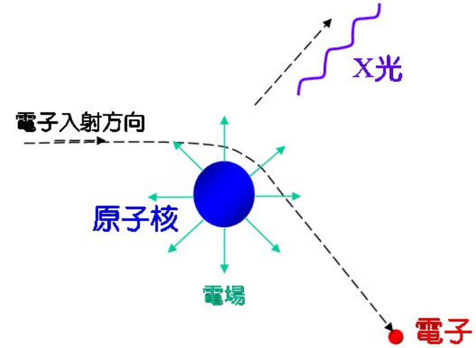

Wilhelm Röntgen produced and detected electromagnetic radiation in a wavelength range known as x-rays today; this achievement earned him the first Nobel Prize in Physics in 1901.

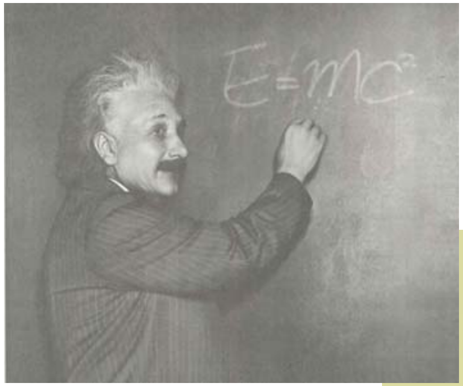

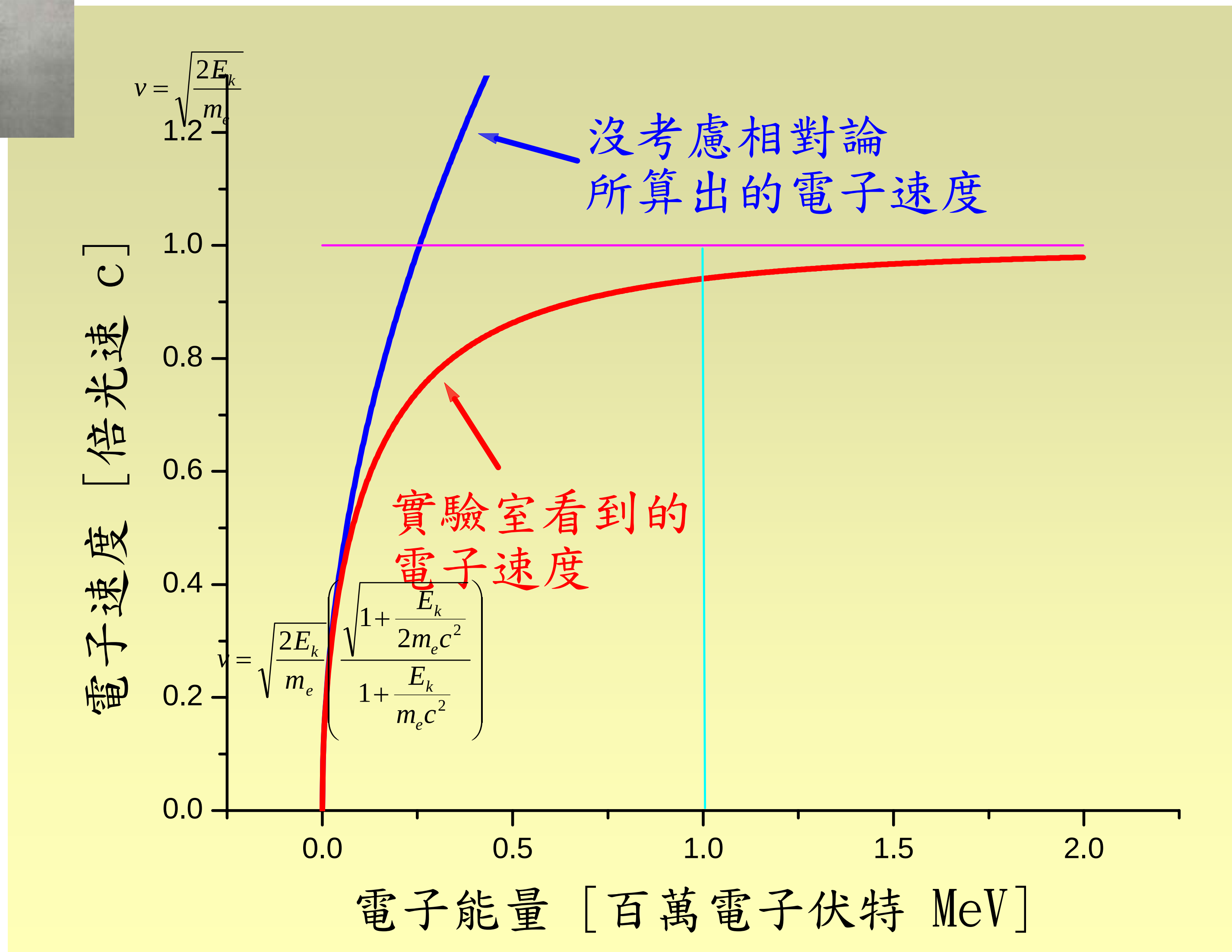

$v=\sqrt{\frac{2E_k}{m_e}}$
沒考慮相對論
所算出的電子速度
實驗室看到的
電子速度
$v=\sqrt{\frac{2E_k}{m_e}}\left(\frac{\sqrt{1+\frac{E_k}{2m_ec^2}}}{1+\frac{E_k}{m_ec^2}}\right)$
電子速度［倍光速 C］
電子能量［百萬電子伏特 MeV］
0.0
0.2
0.4
0.6
0.8
1.0
1.2
0.0
0.5
1.0
1.5
2.0

High Energy Accelerators

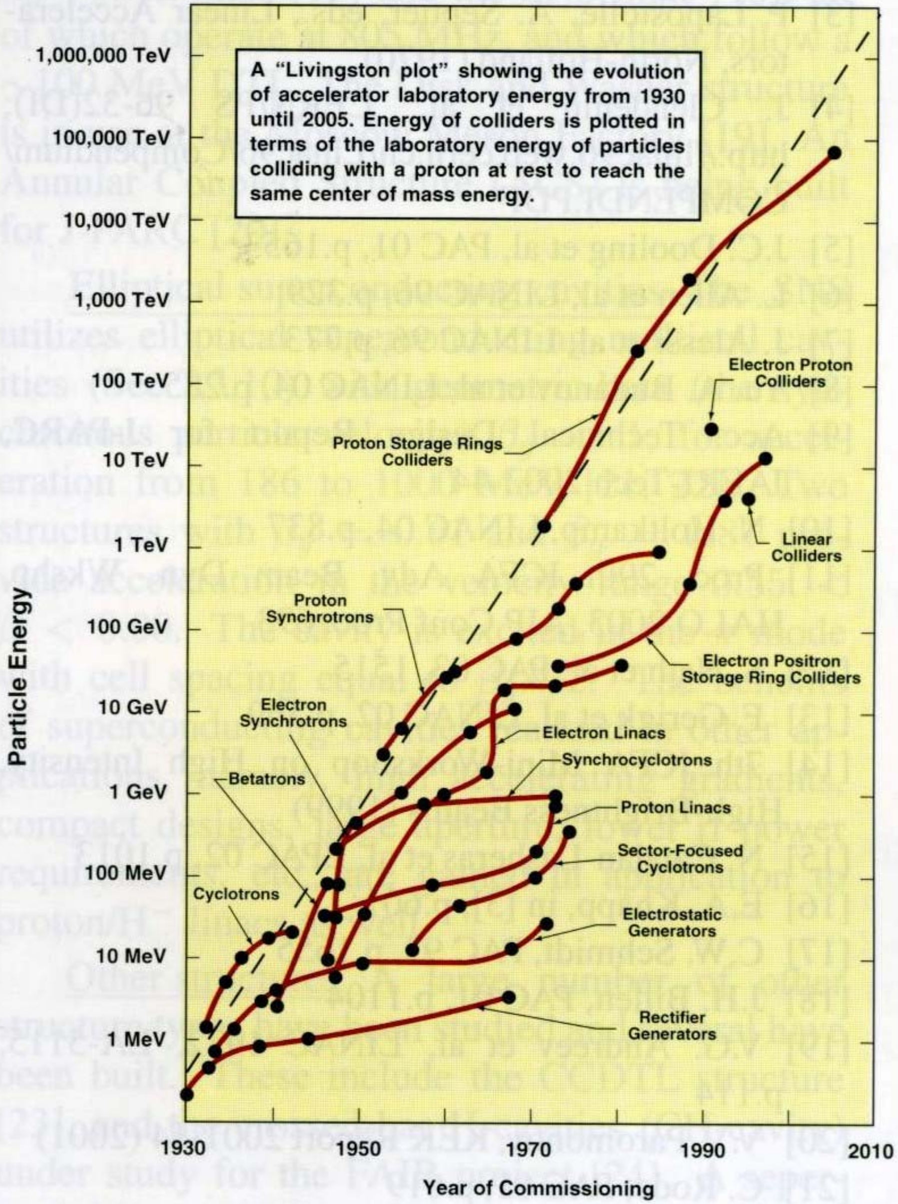

Figure 1: Livingston chart. 2-017

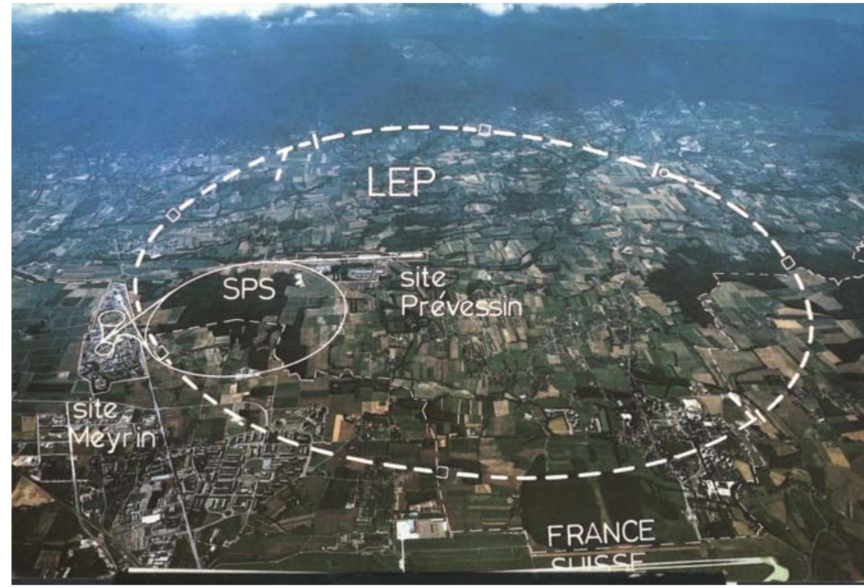

Synchrotron Radiation

Year 1947: First Synchrotron Radiation observed in weak focusing synchrotron betatrons

1st G :1960-1970

2nd G :1970-1980

3rd G :1980-

- Straight sections for insertion devices
- Low emittance

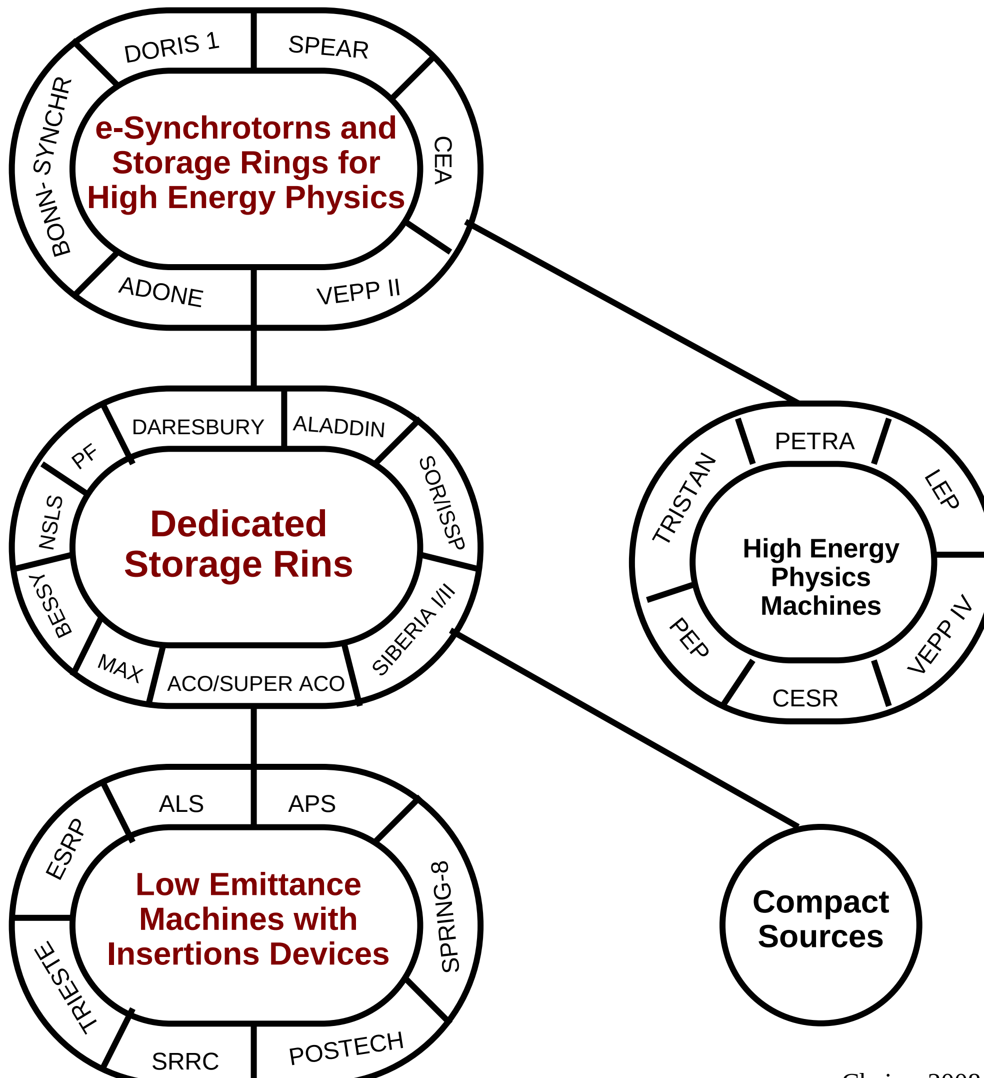

SR Facilities in Asia Oceania Region

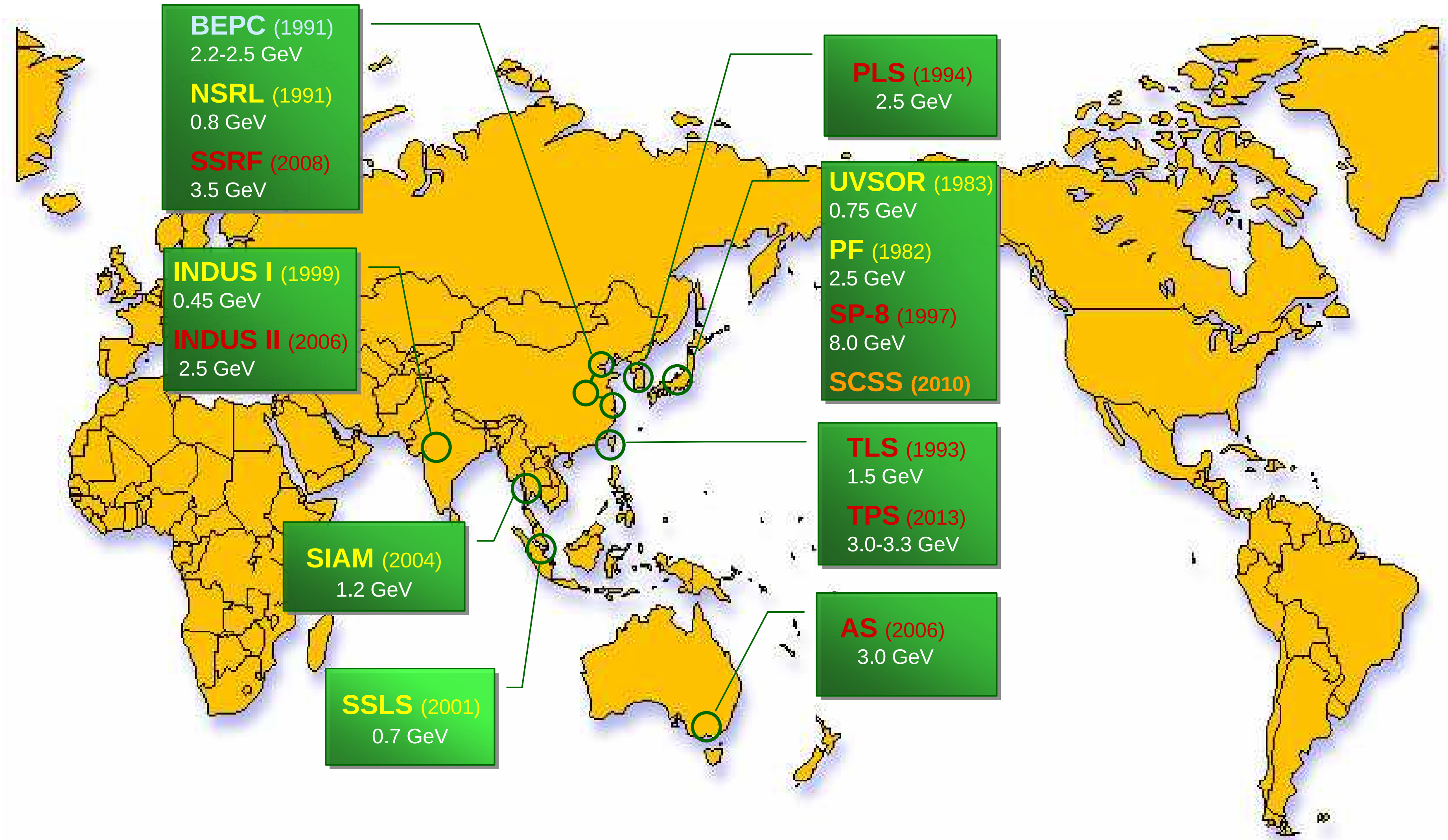

Basic Parameters of Taiwan Light Source

- Interval between bunches: 2ns
- Bunch length (1σ@1.6MV): 6.5 mm
- Bunch duration (1σ): 21 ps
- SC Cavity length: 24 cm
- Flight time through SC cavity: 0.8 ns

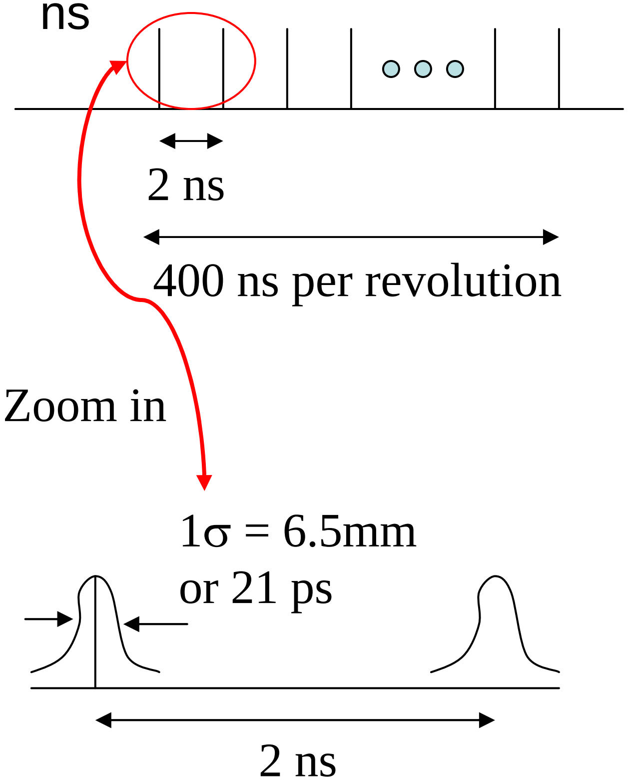

- Bunch current (180/200 filling to I_{avg}=300 mA): 1.67 mA/bunch or $4.17*10^9$ electrons/bunch

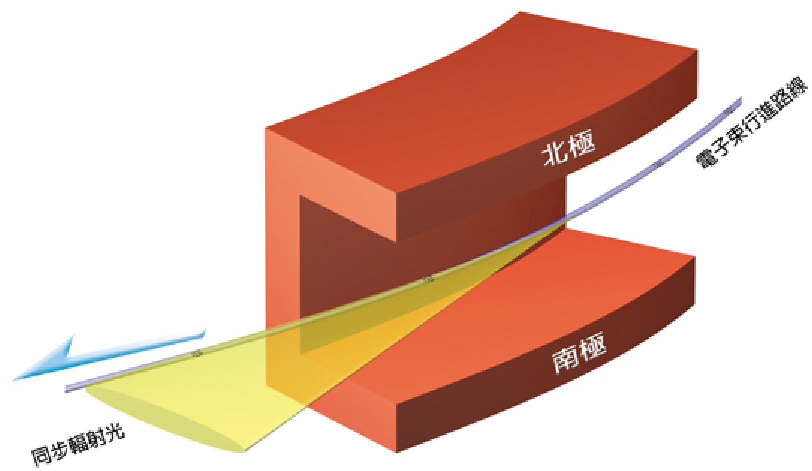

- Critical energy of SR

$$E_c(\text{keV}) = 0.665\ E^2\ (\text{GeV})\ B(\text{T})$$

Insertion Devices

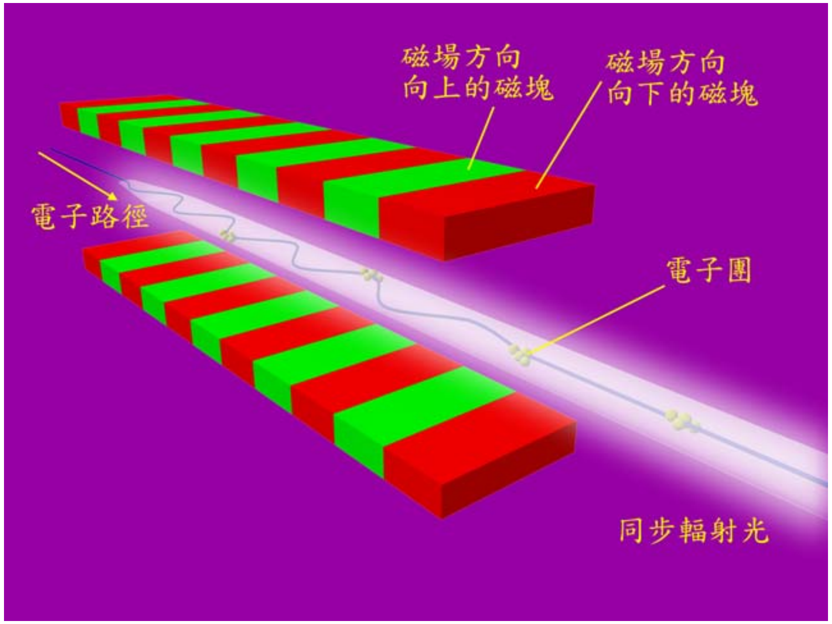

Wiggler: radiation adds incoherently (I~2N, N: number of magnet periods)

Undulator: radiation interferences coherently

Superconducting RF Cavity

Goals：

- To increase the maximum electron beam current of the storage ring from 240 mA to 500 mA
- To eliminate beam instabilities caused by the strong higher-order modes (HOMs) of the existing RF cavities

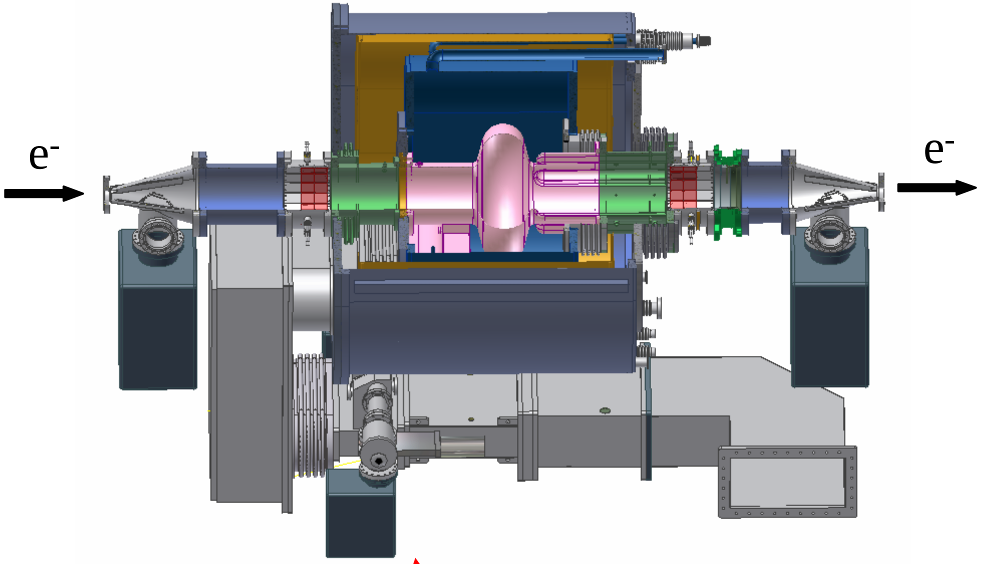

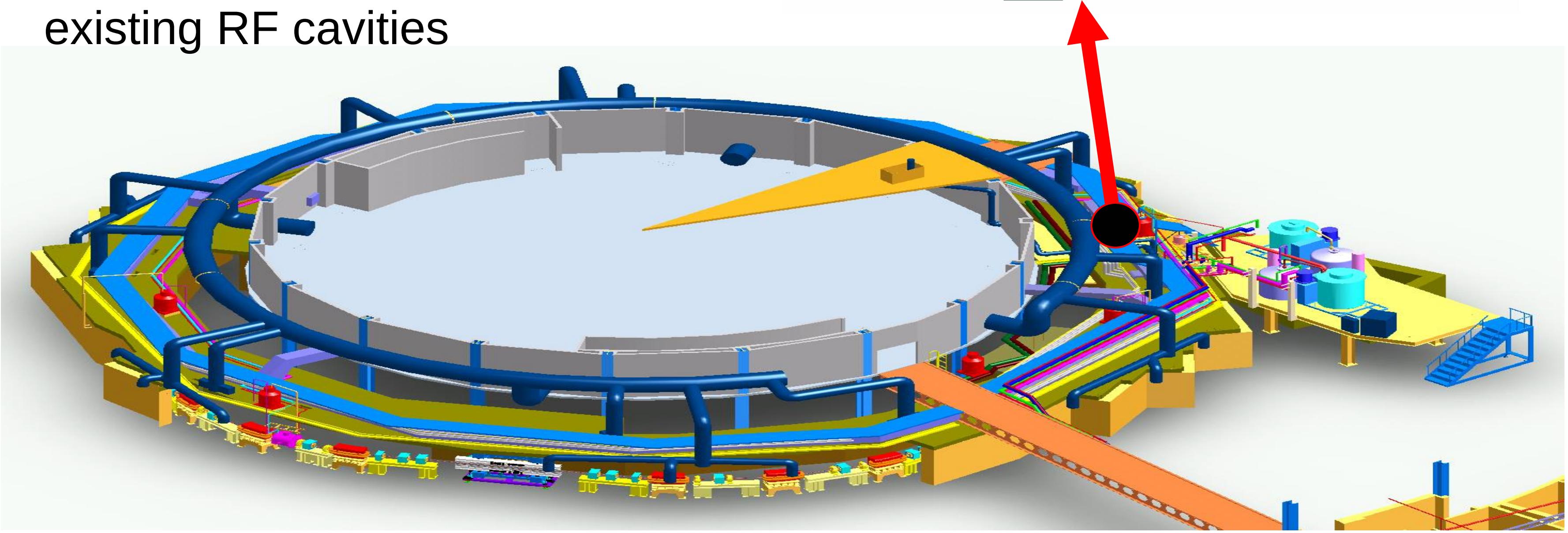

Low-emittance Medium Energy Rings

Date	Location	Name	E [GeV]	Emit. [nm-rad]	C [m]	Straights m*section	Cell	Status
2001	Switzerland, Villigen	SLS	2.4	4.8 (4.1)	288	11.76m*3+7m*3+4m*6	12 TBA	Operation
2006	France, Orsay	SOLEIL	2.75	(3.7)	351	12m*4+7m*12+3.6m*8	16 DBA	Operation
2006	UK, Oxfordshire	DIAMOND	3.0	6.5 (2.7)	562	11.34m*6+8.34m*18	24 DBA	Operation
2008	China, Shanghai	SSRF	3.5	7.8 (3.0)	432	12m*4+6.7m*16	20 DBA	Commiss.
2009	Spain, Barcelona	ALBA	3.0	(4.2)	268	8m*4+4.2m*12+2.6m*8	16 DBA	Construct.
2013	Taiwan, Hsinchu	TPS	3.0	1.7(1.46)	518	12m*6+7m*18	24 DBA	Approved
2013	USA, Brookhaven	NSLS-II	3.0	1.9 (0.5)	780	8m*15+5m*15	30 DBA	Approved

Emittance of Synchrotrons

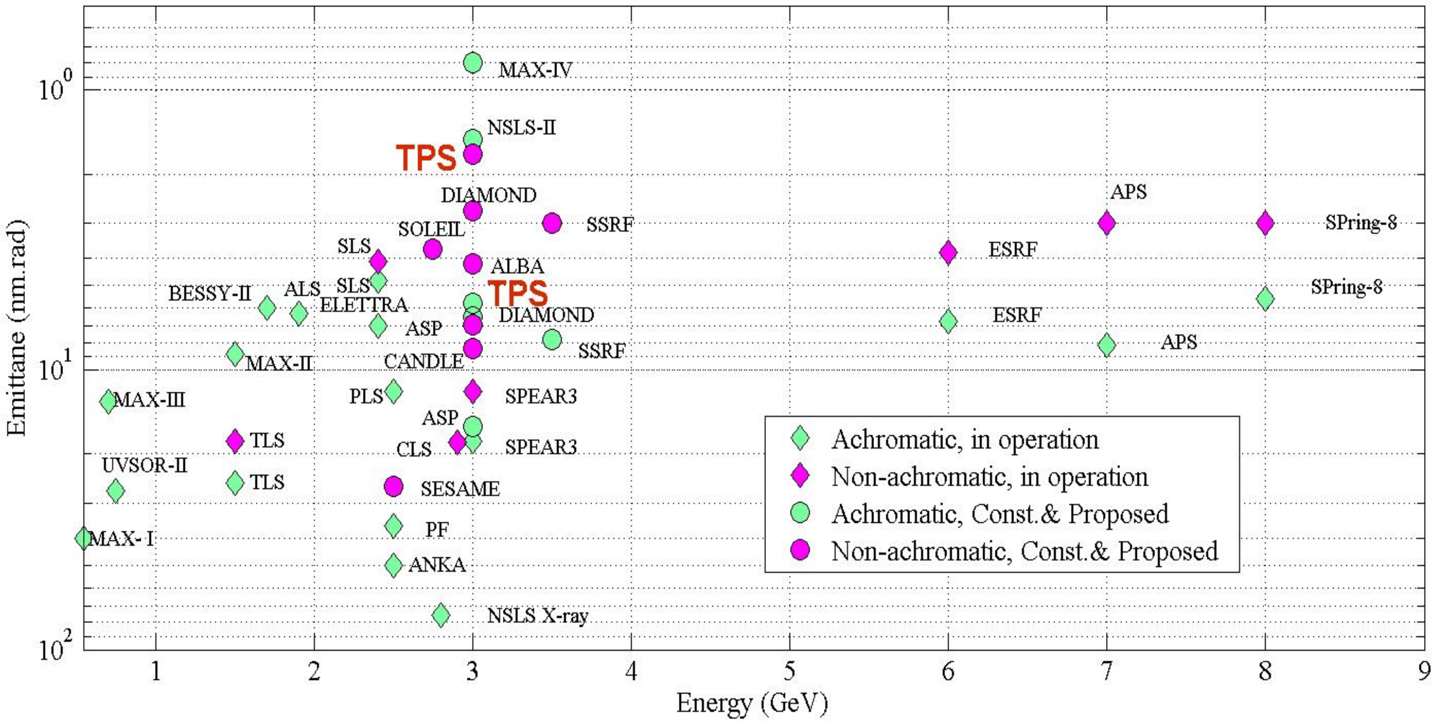

Storage Ring

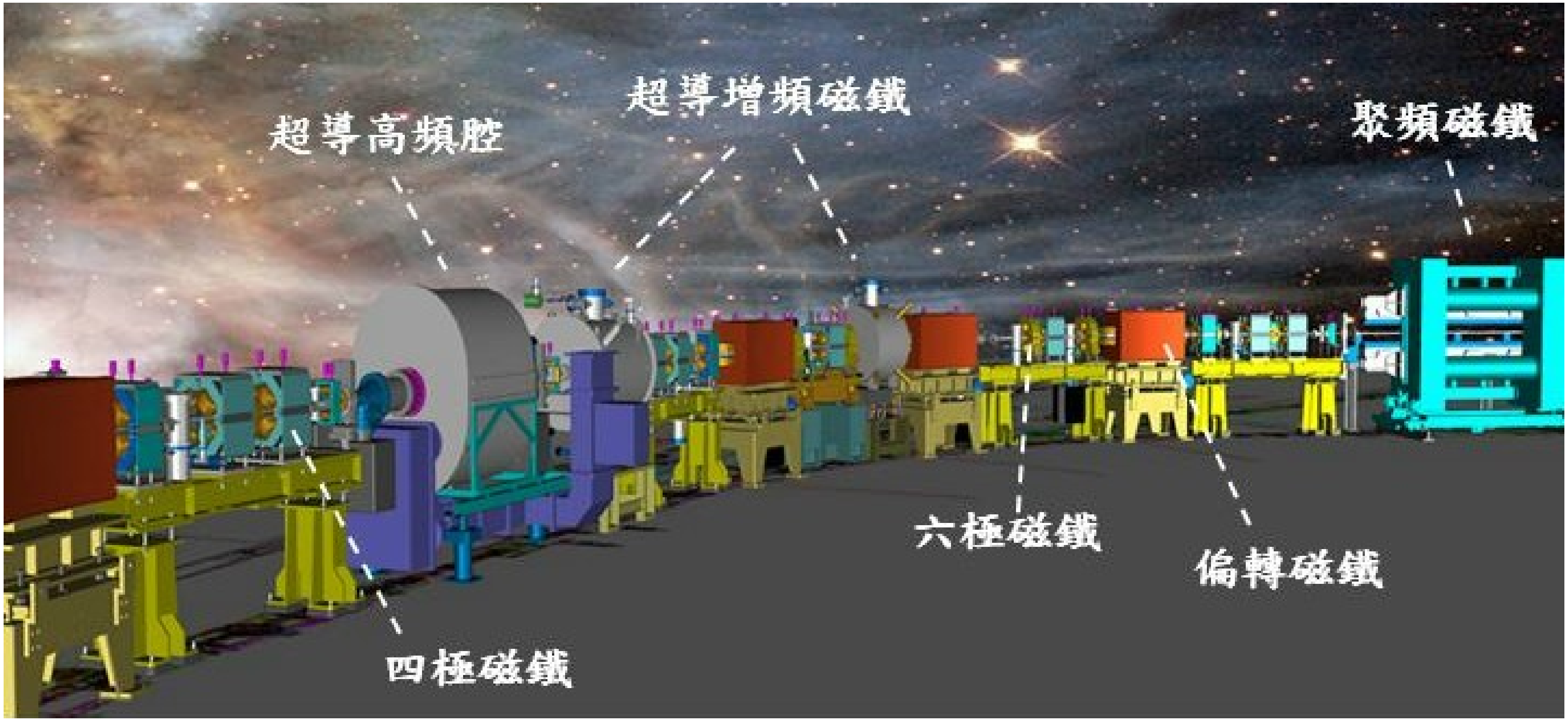

TPS DBA Lattice Cell and Engineering Layout

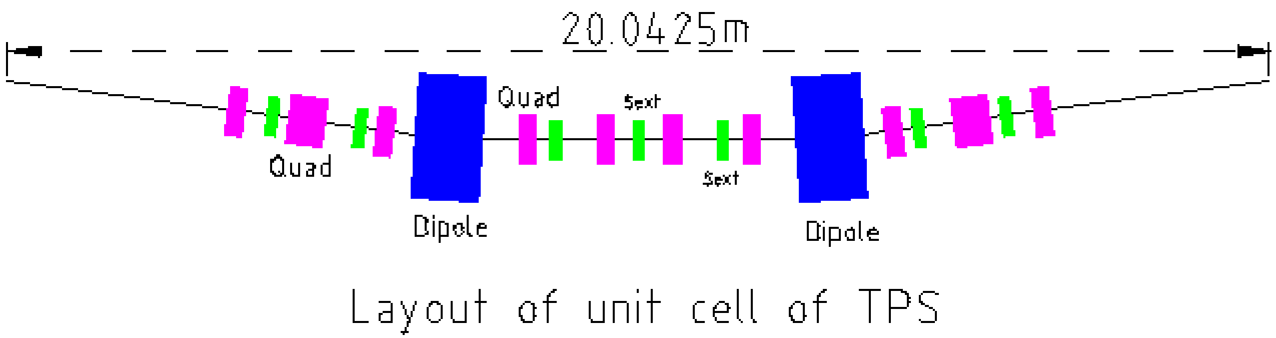

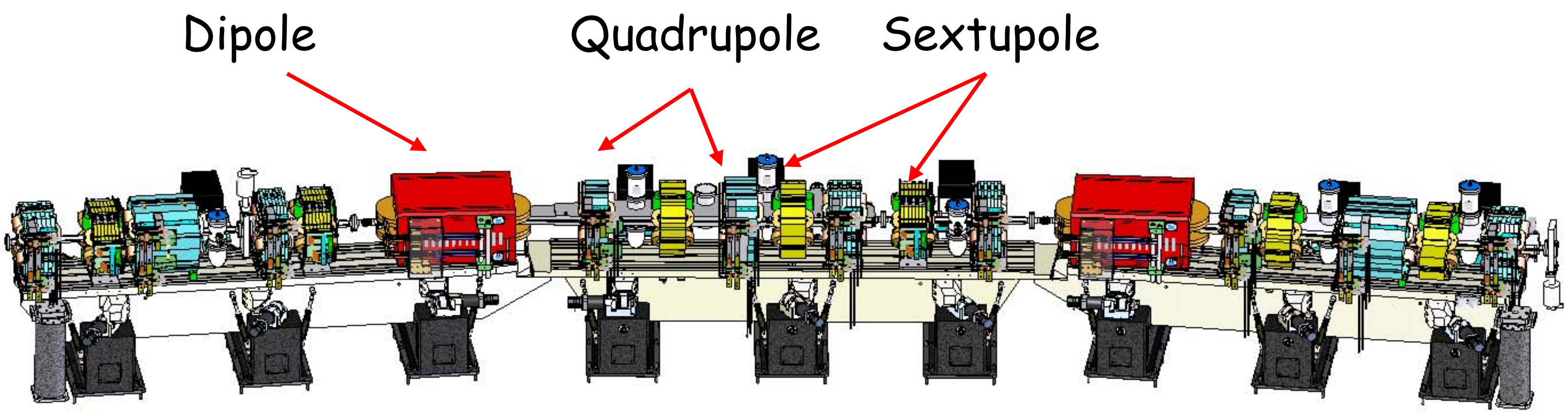

Optical Functions and Dynamic Aperture of Three Modes

Zero dispersion, 4.9 nm-rad

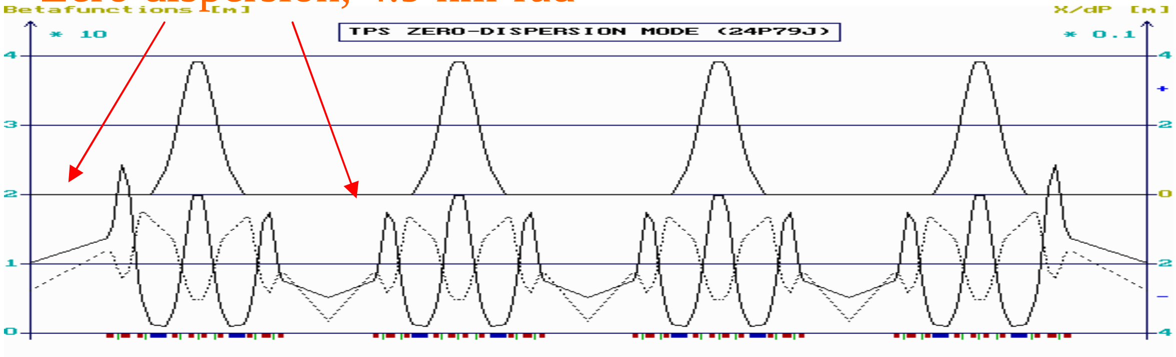

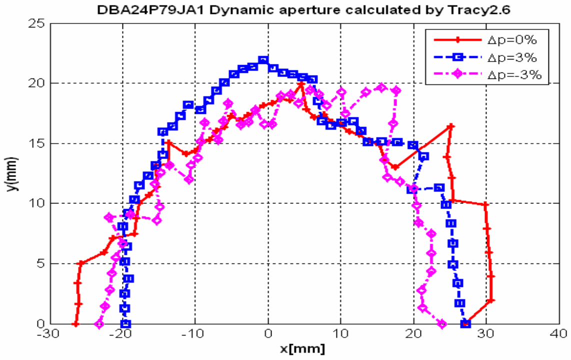

Low dispersion 2.5 nm-rad

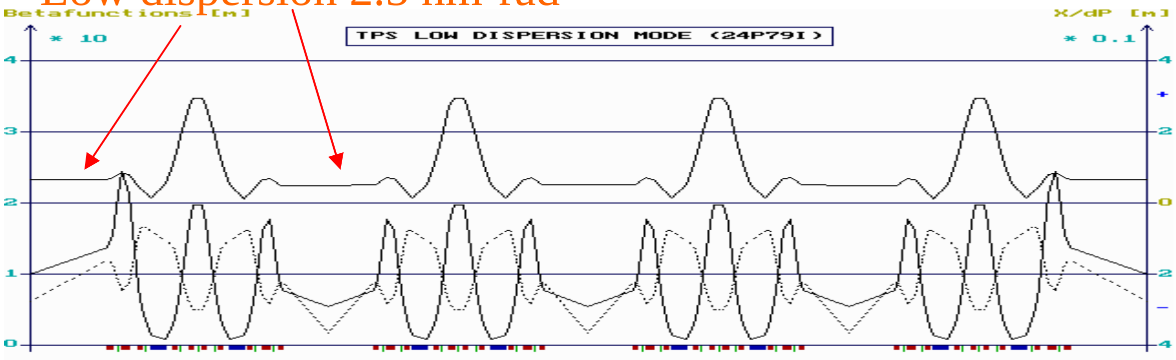

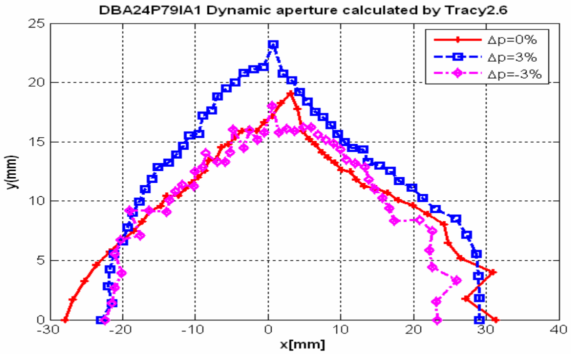

High dispersion, 1.6 nm-rad

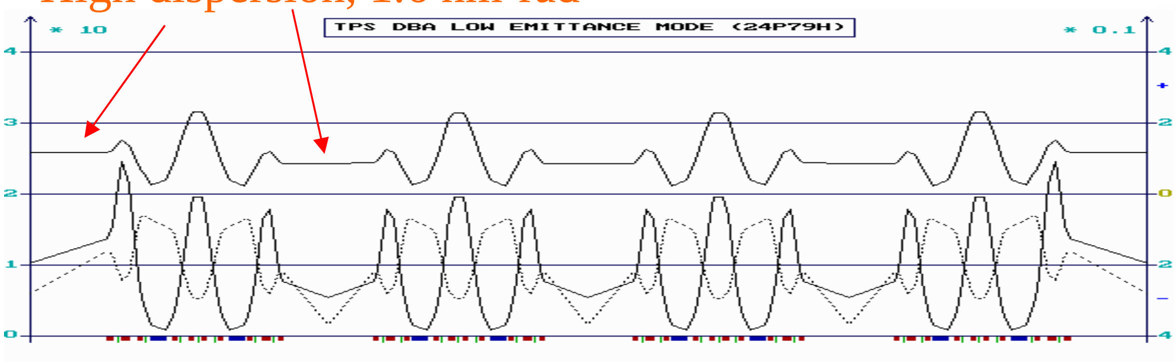

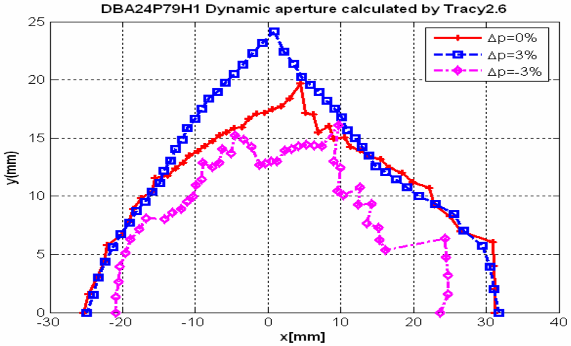

Brightness of Insertion Devices

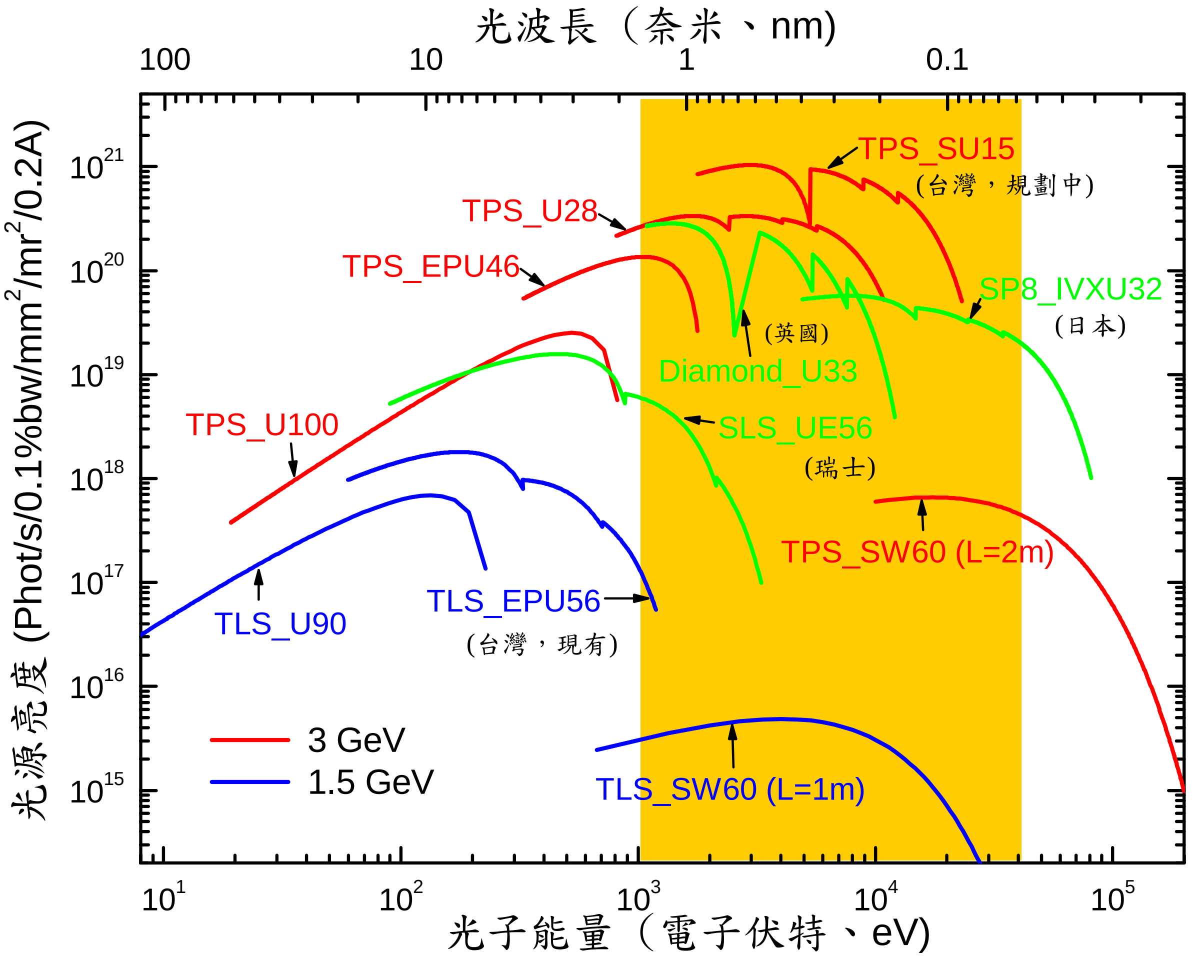

- Critical energy of SR spectrum Ec(keV) = 0.665 E^2 (GeV) B(T)

  TLS: 1.5 GeV, operation since Oct. 1993; the first 3rd generation synchrotron facility in Asia

  TPS: 3 GeV, operation planned for 2013

Fully coherent radiation.......

J.M. Byrd

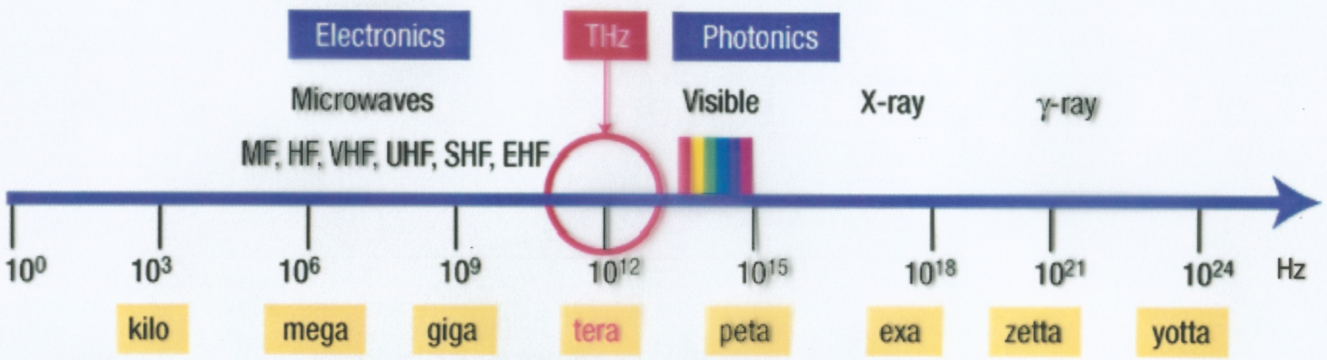

1 THz
= 4.1 meV
= 33 cm^{-1}
= 300 μm

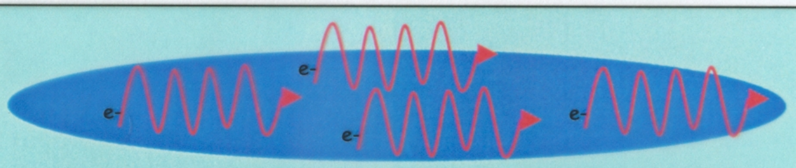

Incoherent emission for long bunches, P~N

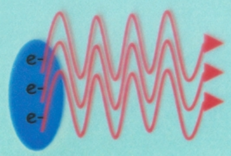

Coherent emission for short bunches $P{\sim}N^2$

Achieved at BESSY-II: 10^4 more flux than from conventional IR sources

Plans for CIRCE @ ALS
$10^6 – 10^{10}$ more flux

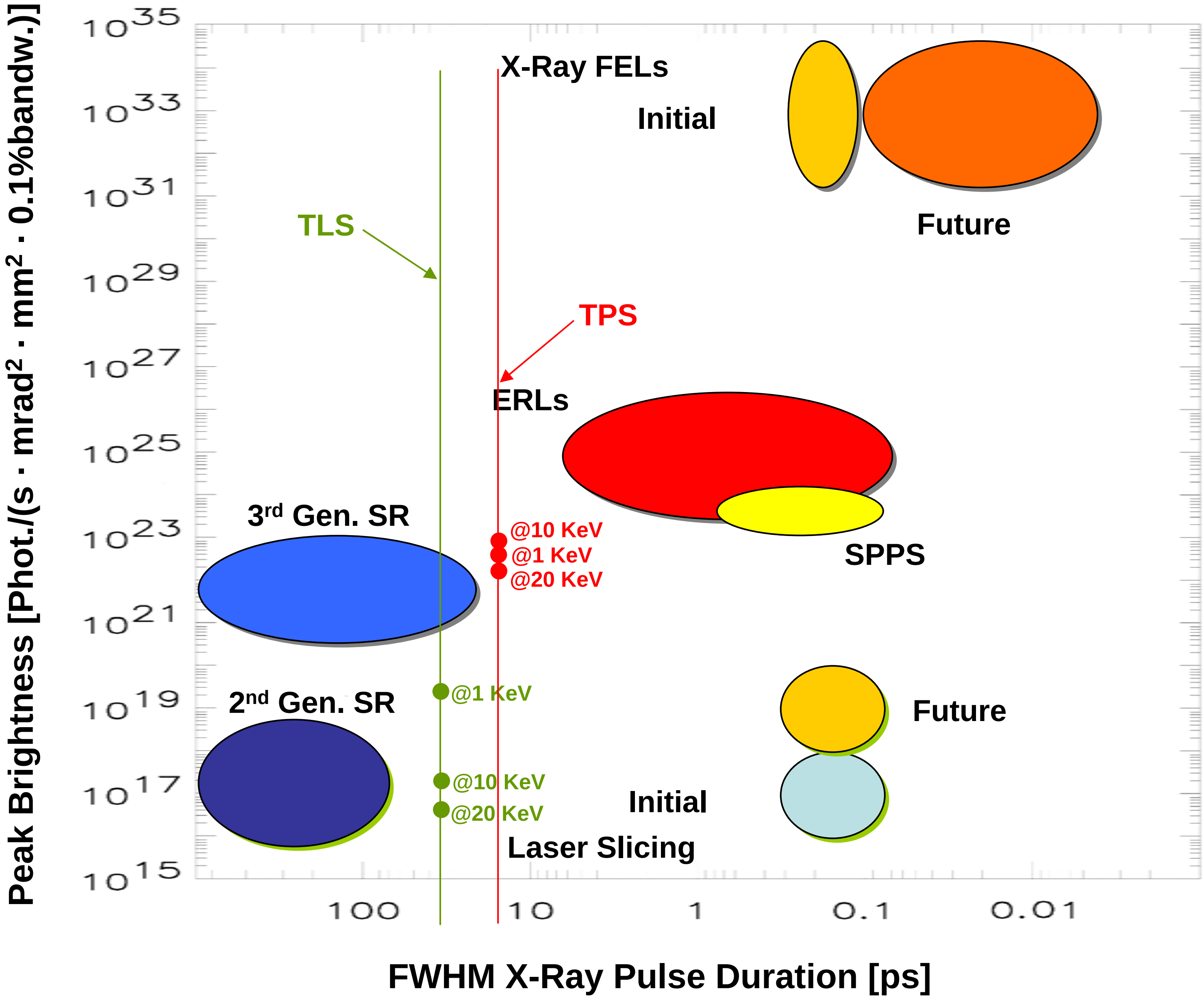

Courtesy of H. Winick

Electron Binding Energies

Electron binding energies, in electron volts, for the elements in their natural forms

Element	K 1s	L_{I} 2s	L_{II} $2p_{1/2}$	L_{III} $2p_{3/2}$	M_{I} 3s	M_{II} $3p_{1/2}$	M_{III} $3p_{3/2}$	M_{IV} $3d_{3/2}$	M_{V} $3d_{5/2}$	N_{I} 4s	N_{II} $4p_{1/2}$	N_{III} $4p_{3/2}$
1 H	16*											
2 He	24.6*											
3 Li	54.7*											
4 Be	111.5*											
5 B	188*											
6 C	284.2*											
7 N	409.9*	37.3*										
8 O	543.1*	41.6*										
9 F	696.7*											
10 Ne	870.2*	48.5*	21.7*	21.6*								
11 Na	1070.8†	63.5†	30.4†	30.5†								
12 Mg	1303.0†	88.6*	49.6†	49.2†								
13 Al	1558.98*	117.8*	72.9*	72.5*								
14 Si	1839	149.7*b	99.8*	99.2*								
15 P	2149	189*	136*	135*								
16 S	2472	2309*b	163.6*	162.5*								
17 Cl	2833	270*	202*	200*								
18 Ar	3205.9*	326.3*	250.6*	248.4*	29.3*	15.9*	15.7*					
19 K	3608.4*	378.6*	297.3*	294.6*	34.8*	18.3*	18.3*					
20 Ca	4038.5*	438.4†	349.7†	346.2†	44.3†	25.4†	25.4†					
21 Sc	4492	498.0*	403.6*	398.7*	51.1*	28.3*	28.3*					
22 Ti	4966	560.9†	461.2†	453.8†	58.7†	32.6†	32.6†					
23 V	5465	626.7†	519.8†	512.1†	66.3†	37.2†	37.2†					
24 Cr	5989	695.7†	583.8†	574.1†	74.1†	42.2†	42.2†					
25 Mn	6539	769.1†	649.9†	638.7†	82.3†	47.2†	47.2†					
26 Fe	7112	844.6†	719.9†	706.8†	91.3†	52.7†	52.7†					
27 Co	7709	925.1†	793.3†	778.1†	101.0†	58.9†	58.9†					
28 Ni	8333	1008.6†	870.0†	852.7†	110.8†	68.0†	66.2†					
29 Cu	8979	1096.7†	952.3†	932.5†	122.5†	77.3†	75.1†					
30 Zn	9659	1196.2*	1044.9*	1021.8*	139.8*	91.4*	88.6*	10.2*	10.1*			
31 Ga	10367	1299.0*b	1143.2†	1116.4†	159.5†	103.5†	103.5†	18.7†	18.7†			
32 Ge	11103	1414.6*b	1248.1*b	1217.0*b	180.1*	124.9*	120.8*	29.0*	29.0*			
33 As	11867	1527.0*b	1359.1*b	1323.6*b	204.7*	146.2*	141.2*	41.7*	41.7*			
34 Se	12658	1652.0*b	1474.3*b	1433.9*b	229.6*	166.5*	160.7*	55.5*	54.6*			
35 Br	13474	1782*	1596*	1550*	257*	189*	182*	70*	69*			
36 Kr	14326	1921	1730.9*	1678.4*	292.8*	222.2*	214.4	95.0*	93.8*	27.5*	14.1*	14.1*
37 Rb	15200	2065	1864	1804	326.7*	248.7*	239.1*	113.0*	112*	30.5*	16.3*	15.3*
38 Sr	16105	2216	2007	1940	358.7†	280.3†	270.0†	136.0†	134.2†	38.9†	20.3†	20.3†
39 Y	17038	2373	2156	2080	392.0*b	310.6*	298.8*	157.7†	155.8†	43.8*	24.4*	23.1*
40 Zr	17998	2532	2307	2223	430.3†	343.5†	329.8†	181.1†	178.8†	50.6†	28.5†	27.7†
41 Nb	18986	2698	2465	2371	466.6†	376.1†	360.6†	205.0†	202.3†	56.4†	32.6†	30.8†
42 Mo	20000	2866	2625	2520	506.3†	410.6†	394.0†	231.1†	227.9†	63.2†	37.6†	35.5†
43 T_c	21044	3043	2793	2677	544*	447.6*	417.7*	257.6*	253.9*	69.5*	42.3*	39.9*
44 Ru	22117	3224	2967	2838	586.2†	483.3†	461.5†	284.2†	280.0†	75.0†	46.5†	43.2†
45 Rh	23220	3412	3146	3004	628.1†	521.3†	496.5†	311.9†	307.2†	81.4*b	50.5†	47.3†
46 Pd	24350	3604	3330	3173	671.6†	559.9†	532.3†	340.5†	335.2†	87.1*b	55.7†a	50.9†a
47 Ag	25514	3806	3524	3351	719.0†	603.8†	573.0†	374.0†	368.0†	97.0†	63.7†	58.3†

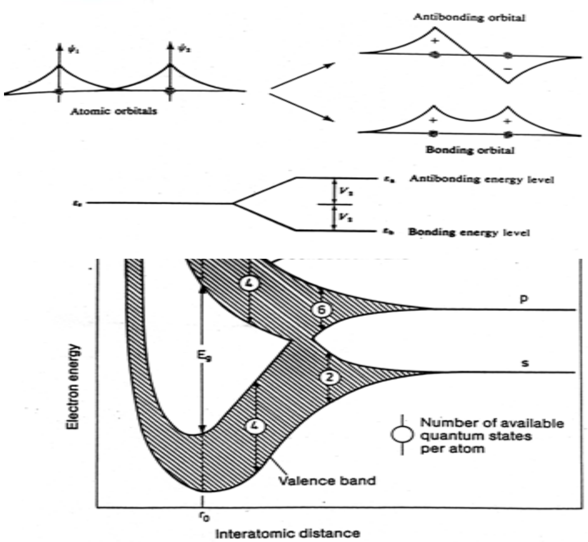

VUV

Soft X-ray

Hard X-ray

Unique Characteristics of SR

+ High brilliance/flux

  (coherence & emittance)

+ Energy tunability

  (element sepecificity)

+ Polarization

  (spin probe)

+ Time structure

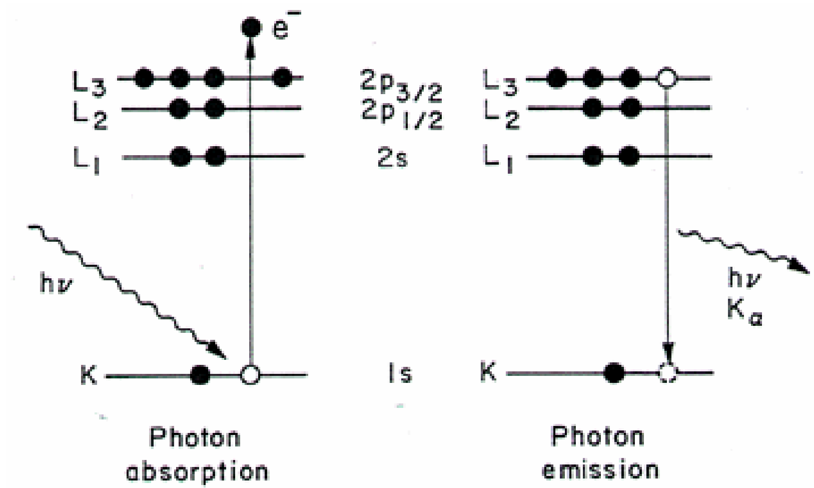
e⁻
L3
L2
L1
hν
K
2p3/2
2p1/2
2s
1s
L3
L2
L1
hν
Kα
K
Photon
absorption
Photon
emission

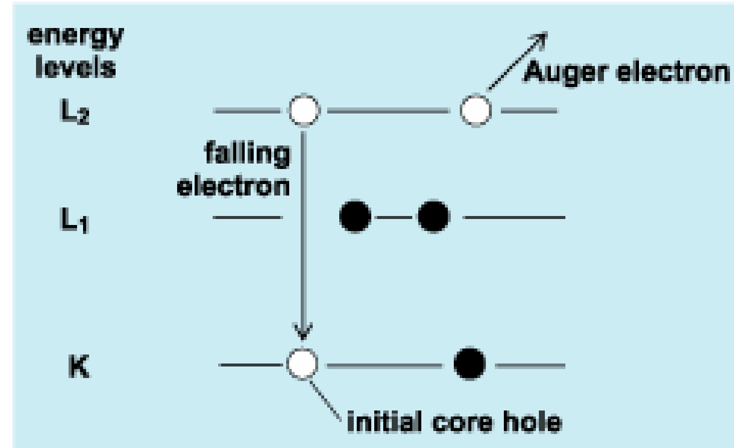
energy
levels
L2
L1
K
falling
electron
Auger electron
initial core hole

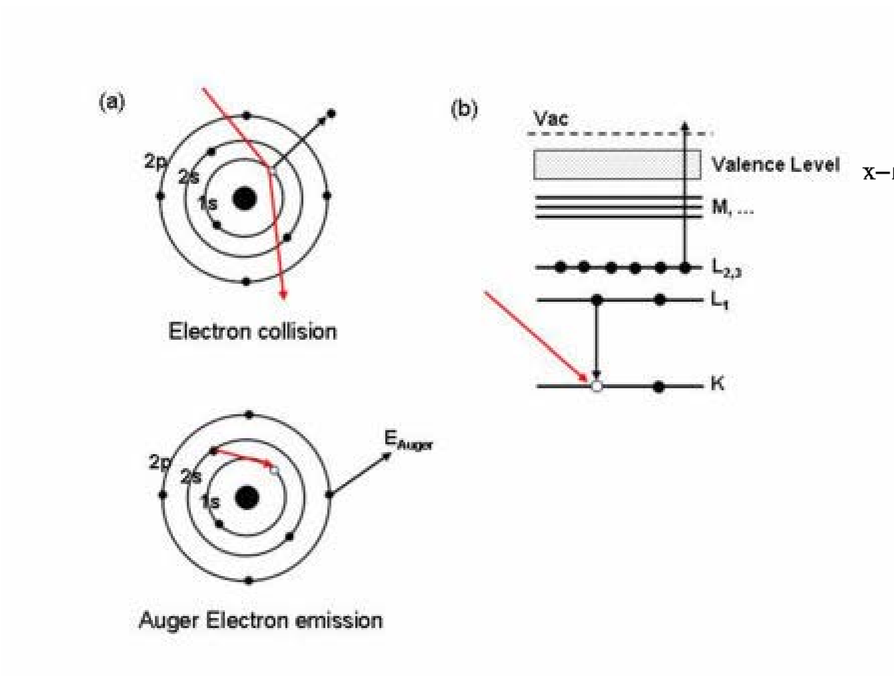
(a)
2p
2s
1s
Electron collision
(b)
Vac
Valence Level
M, ...
L2,3
L1
K
2p
2s
1s
EAuger
Auger Electron emission

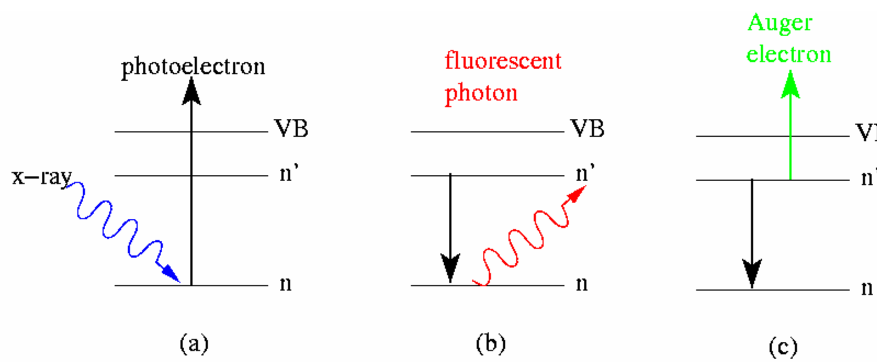
photoelectron
x–ray
VB
n'
n
(a)
fluorescent
photon
VB
n'
n
(b)
Auger
electron
VB
n'
n
(c)

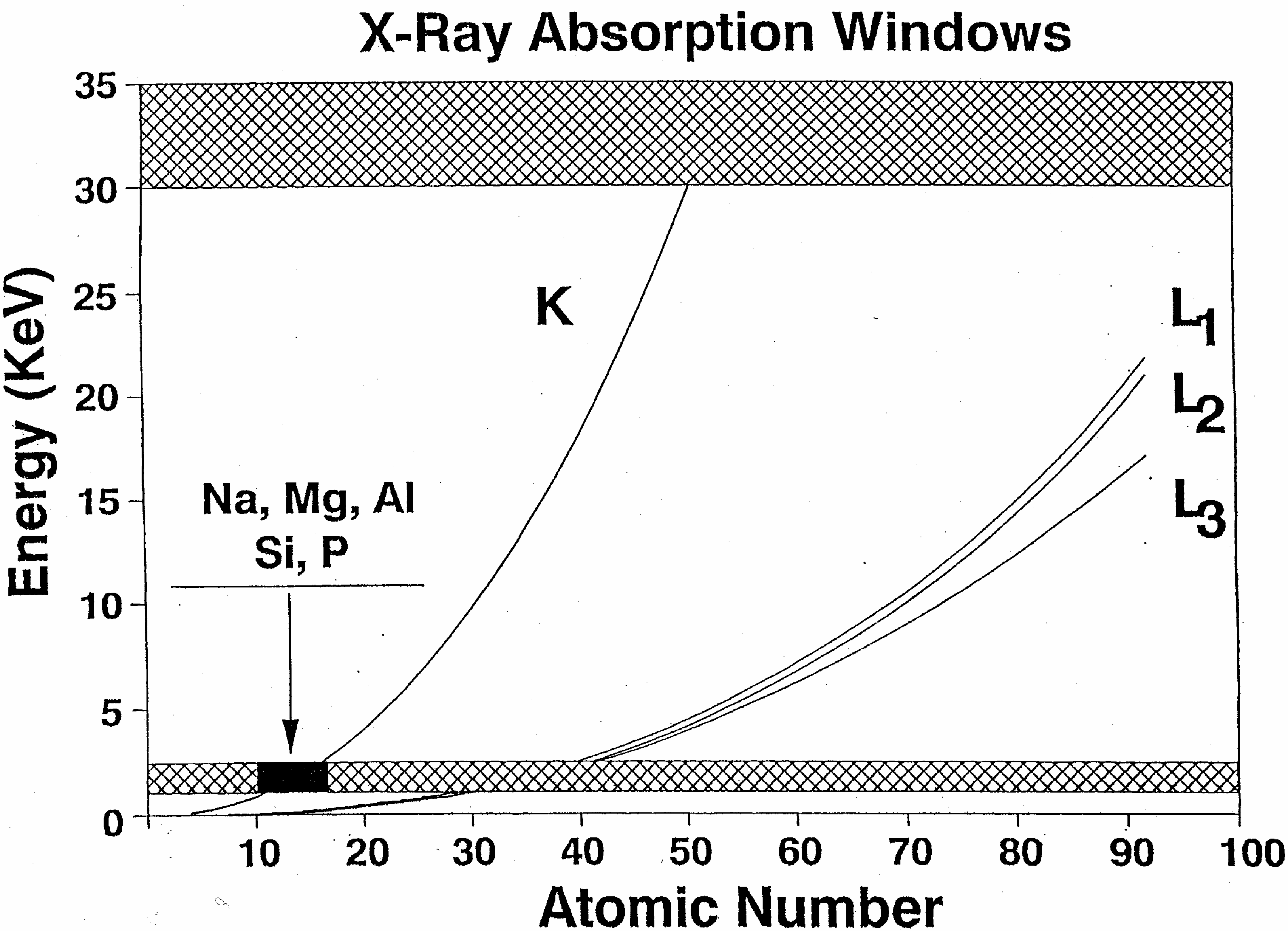
X-Ray Absorption Windows
Energy (KeV)
35
30
25
20
15
10
5
0
K
L1
L2
L3
Na, Mg, Al
Si, P
10
20
30
40
50
60
70
80
90
100
Atomic Number

EXAFS

$$\chi(k) = \sum_j \frac{N_j}{kR_j^2} S_j(k) F_j(k) \exp(-2\sigma_j^2 k^2) \exp\left[-2R_j / \lambda(k)\right] \sin\left[2kR_j + \delta_{ij}(k)\right]$$

Probe of Atomic Arrangements in disordered matters – beyond crystallography

EXTENDED X-RAY ABSORPTION FINE STRUCTURE
EXAFS

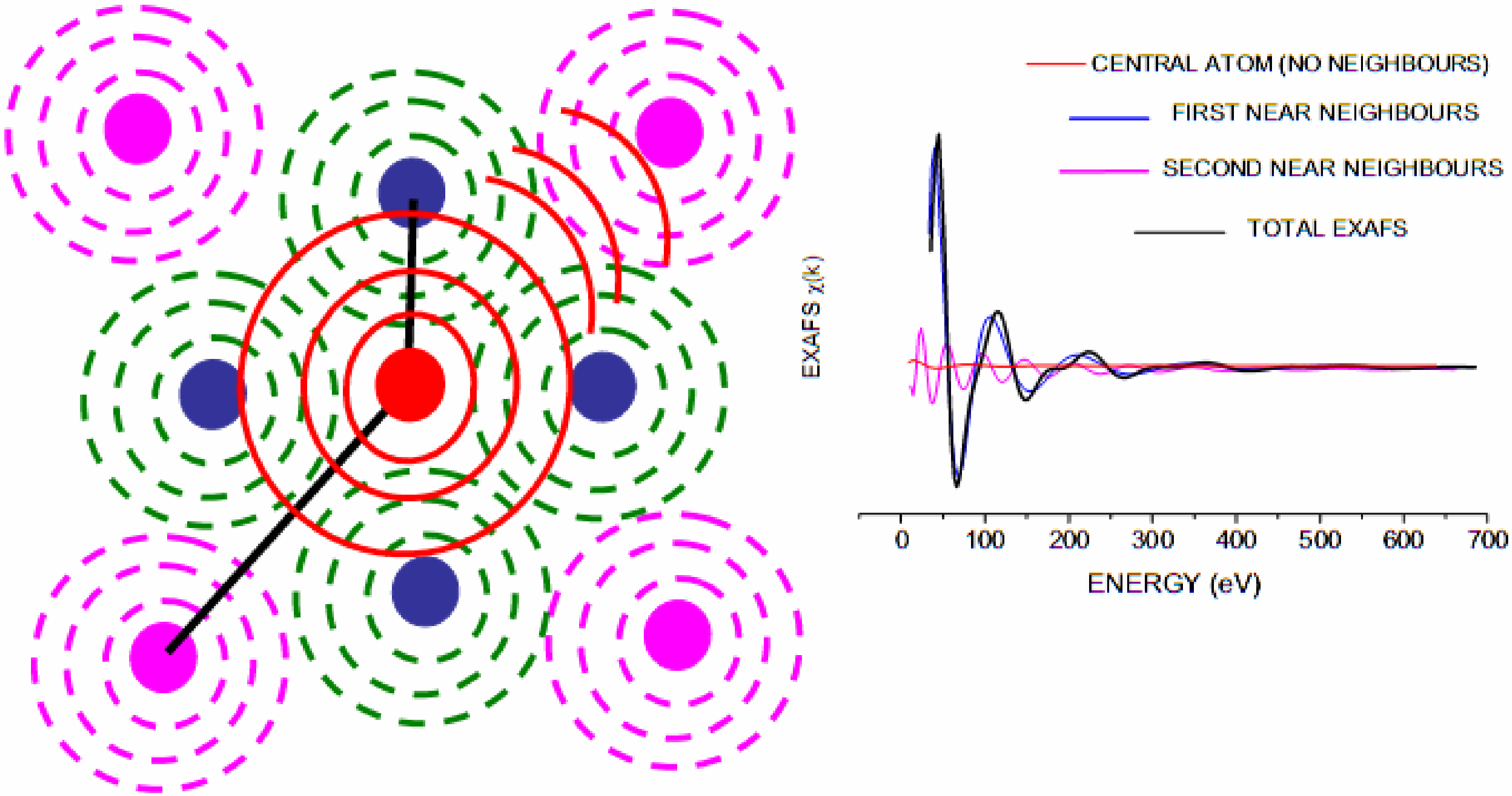

$$\chi(k) = \sum_j (N_j/R_j^2 k) \exp(-2\sigma^2 k^2) F_j(k) \text{ SIN } (2R_j k + \phi_j(k))$$

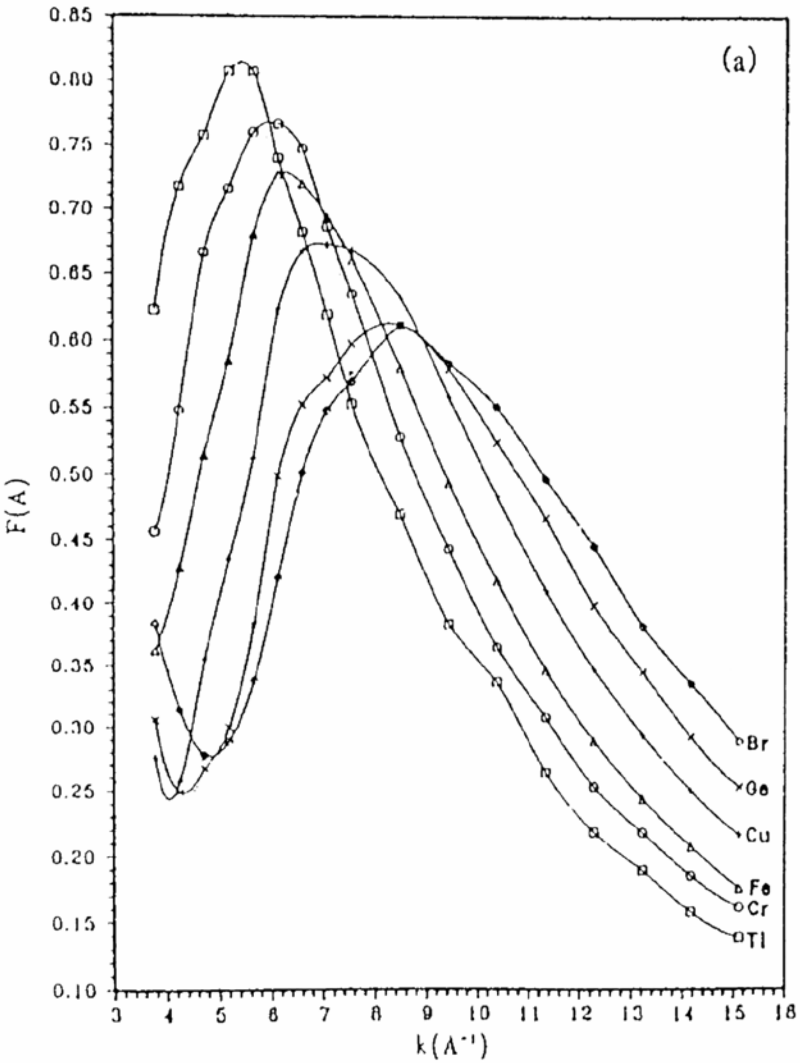
(a)
F(A)
k(Å⁻¹)
Br
Ge
Cu
Fe
Cr
Ti

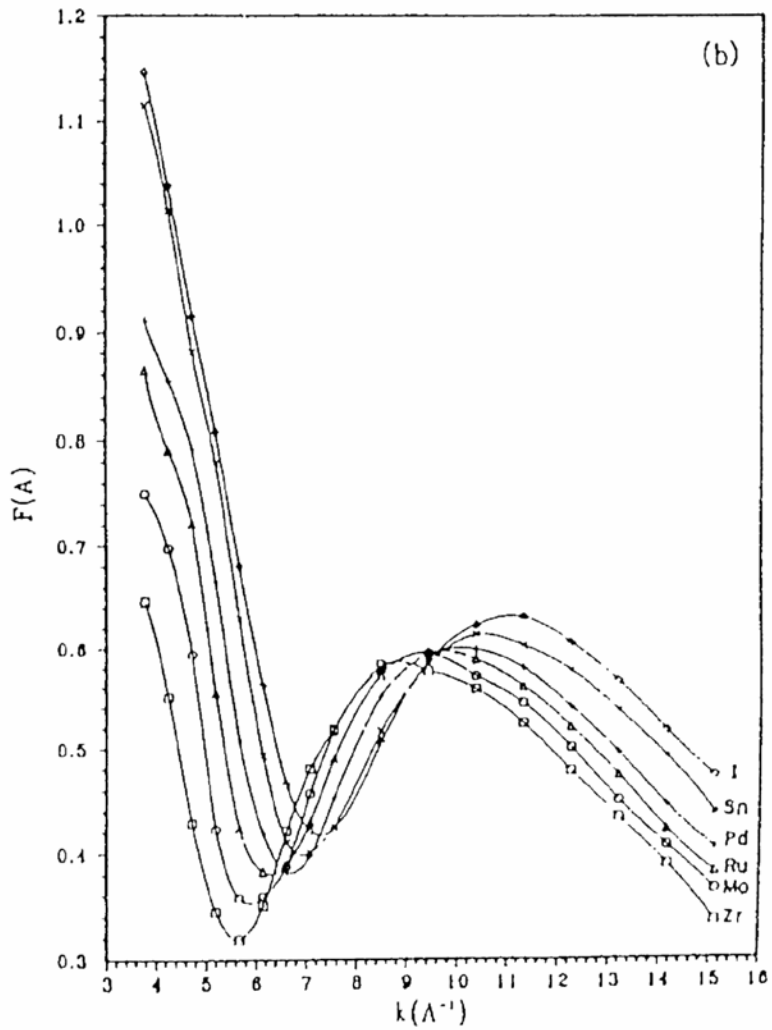
(b)
F(A)
k(Å⁻¹)
I
Sn
Pd
Ru
Mo
Zr

Total phase shift experienced by the photoelectron is given by $\delta_{ij}(k) = 2\,\delta_l^c(k) + \theta(k)$

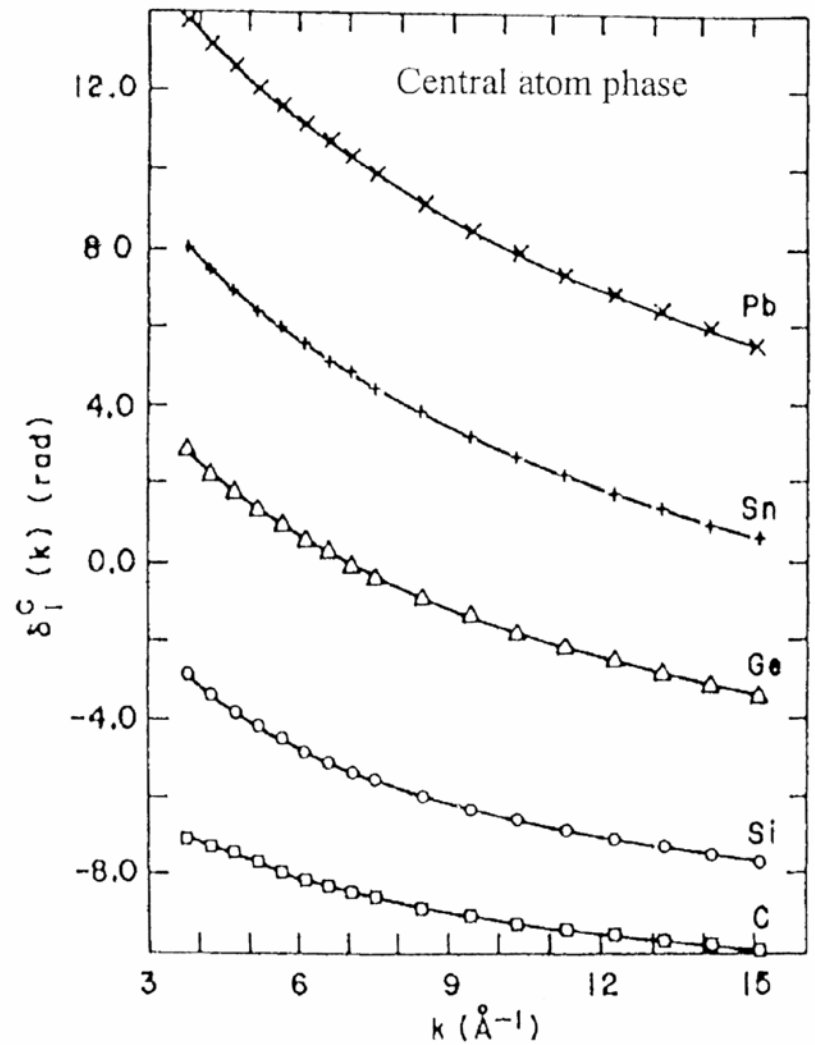

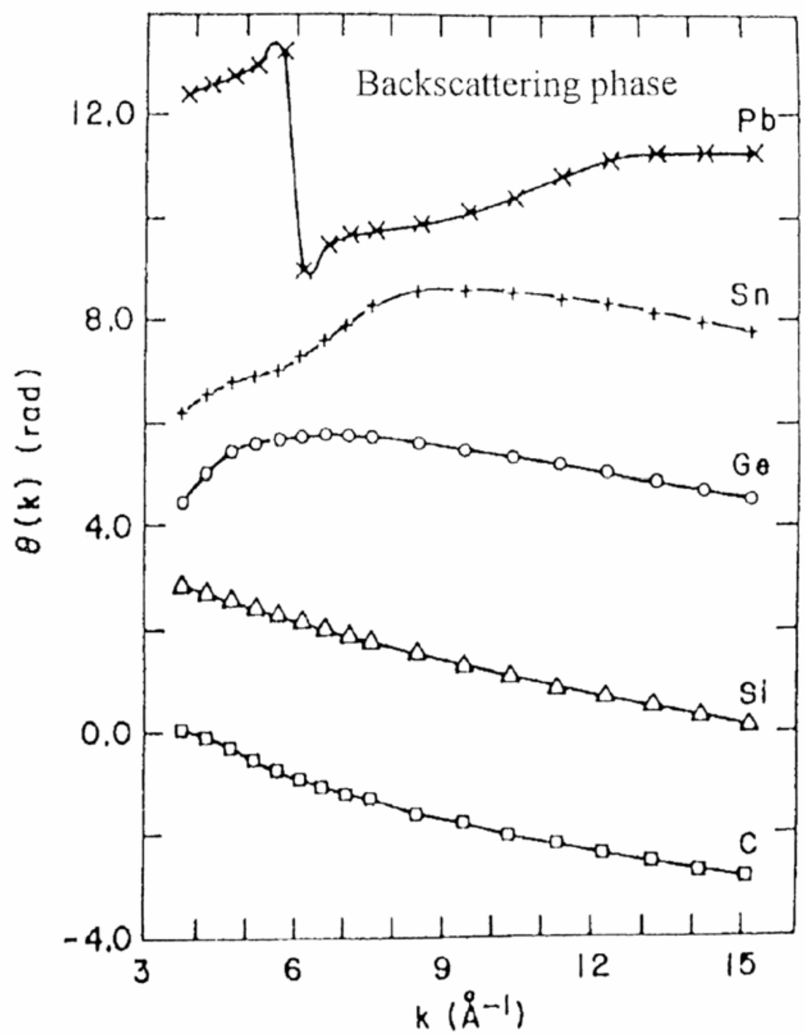

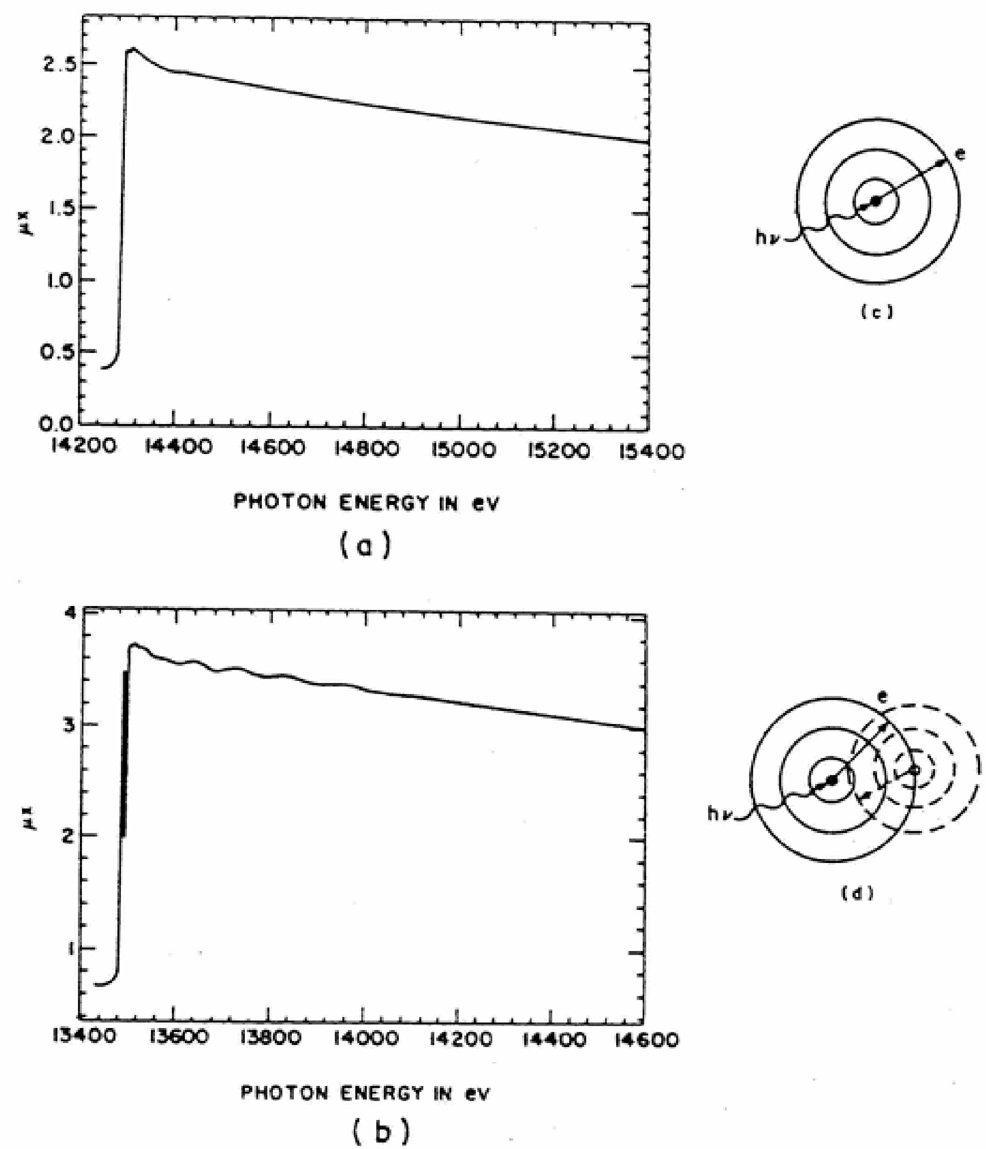

Fig. 2.2. Qualitative rationalization of the absence and presence, respectively, of EXAFS in a monatomic gas such as Kr (a and c) and a diatomic gas such as Br_2 (b and d).

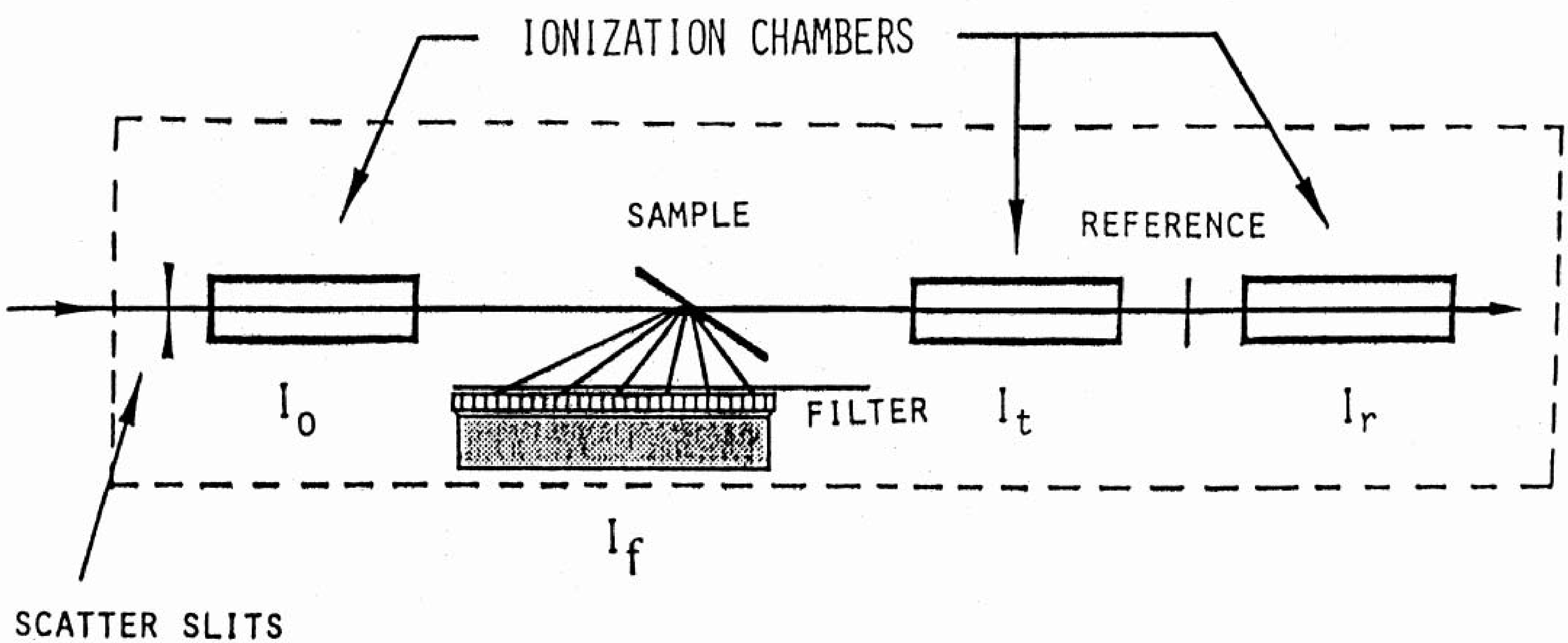

典型的 X 光吸收光譜術實驗配置圖 (其中虛線表示實驗站的輻射屏蔽屋)

Supported Metal Catalyst

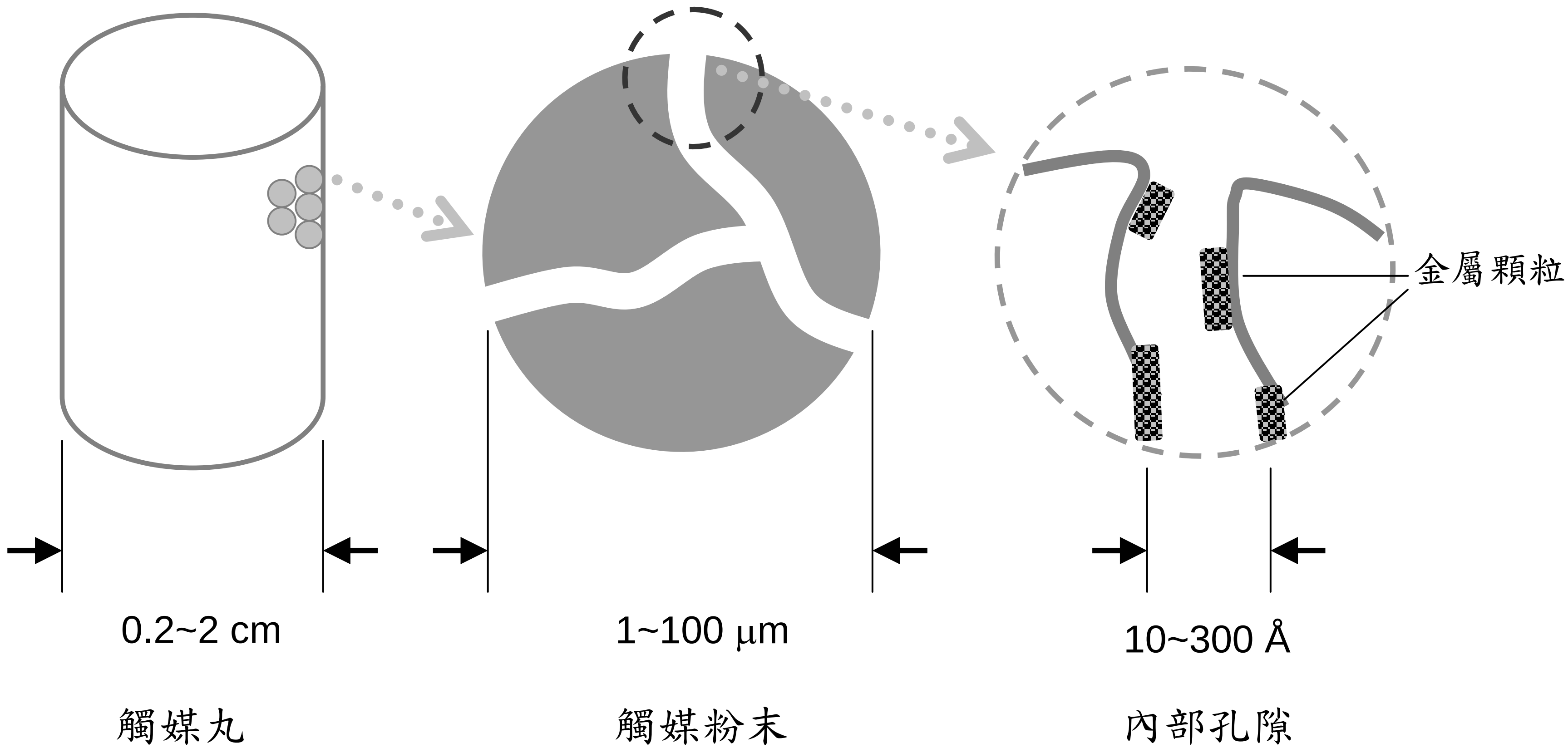

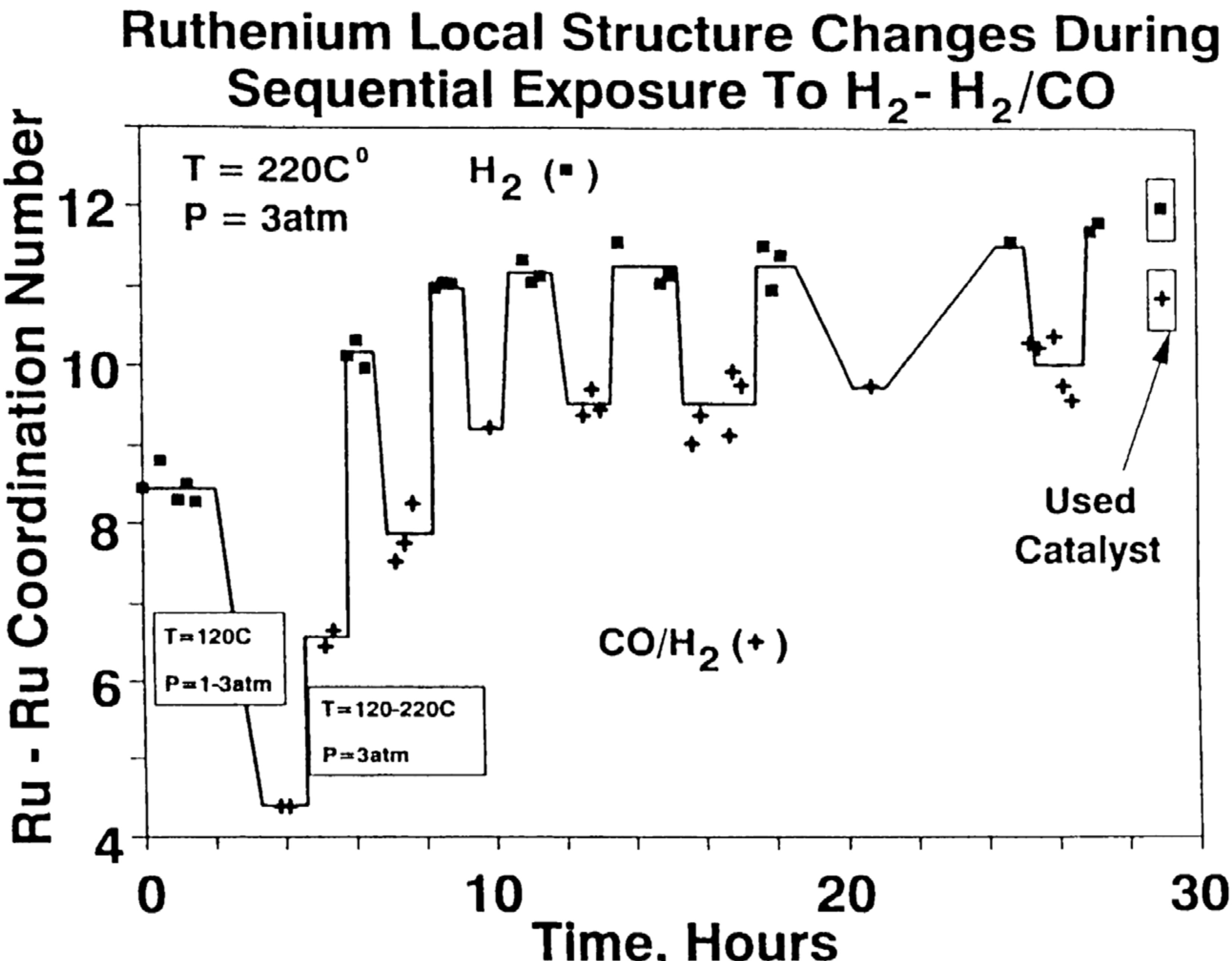
Ruthenium Local Structure Changes During Sequential Exposure To H2- H2/CO
T = 220C0
P = 3atm
H2 (▪)
T=120C
P=1-3atm
T=120-220C
P=3atm
CO/H2 (+)
Used Catalyst
Ru - Ru Coordination Number
Time, Hours
12
10
8
6
4
0
10
20
30

Fuel Cell Research

燃料電池工作示意圖

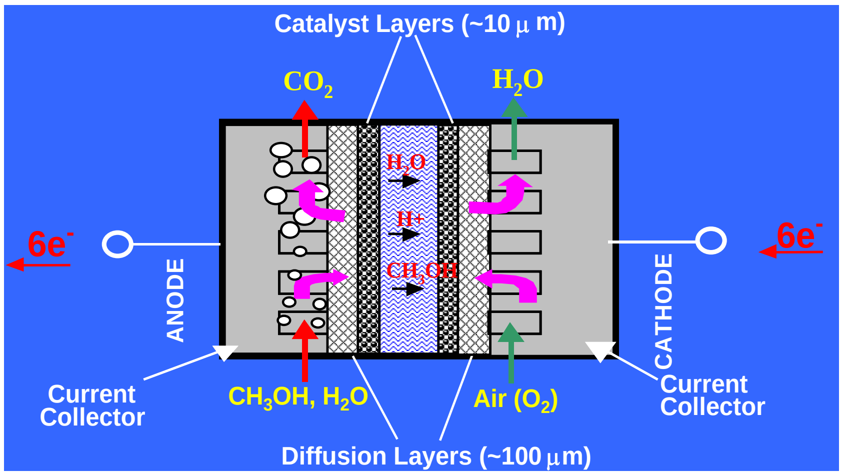

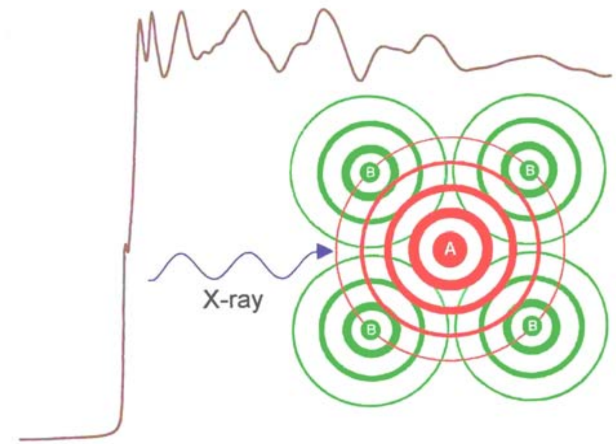

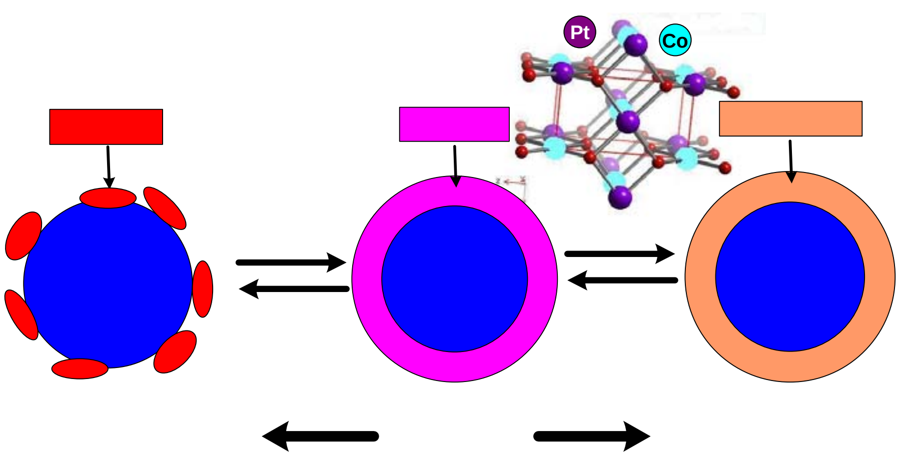

利用X光吸收光譜分析可獲知材料中特定元素的電子性質與局部幾何結構，並經由充放電過程之臨場量測，直接與電化學行為建立關聯性，成為改進電極材料特性之依據。

Atomic Scattering Factors of X-rays

Atomic scattering factor ***f (q,E)= f₀(q) + f'(E)+ i f"(E)***

Intensity

$$I \approx \left|F_{HKL}\right|^2 = \left|\sum_i f_i \cdot e^{i\vec{q}_{HKL}\cdot\vec{r}_i}\right|^2$$

X-ray Anomalous Scattering Factor of PT

$$f(E) = f_0 + f'(E) + i\,f''(E)$$

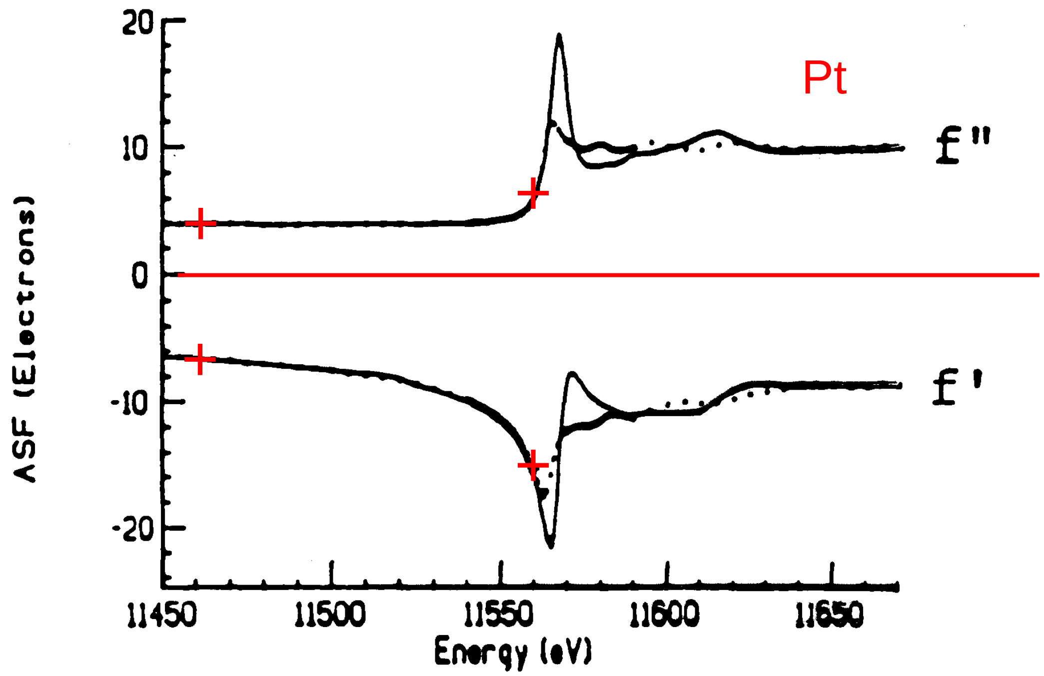

Element-specific diffraction pattern <u>or</u> X-ray partial structure factor

Anomalous X-ray Scattering

Atomic scattering factor $f\,(q,E) = f_0(q) + f'(E) + i\,f''(E) = f_1 + i\,f_2$

Intensity $$I \approx \left|F_{HKL}\right|^2 = \left|\sum_i f_i \cdot e^{i\vec{q}_{HKL}\cdot\vec{r}_i}\right|^2$$

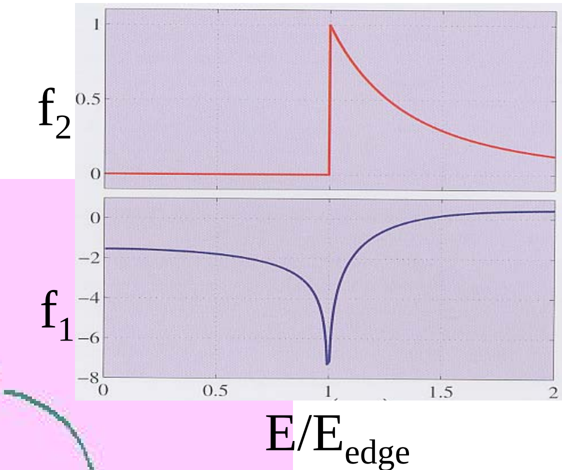

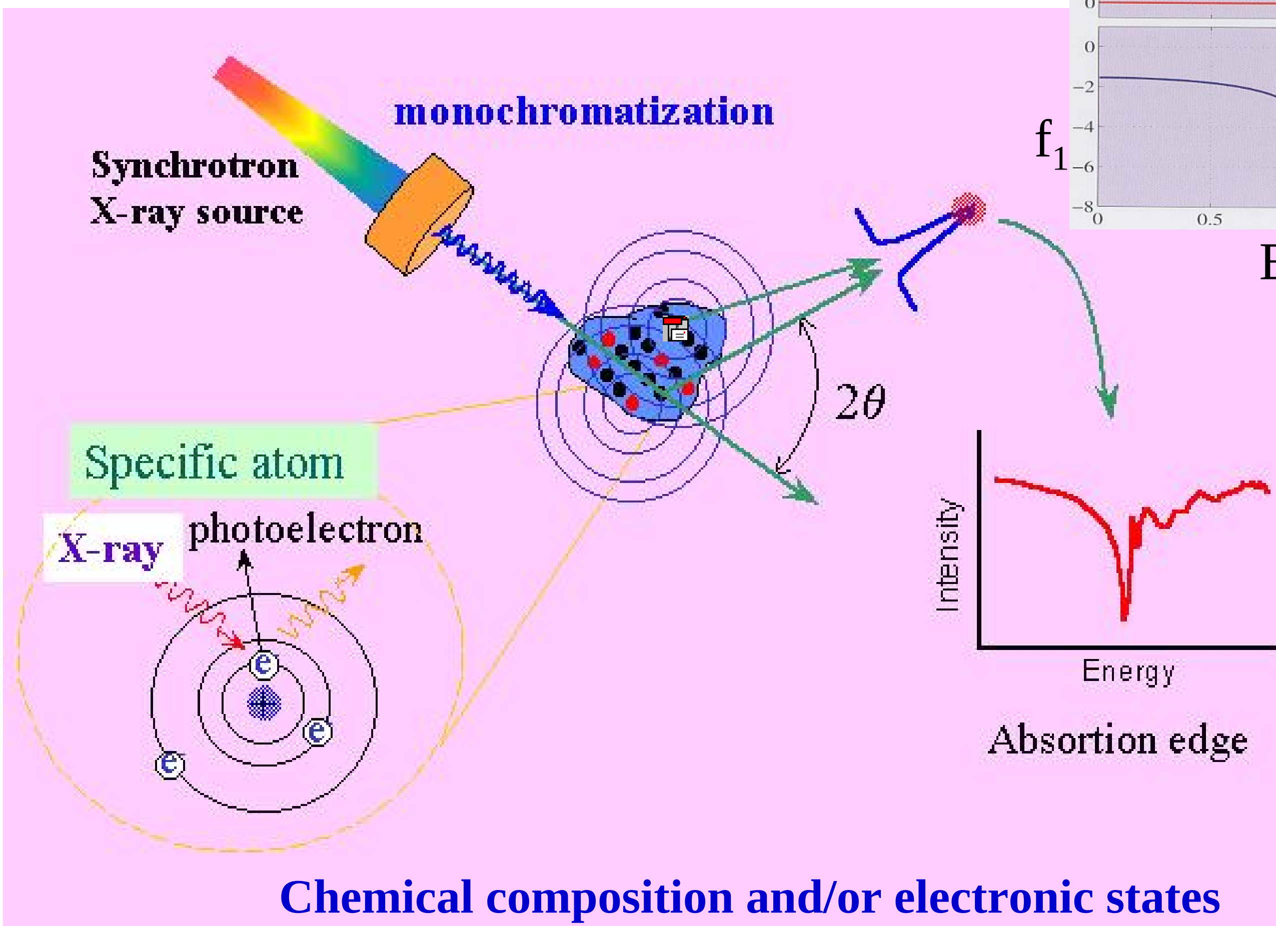

Uncapped $In_{0.5}Ga_{0.5}As$ Quantum Dots

Grown by MEE

$In_{0.5}Ga_{0.5}As$ 5.85 ML/ Ga (4x2)

grown @ 520^{o}C 0.7 ML/s.

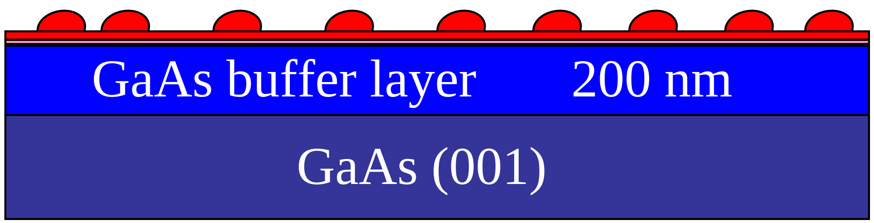

AFM image

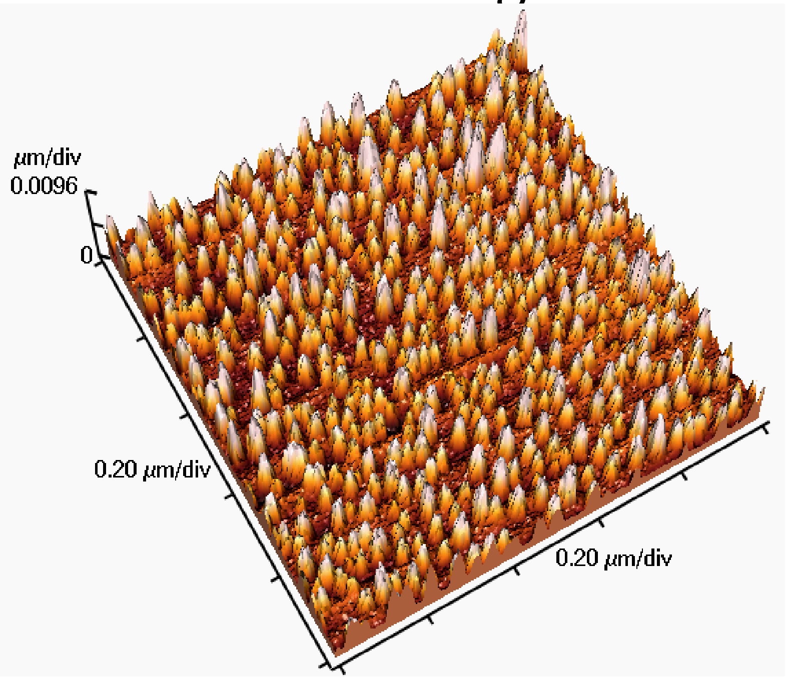

a_{InAs} = 6.0583Å
a_{GaAs} = 5.65325Å

misatch = 7.2 %

n ~ 5 x10^{10} cm^{-2}

J. Cryst. Growth, 175/176, 777 (1997).

A New Era of Biological Science

The Atoms: God's Creation

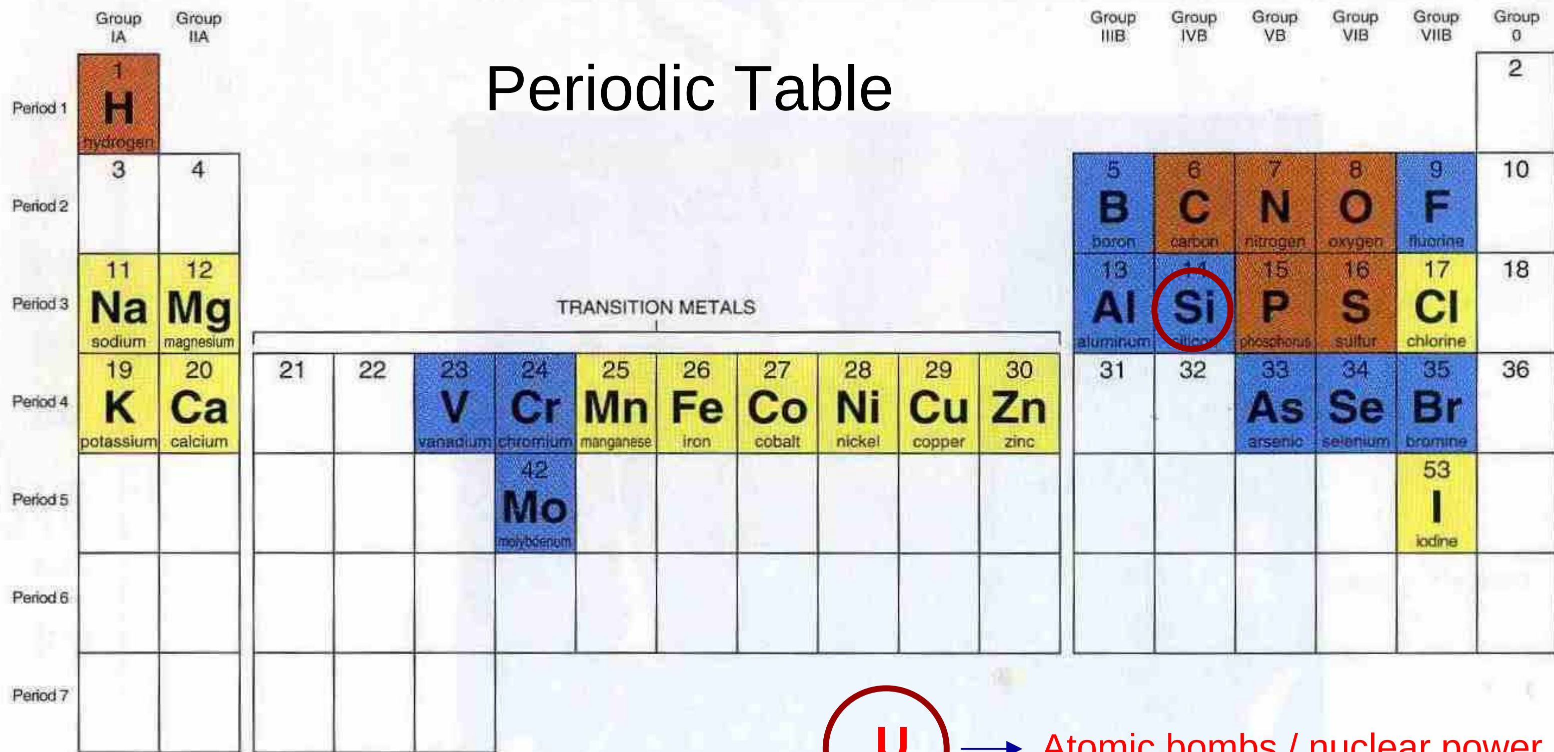

U
92

→ Atomic bombs / nuclear power plants

FIGURE 1.3

The biochemist's periodic table. Elements in red are present in bulk form in living cells and are essential for life. Those in yellow are trace elements that are very likely essential. Those elements in blue may be essential.

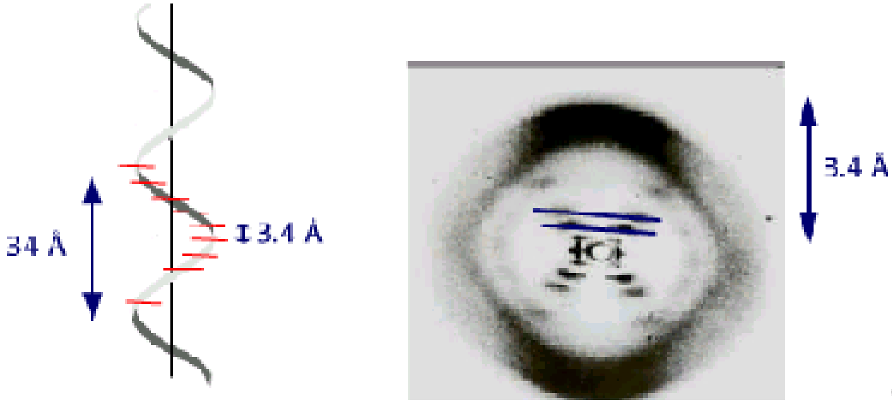

X-ray Diffraction of DNA

(Rosalind Franklin)

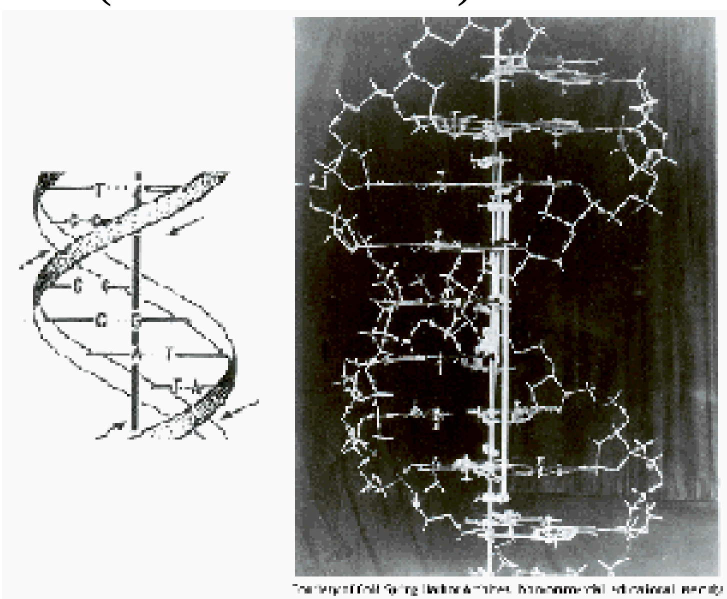

Double Helix DNA

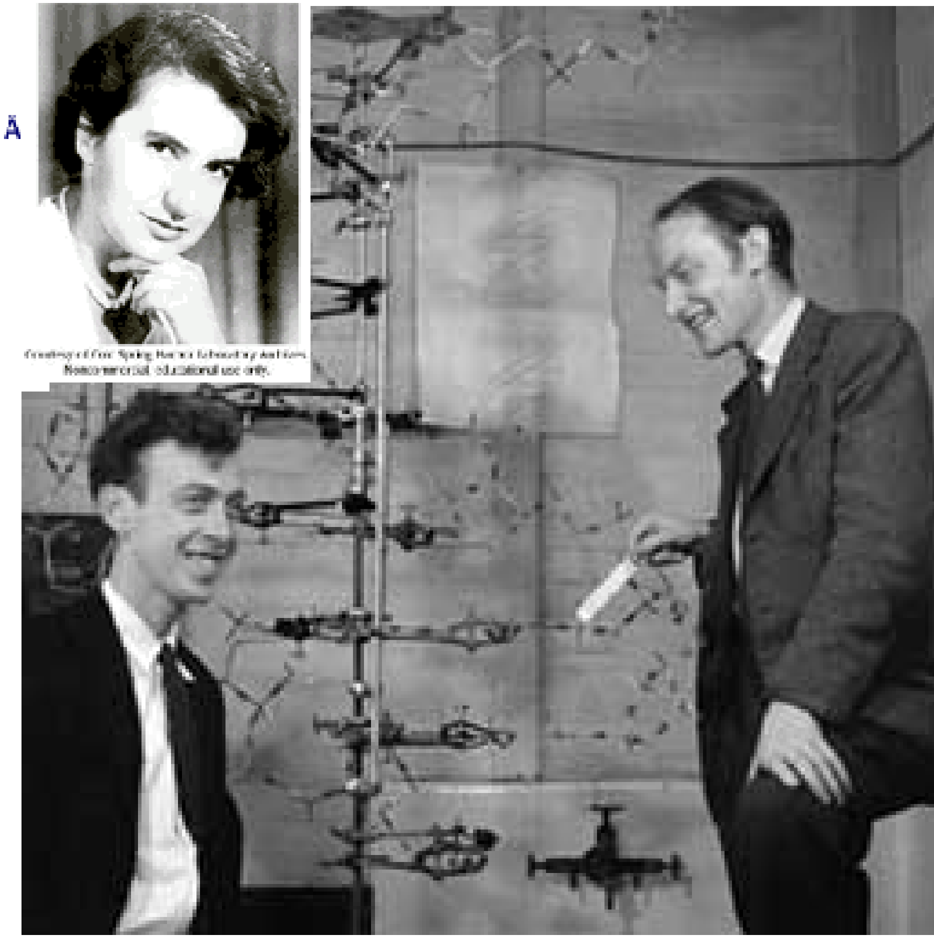

Watson, Crick and their DNA model in 1953.

華生與克里克(1962年諾貝爾生醫獎得主)

利用X光繞射發現DNA雙螺旋結構

Source：James D. Watson , Francis Crick .
Molecular Structure of nucleic acids, **Nature**, 171(1953):737-138

DNA Structure

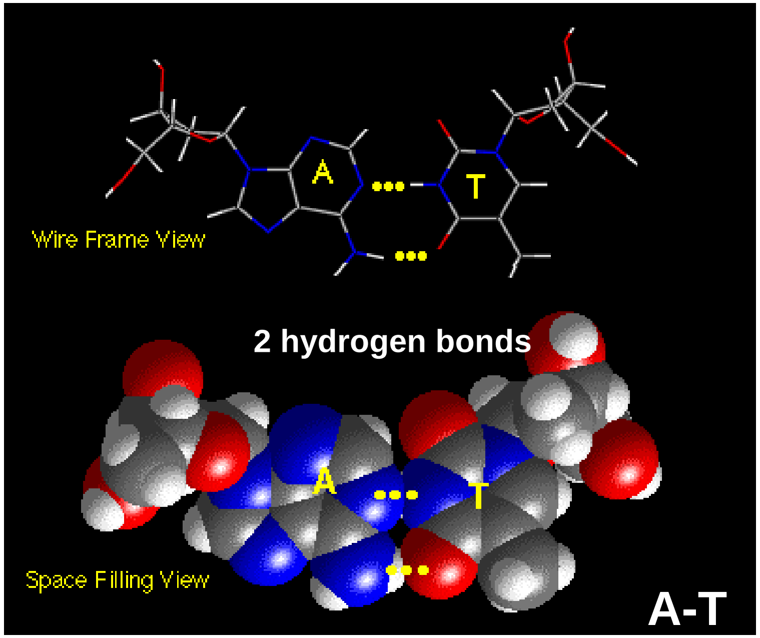

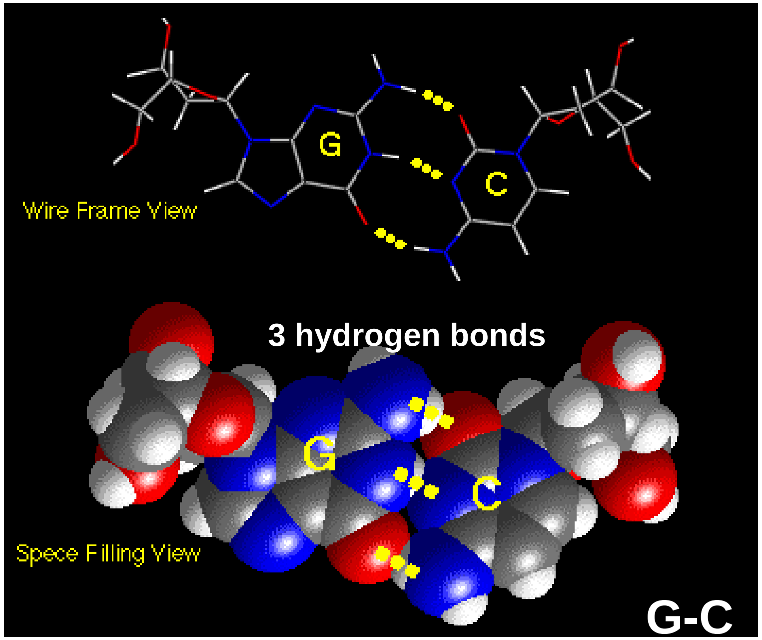

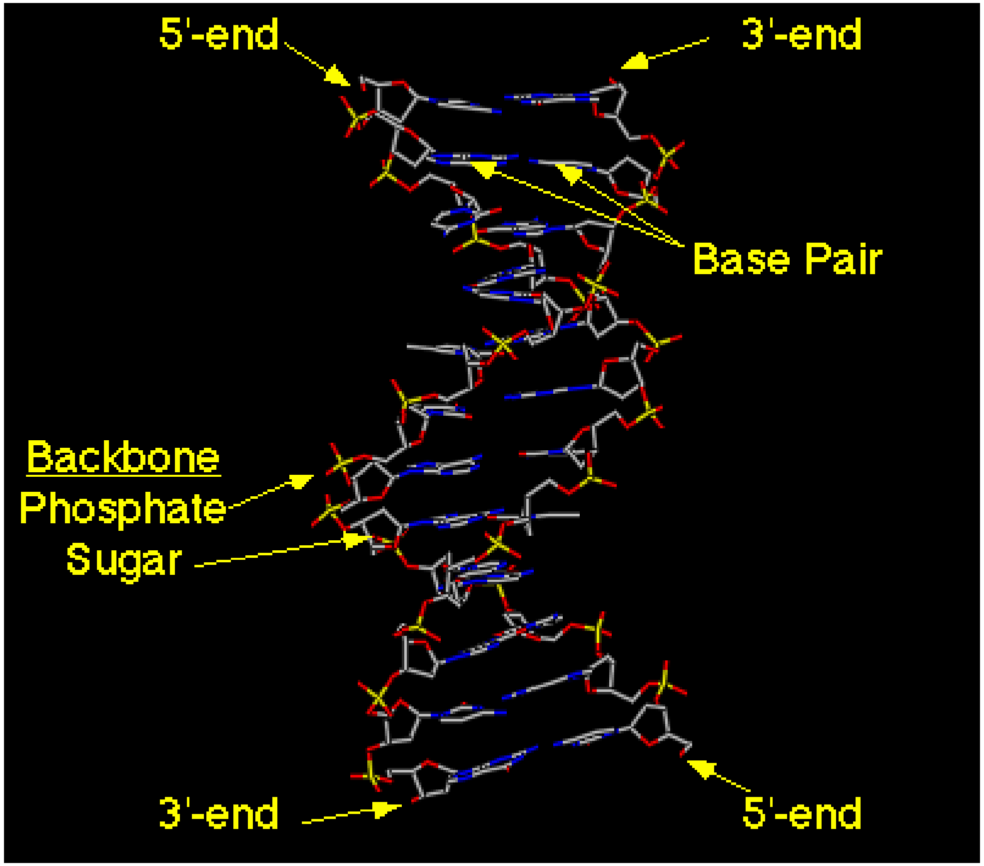

Double helix DNA of 12 base pairs

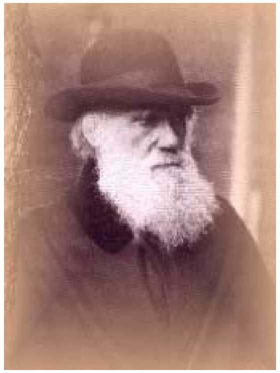

Charles Darwin

The Genome Map of living matters

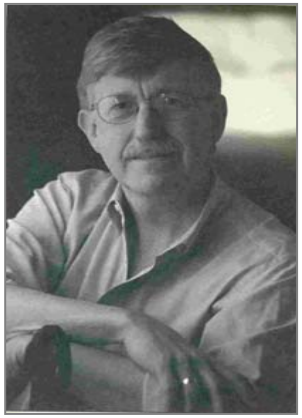

Francis Collins

DECIPHERING GOD'S INSTRUCTION BOOK

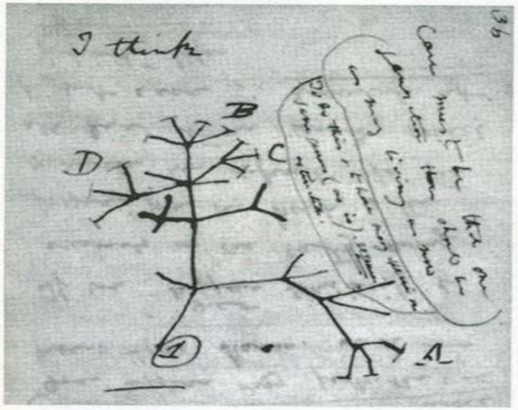

descent from a common ancestor with natural selection operating on randomly occurring variations. At the level of the genome as a whole, a computer can construct a tree of life based solely upon the similarities of the DNA sequences of multiple organisms. The result is shown in Figure 5.1. Bear in mind that this analysis does not utilize any information from the fossil record, or from anatomic observations of current life forms. Yet its similarity to conclusions drawn from studies of comparative anatomy, both of existent organisms and of fossilized remains, is striking. Second, within the genome, Darwin's theory predicts that mutations that do not affect function (namely,

129

The Language of God

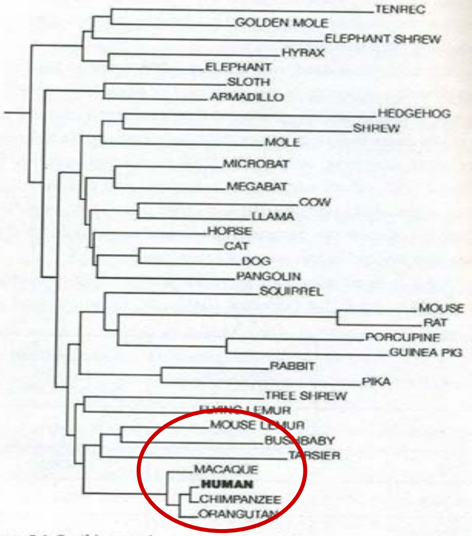

Figure 5.1 On this page is a current view of the tree of life, where relationships between different mammalian species are inferred solely by a comparison of their DNA sequences. The length of the branches represents the degree of difference between species—thus the DNA sequences of mouse and rat are more closely related than those of mouse and squirrel, and the DNA sequences of human and chimpanzee are more closely related than those of human and macaque. Opposite, for an interesting historical comparison, is a page from Darwin's 1837 notebook, where the words "I think" are followed by his own idea of the tree of life that connects different species.

128

From "The Language of God" by F. Collins (Free Press, 2006)

BL13B1 PX Experimental Station
- for drug design

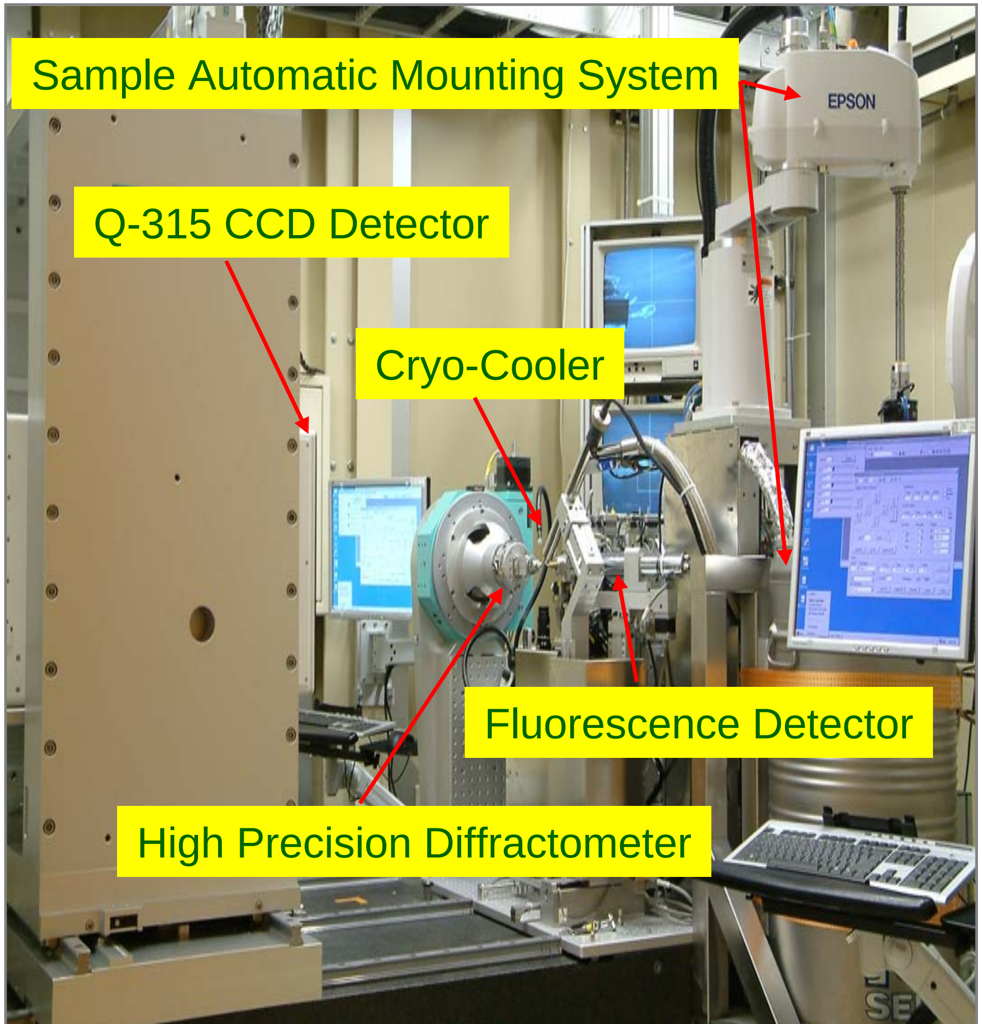

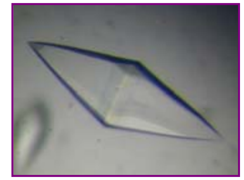

Protein Crystal

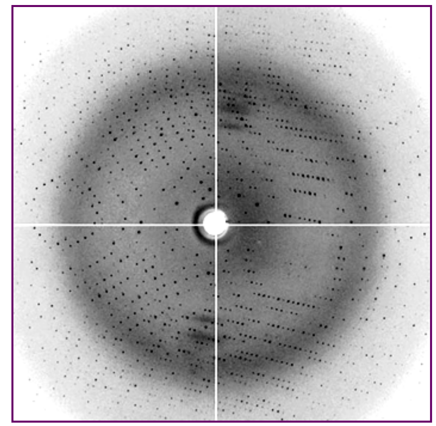

X-ray Diffraction Pattern

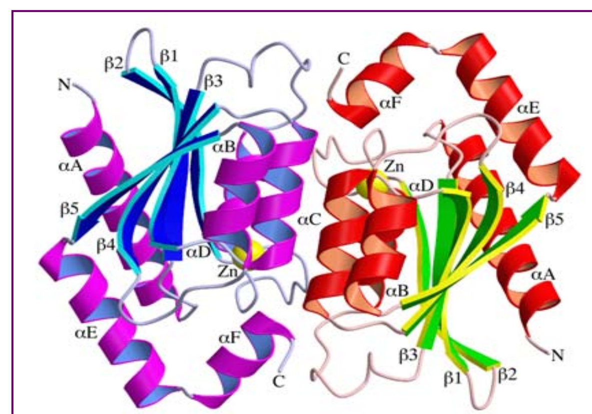

Protein Structure

Structure of SARS 3CL^{pro} with substrate

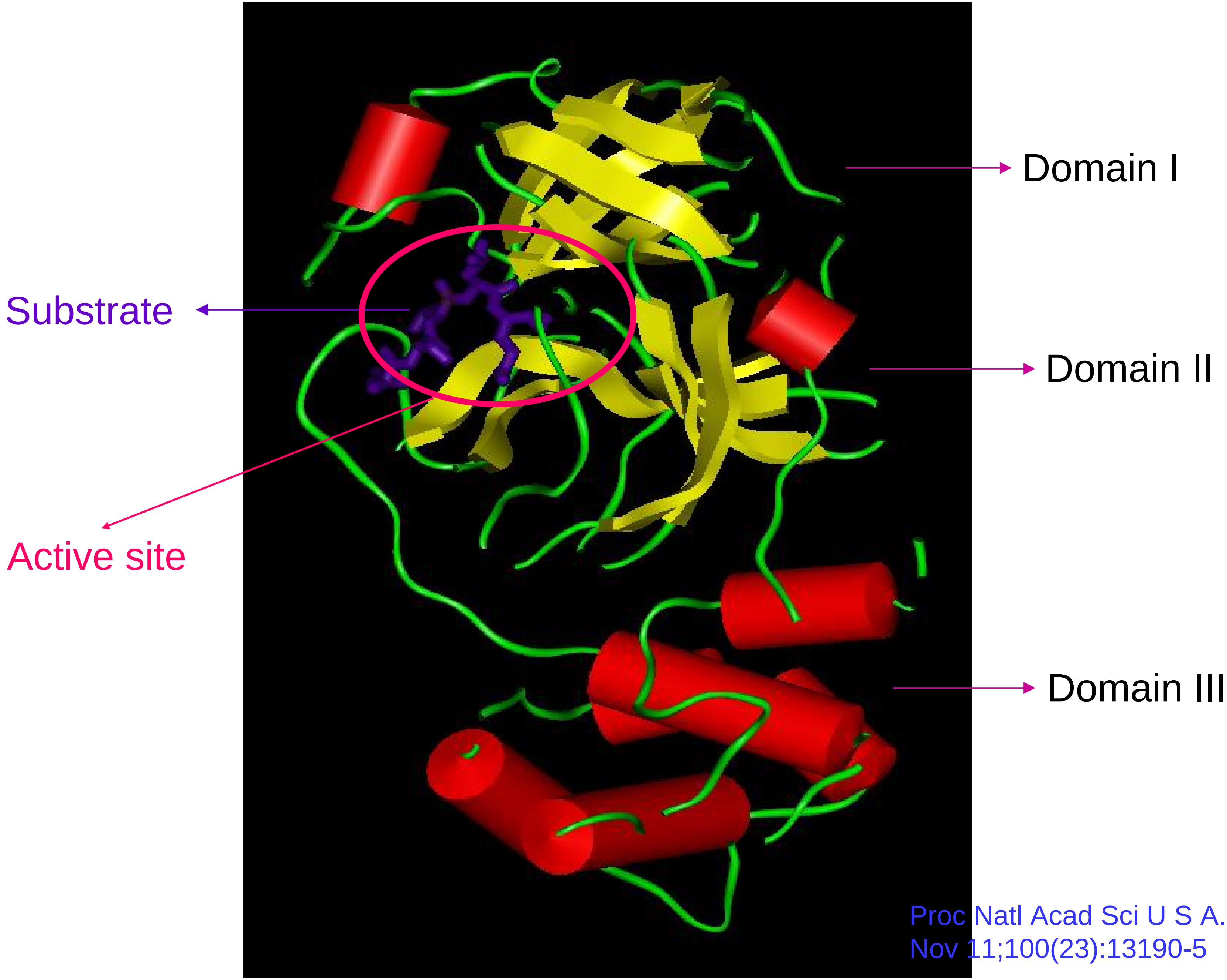

Proc Natl Acad Sci U S A. 2003 Nov 11;100(23):13190-5

Valence States of Condensed Matter

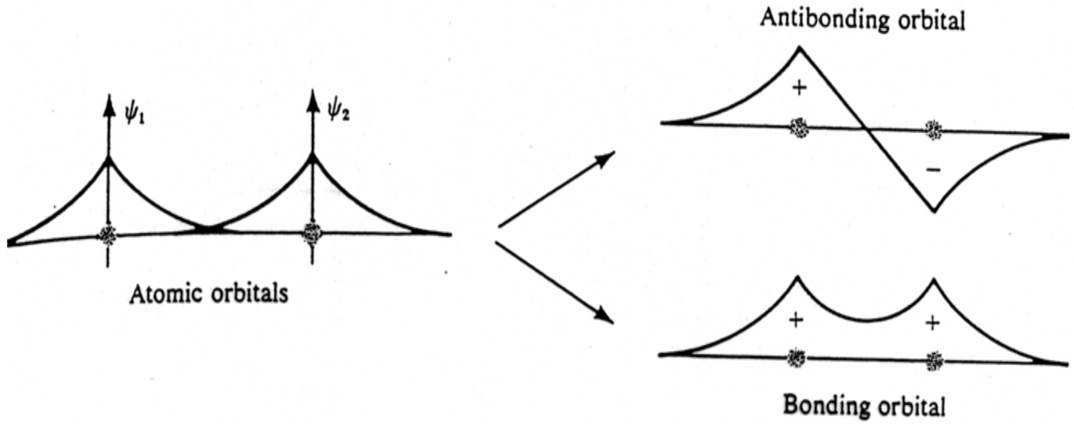
Antibonding orbital
ψ_1
ψ_2
+
−
Atomic orbitals
+
+
Bonding orbital

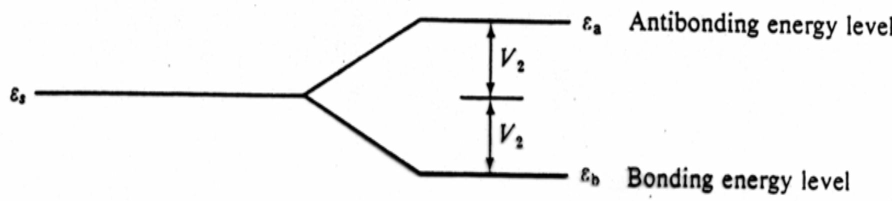
ε_a Antibonding energy level
V_2
ε_s
V_2
ε_b Bonding energy level

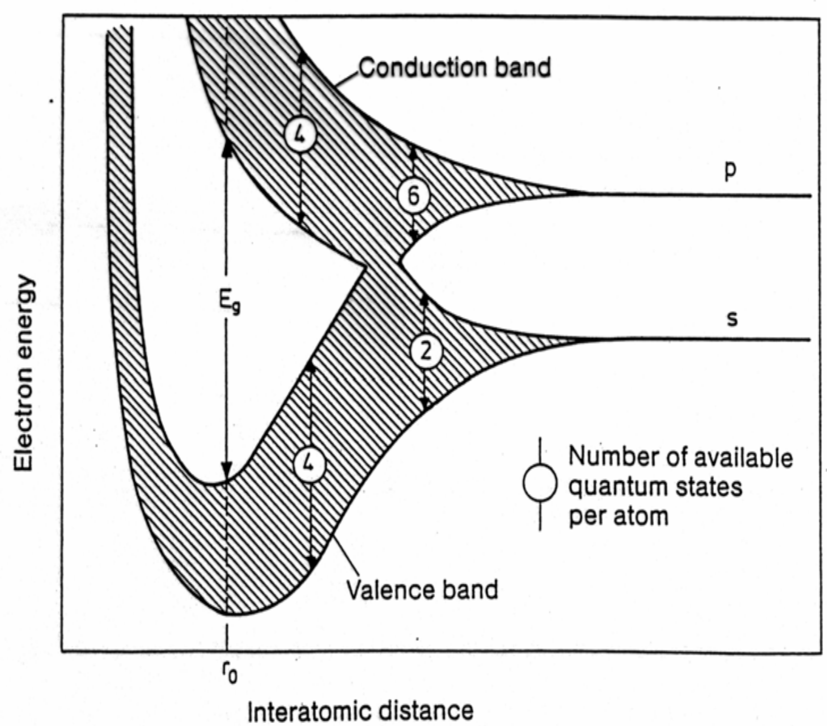
Conduction band
4
6
p
E_g
s
2
Electron energy
4
Number of available
quantum states
per atom
Valence band
r_0
Interatomic distance

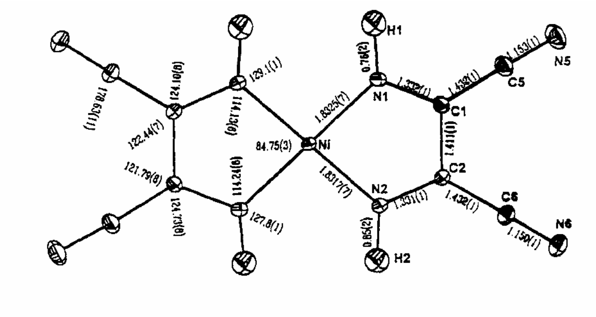

圖一 $Ni(N_4C_4H_2)_2$ 分子結構圖。

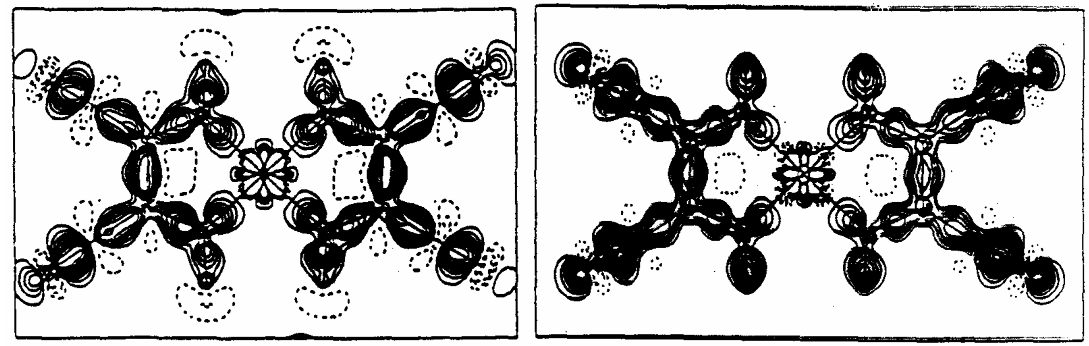

Δρ *M-A, static* Δρ *DFT*

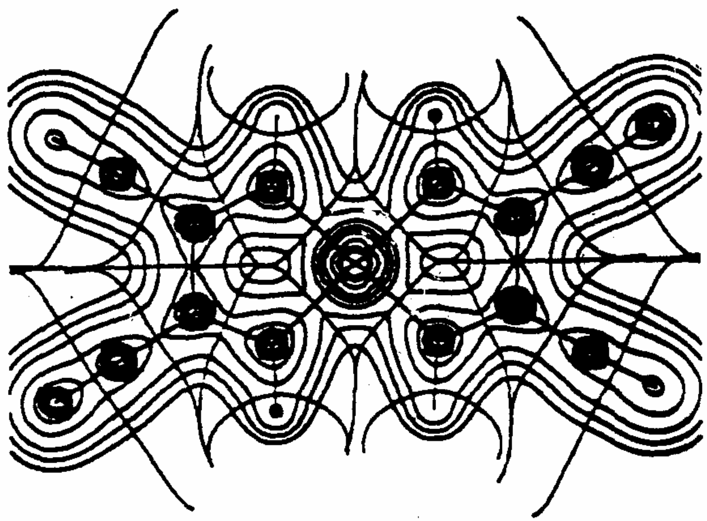

圖六 總電子密度，鍵結路徑及原子範疇。

Courtesy of Y. Wang

Photoelectron Spectroscopy for Valence Structure

1905 Albert Einstein

$$e\,V_{stop} = hf - W$$

Light wave as photon

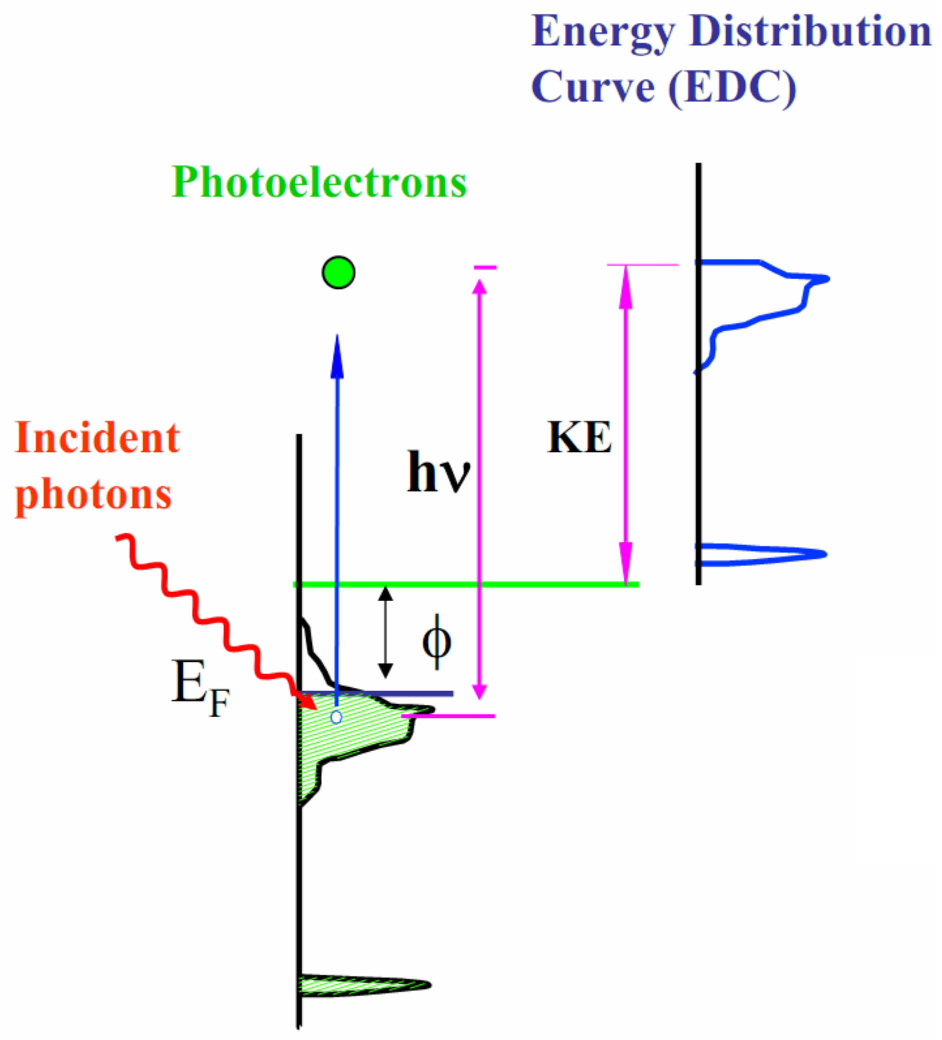

Photoelectron Spectroscopy for Valence Structure

Fermi surfaces

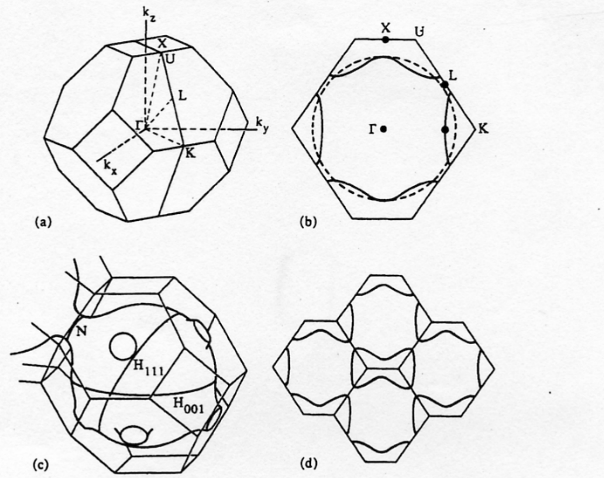

Fig. 10-15 Various aspects of the Fermi surface of Cu. (a) The Brillouin zone of an fcc lattice with some special points labeled. (b) A (110) section of the Brillouin zone. See the text for the meaning of the internal curves. (c) The proposed Fermi surface of Cu. (d) The extended zone picture of a (110) section of the Fermi surface showing the dog bone orbits.

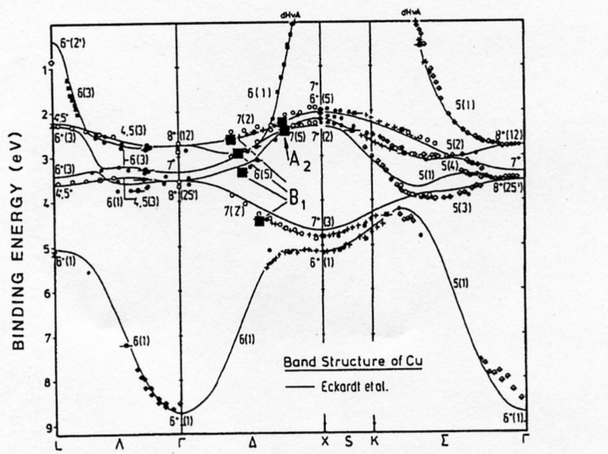

Fig.7.17. Occupied part of the band structure of Cu[7.39] with data points from various sources and a theoretical result [7.53]. Also shown (squares) are the two A_2 points and the four B_1 points from Fig.7.16

$$d\sigma / d\Omega \propto \Sigma \left| \left\langle \Psi_f \middle| \mathrm{A} \bullet \mathrm{P} \middle| \Psi_i \right\rangle \right|^2 \delta\left(E_f - E_i - h\nu\right)$$

Selection rules:

$\Delta l = \pm 1$

$\Delta m_l = 0$ (linearly polarized)

$\Delta m_l = +1$ (L. circularly polarized)

$\Delta m_l = -1$ (R. circularly polarized)

$$k_{//} = \sqrt{2mKE / h^2} \sin\theta$$

Advantages of Soft-x-ray Scattering Spectroscopy

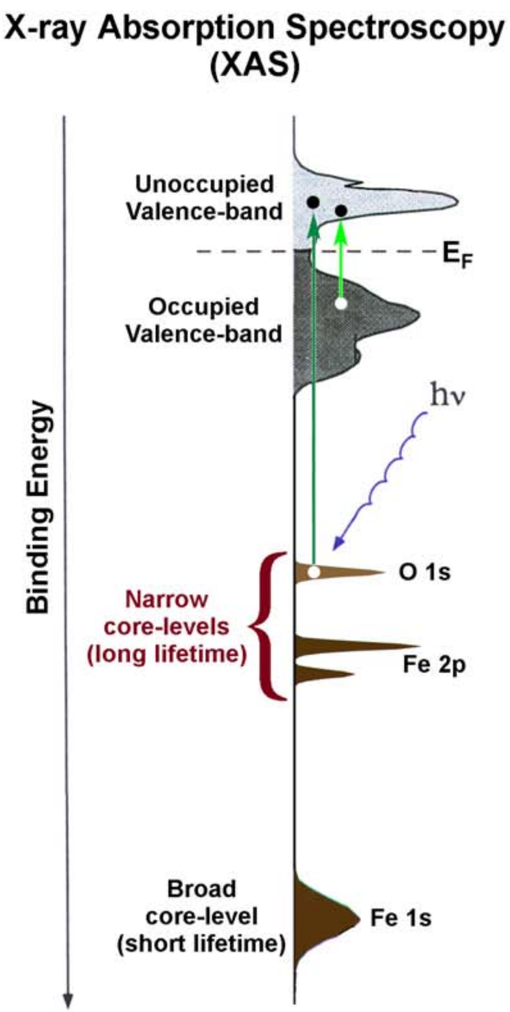

- **Sensitive to spatially order of charge, spin, and orbitals in nanometer scales**

Resonant X-ray scattering

$$\Delta f \sim \sum_i \frac{\langle 0|\vec{\varepsilon}\cdot\vec{r}e^{i\vec{k}\cdot\vec{r}}|i\rangle\langle i|\vec{\varepsilon}'\cdot\vec{r}e^{i\vec{k}'\cdot\vec{r}}|0\rangle}{\hbar\omega-(E_i-E_0-i\Gamma)}$$

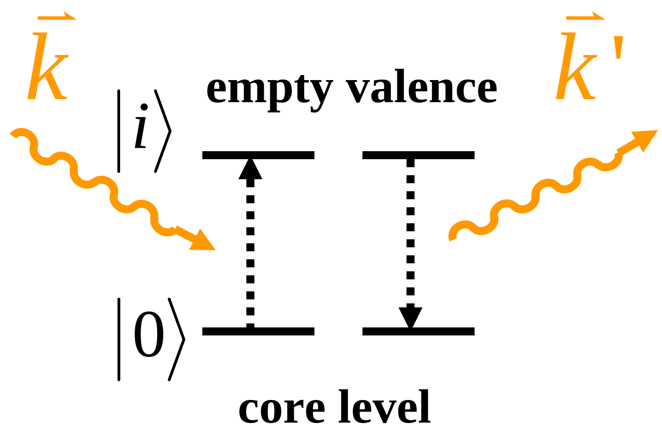

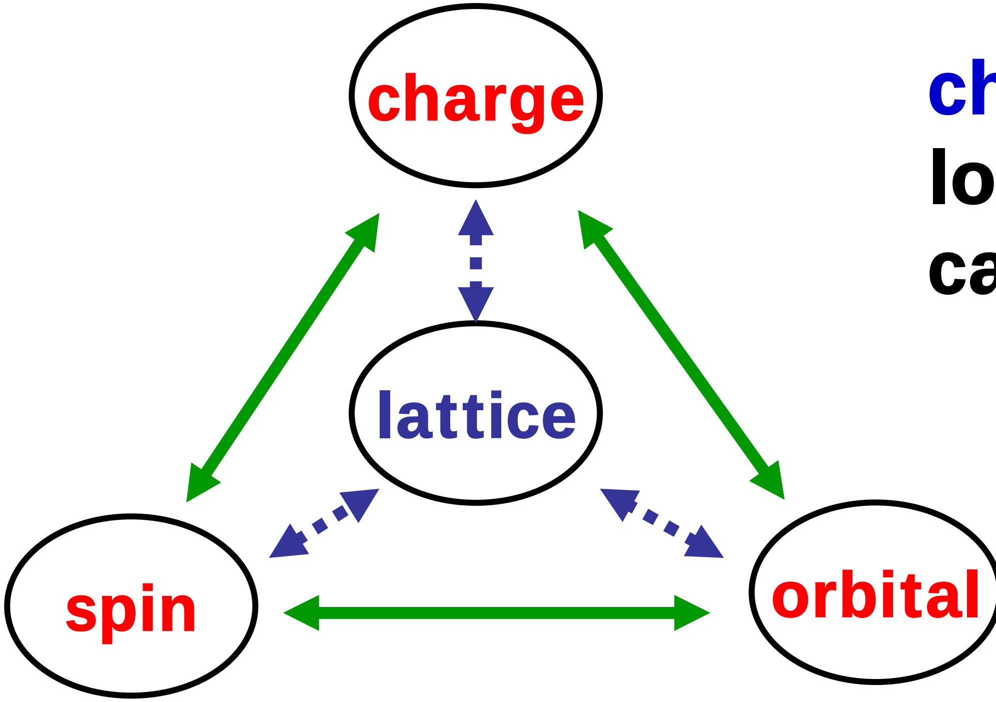

charge ordering: spatial localization of the charge carriers on certain sites

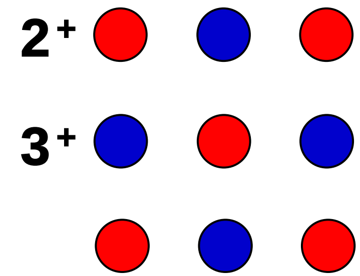

orbital ordering: periodic arrangement of specific electron orbitals

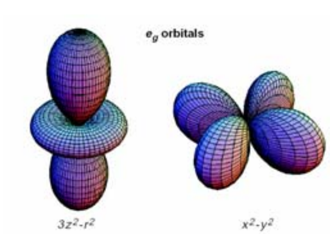

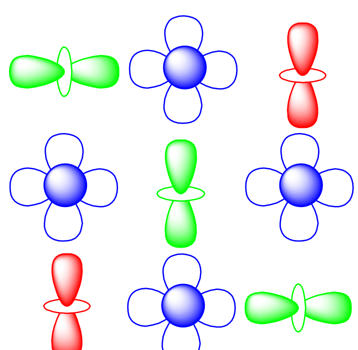

spin ordering: long range ordering of local magnetic moments

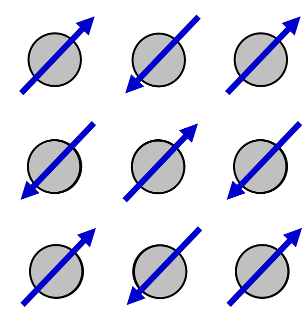

Nano Imaging by X-rays

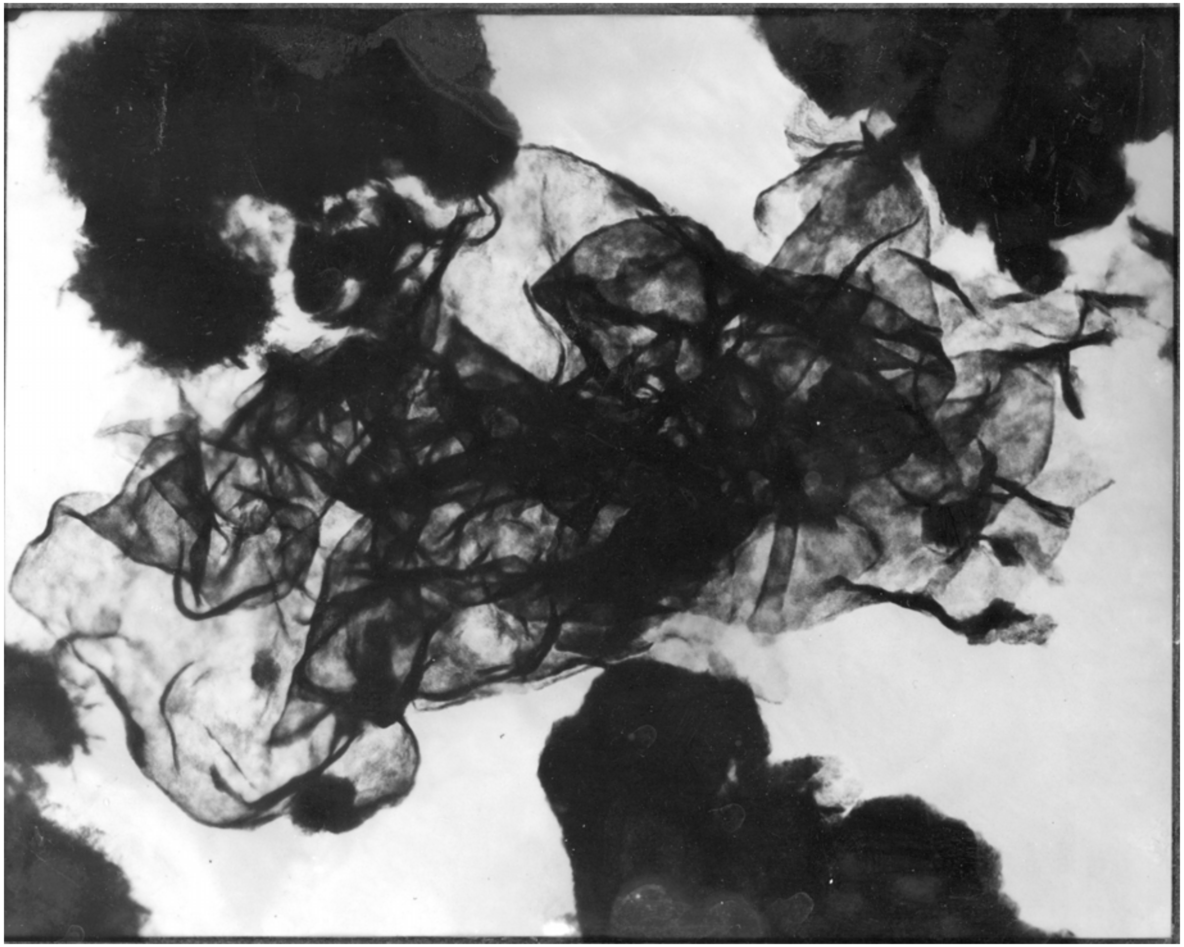

Amorphous MoS_3

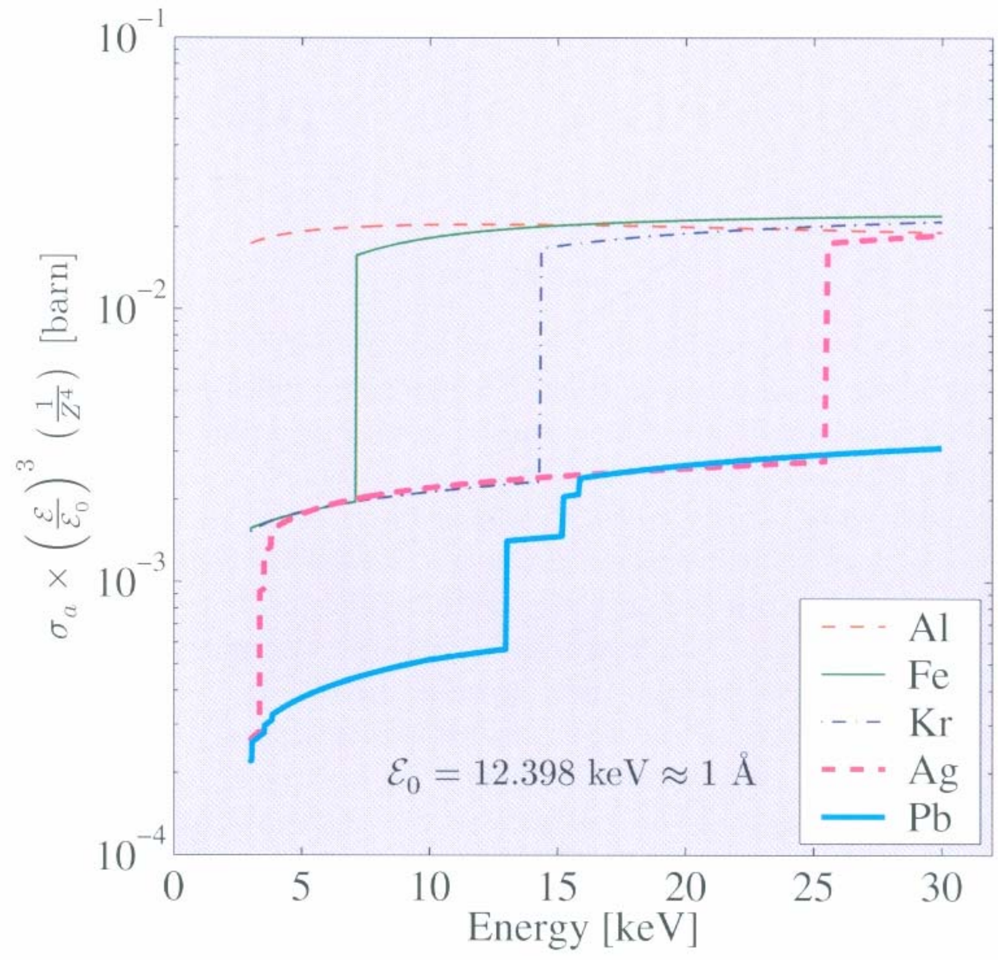

The scaled absorption cross-section as a function of photon energy for a selection of elements. The absorption cross-section per atom, σ_a, has been scaled by dividing it by the atomic number Z to the fourth power, and multiplying it by the photon energy ε to the third power.

From "Elements of Modern X-Ray Physics" by J. Als-Nielsen and D. McMorrow (Wiley 2001)

Zone plate consists of concentric rings (zones) with zone width decreasing with radius

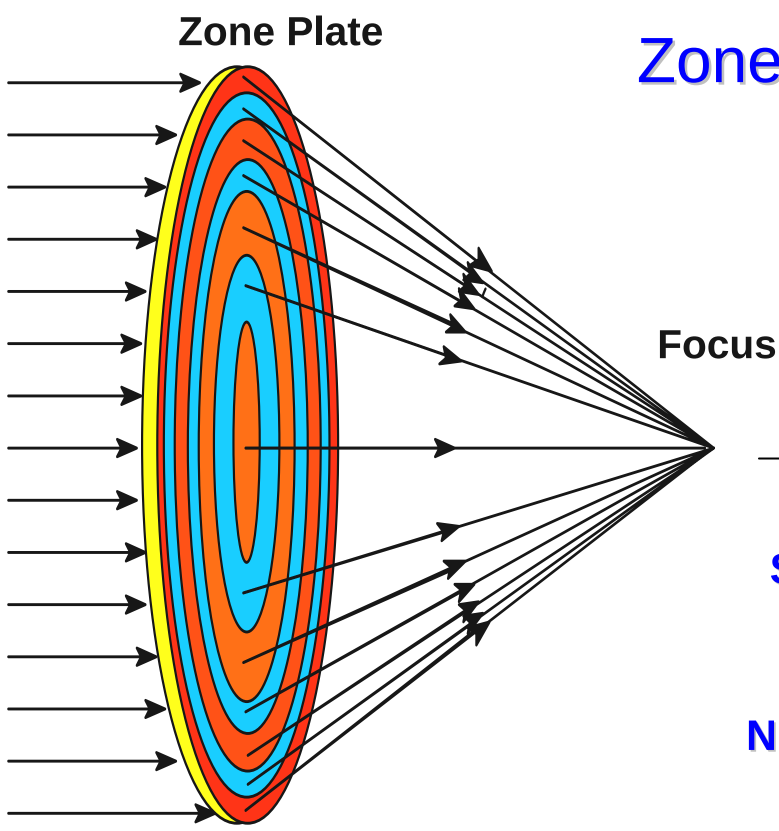

Zone Plate Equations

f : focal length
n : zone index
λ : wavelength
m : diffraction order
r : radius of the zone plate
dr_n: outermost zone width

Zone Radius	$r_n = (n f \lambda)^{1/2}$
Spatial Resolution	$d_m = 1.22 dr_n / m$
Focal Length	$f_m = 2 r\, dr / (m \lambda)$
Numerical Aperture	$NA = \lambda / (2\, dr)$

When NA <<1, the ZP can be treated like an ordinary refractive lens, i.e., $1/q + 1/p = 1/f$ and $M = p/q$.

Nano-TXM at NSRRC

Phase Ring

Zone Plate

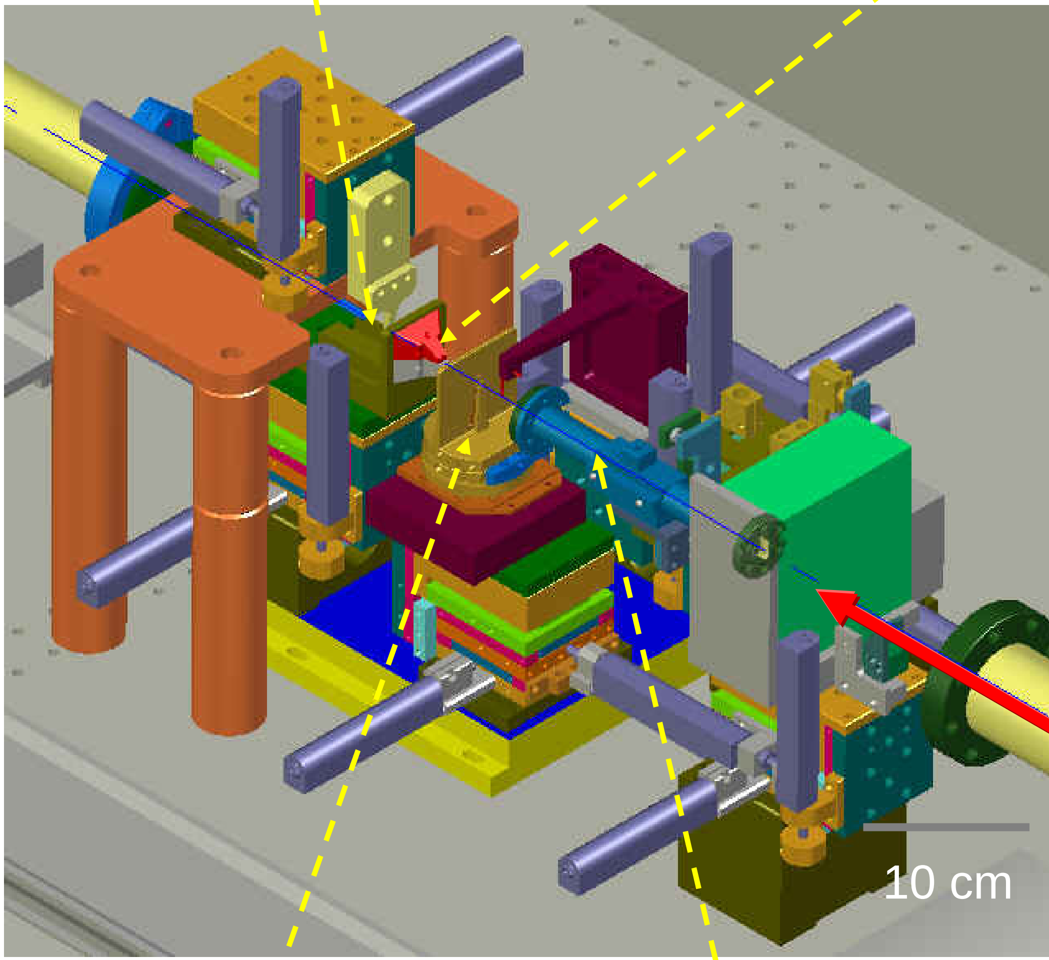

Sample Stage

Condenser Tube

Nanotomography comes of age

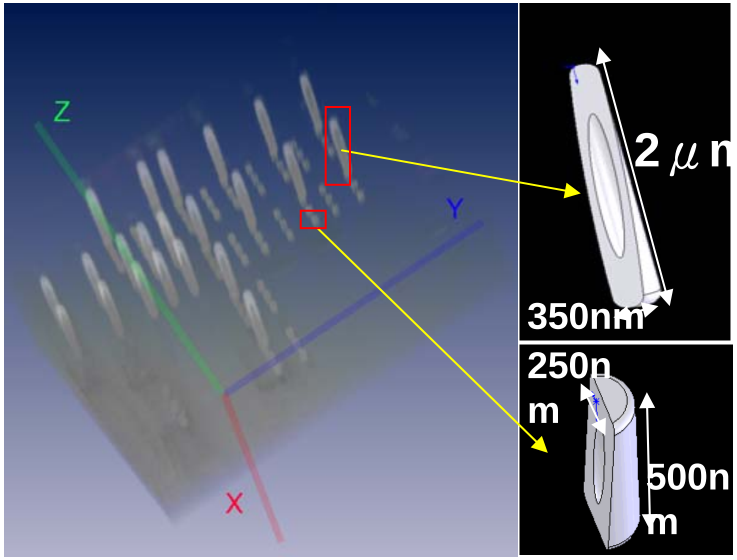

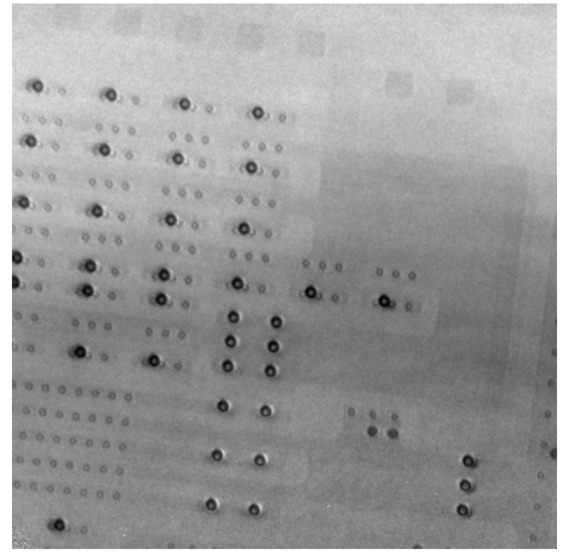

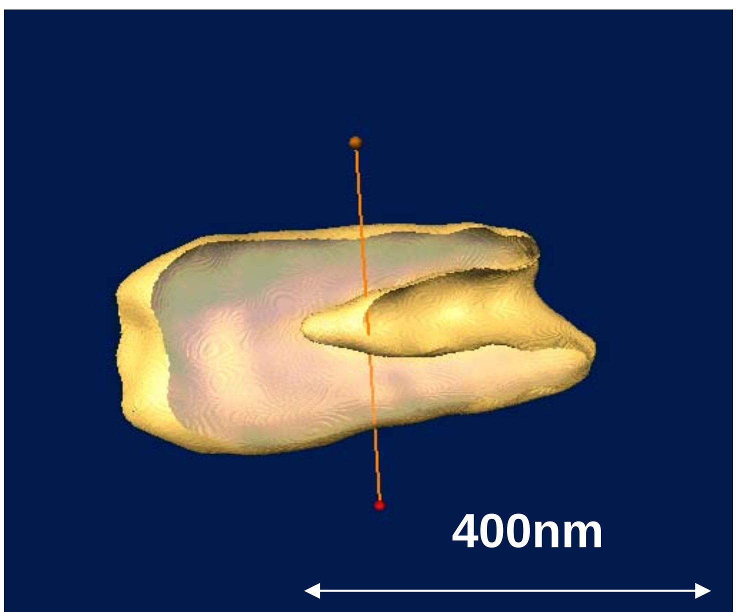

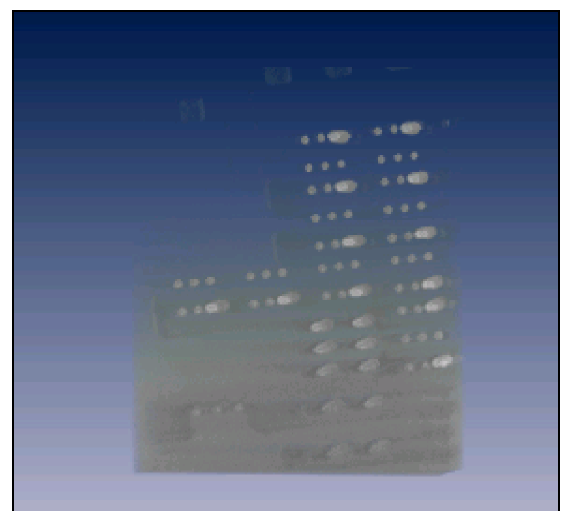

APL 88, 241115 (2006)

「Light」

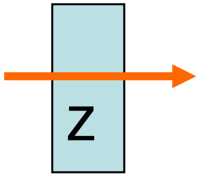

Refraction index : $n = 1-\delta-i\beta$

$$E(z)=E_0 e^{-i2\pi(-\delta-i\beta)\, z/\lambda} = E_0 e^{i2\pi\delta z/\lambda\, -2\pi\beta z/\lambda}$$

$$I(z) \sim |E(z)|^2 \sim I_0 e^{4\pi\beta z/\lambda}$$

Phase Problem

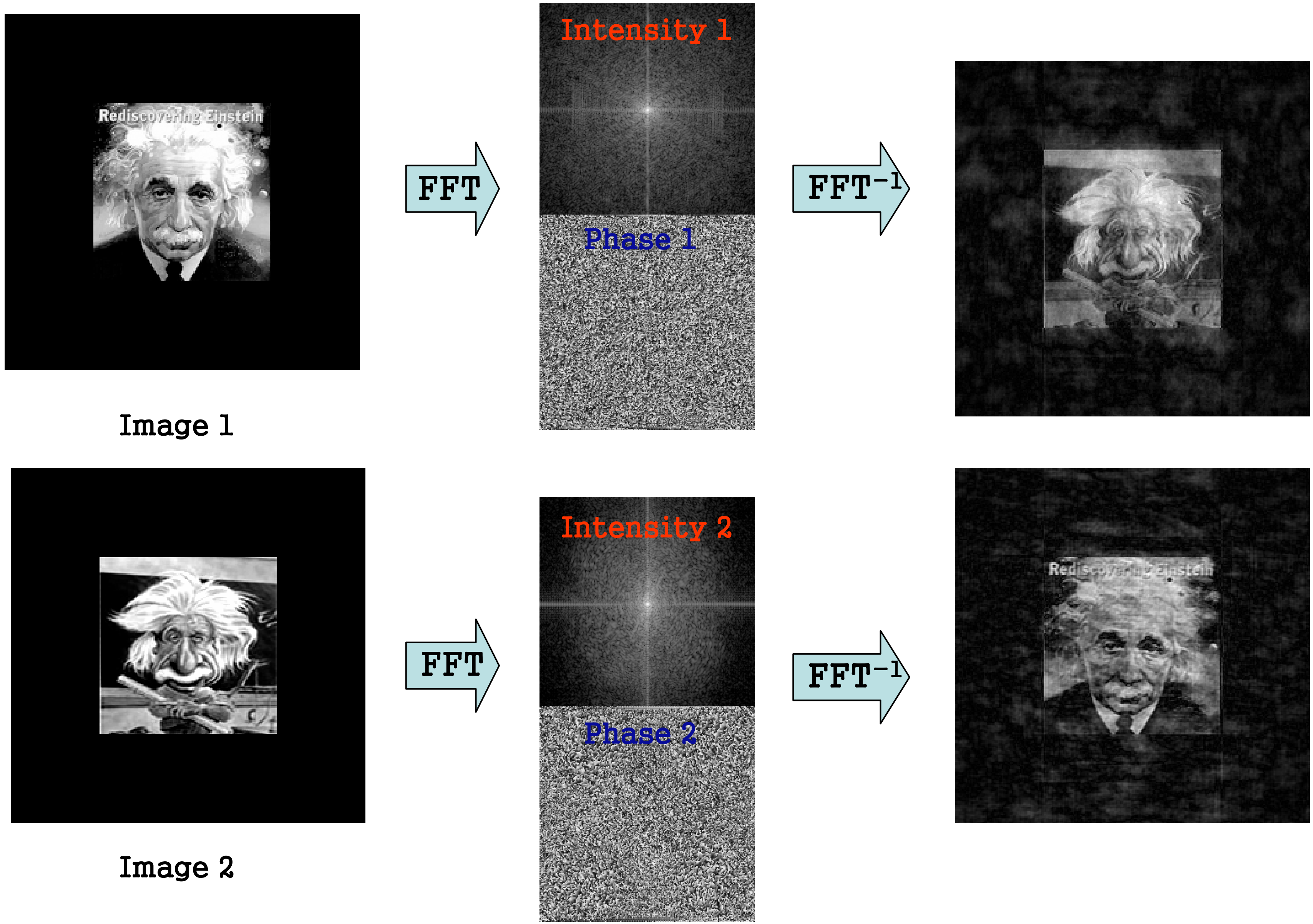

Wilhelm Röntgen @1894

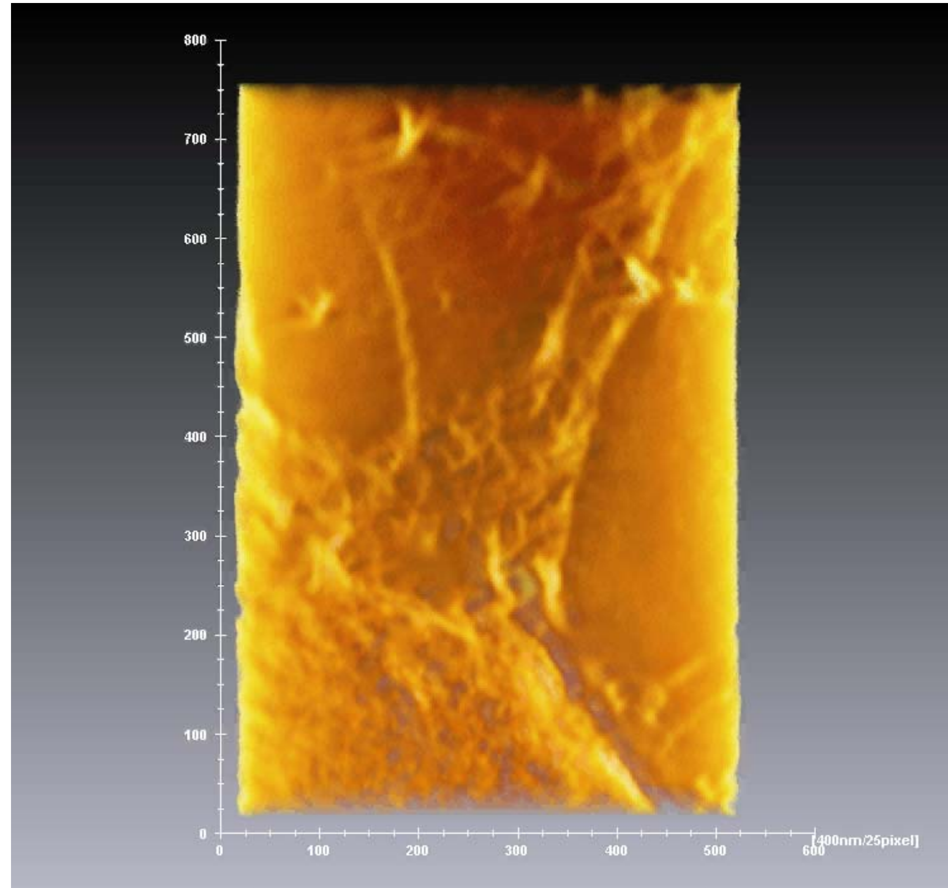

8 μ m

Lung ancer cell
(NSRRC)

Solution of Phase Problem by Coherent Diffraction Imaging

Coherent wave field propagation

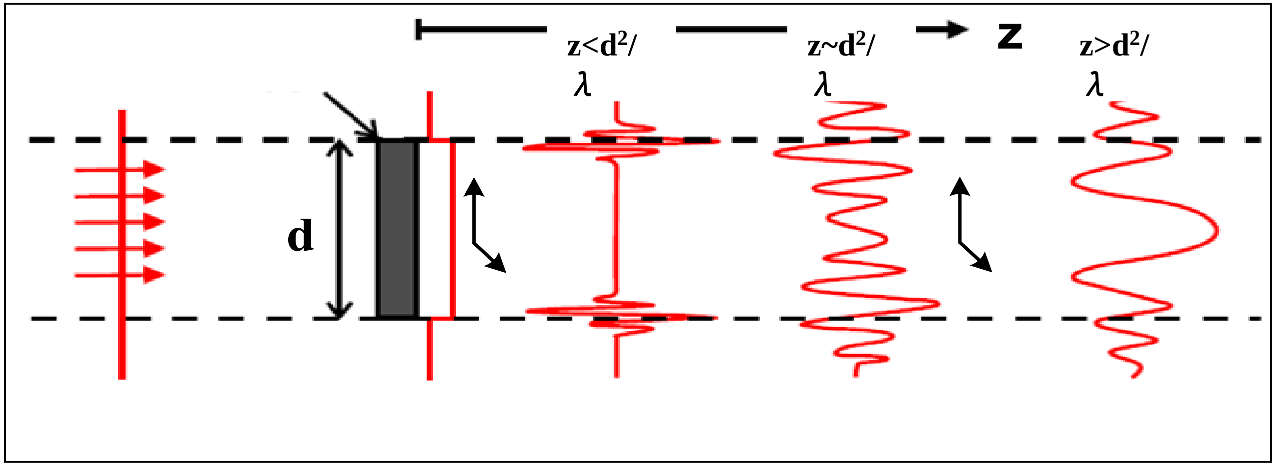

d – sample size;
λ – wavelength;
z – distance from sample

Kinematic approximation

In the Fraunhofer region *complex wavefield* is proportional to the Fourier transform of:
- projected electron density (X-ray)
- projected Coulomb potential (e^-)

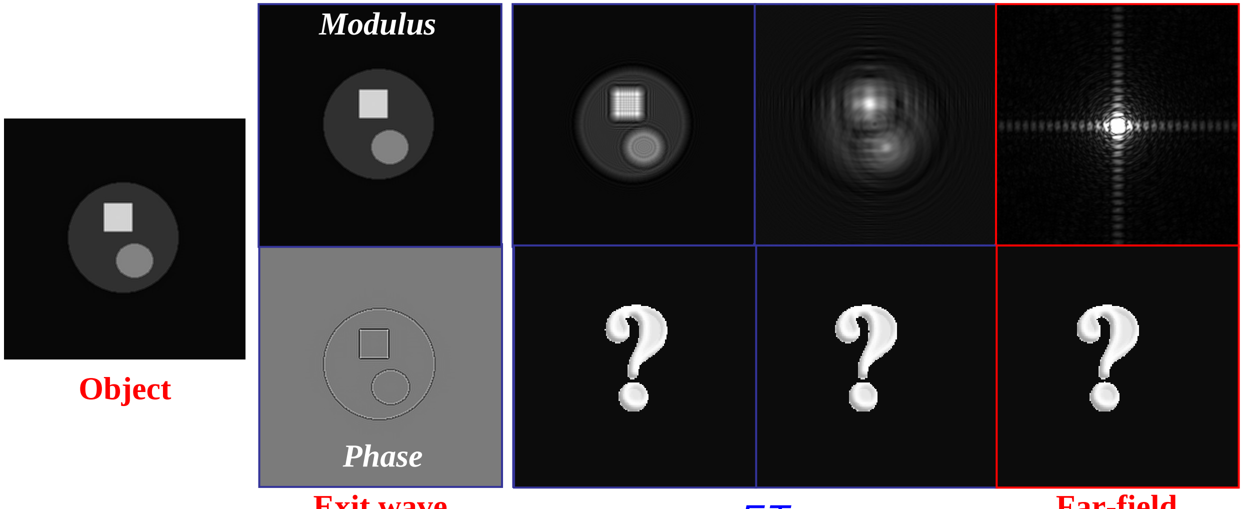

$$\Psi(x,y) \underset{FT^{-1}}{\overset{FT}{\rightleftarrows}} \tilde{\Psi}(u,v)$$

z=0

Phase problem

Detectors measure only diffracted intensity and the phase is lost.

$$I(u,v) = \left|\tilde{\Psi}(u,v)\right|^2$$

Solution of Phase Problem by CDI

Real space

$$\rho(x,y) = \int F(q_x,q_y)\exp\left(-i2\pi(xq_x + yq_y)\right)dq_x dq_y$$

Fourier space

$$F(q_x,q_y) = \int \rho(x,y)\exp\left(i2\pi(xq_x + yq_y)\right)dxdy$$

$$I_{\exp}(q_x,q_y) = \left|F(q_x,q_y)\right|^2$$

Solve system of N² nonlinear equations

$$\left|F(q_x,q_y)\right| = \left|\sum_{x=1}^{N}\sum_{y=1}^{N}\rho(x,y)\exp\left[\frac{2\pi i}{N}(q_x x + q_y y)\right]\right|$$

N

N

N² - unknown variables

known < unknown

N² **2N²**

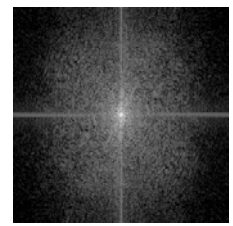

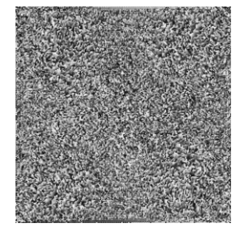

N² - known variables (modulus)
N² - unknown variables (phases)

2N

2N

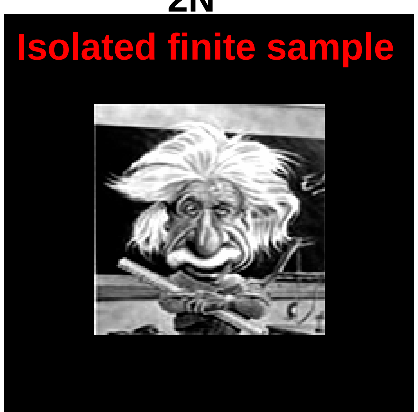

N² - unknown variables
3* N² - known variables (zero)

known > unknown

7N² **5N²**

by Iterative algorithms

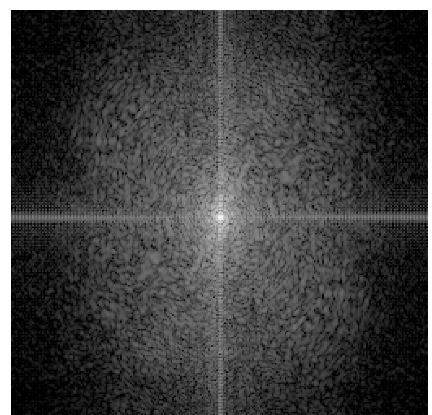

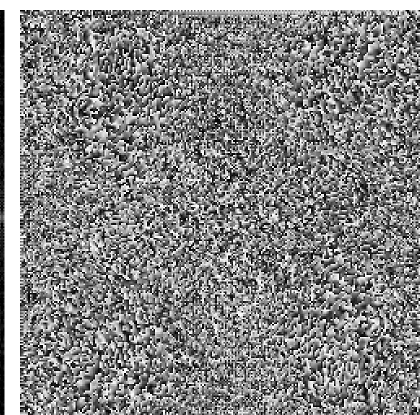

4* N² - known variables (modulus)
4* N² - unknown variables (phases)

CXDI Experiment at BL12XU, SPring-8

-- D. Noh, KIST

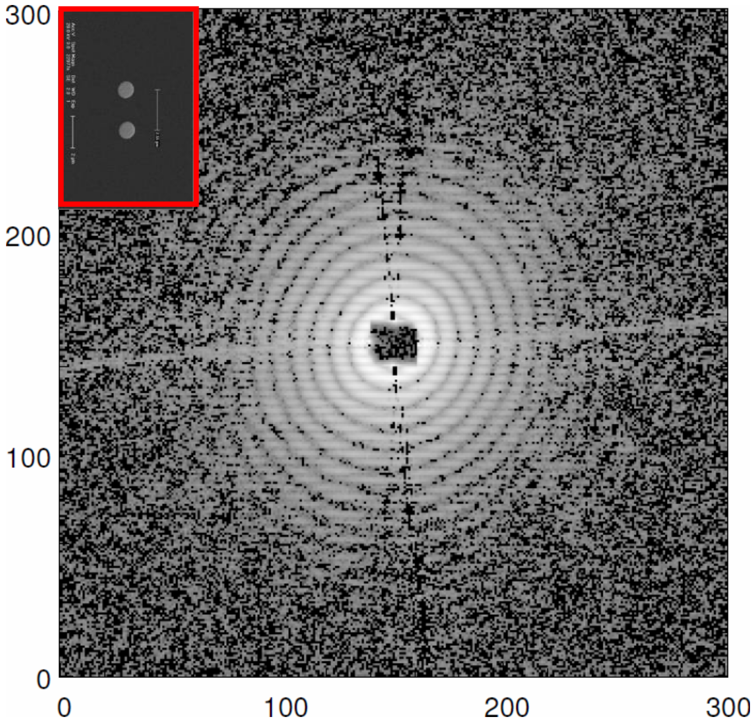

Diffraction Pattern of ~2.5 um spacing Au dots on Si3N4 membrane

- E = 7.5 KeV
- 1.17m Sample to CCD distance
- Centro-symmetry

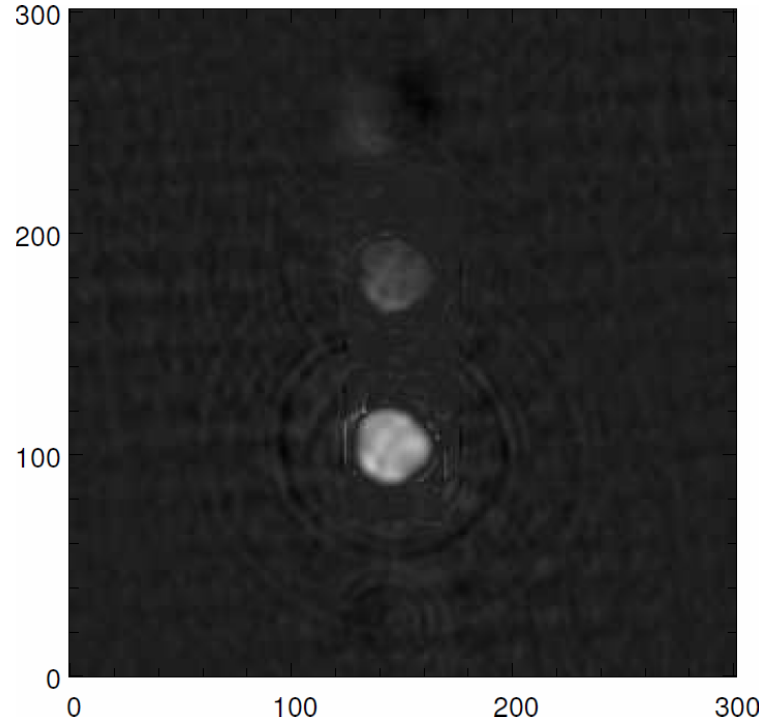

Reconstructed image

- HIO Algorithm (170 iteration)
- Center Patched

Electron Coherent Diffractive Imaging of Single MgO Nano-Particle

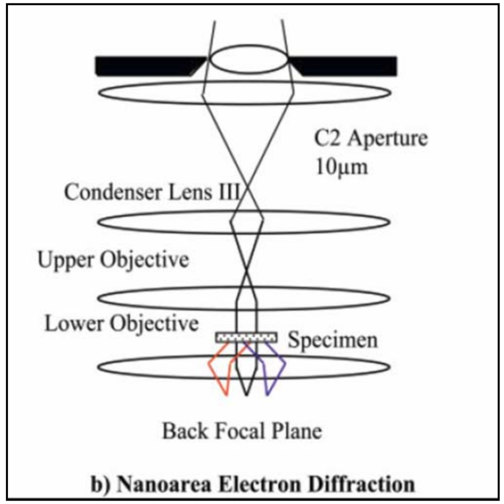

Nano-area electron diffraction (NED)

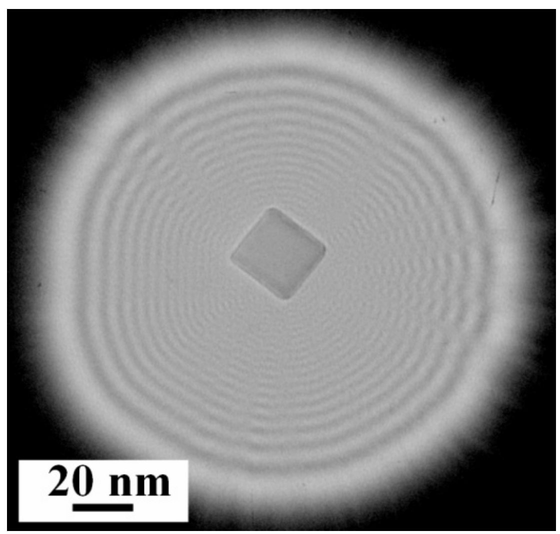

TEM image of the electron nano-probe

Nano-Area Electron Diffraction Experiment

Recorded diffraction pattern from MgO near the [001] zone axis

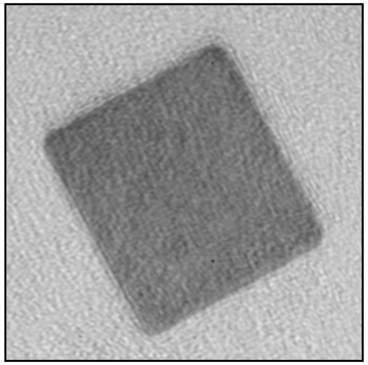

(size ~ 17 nm)

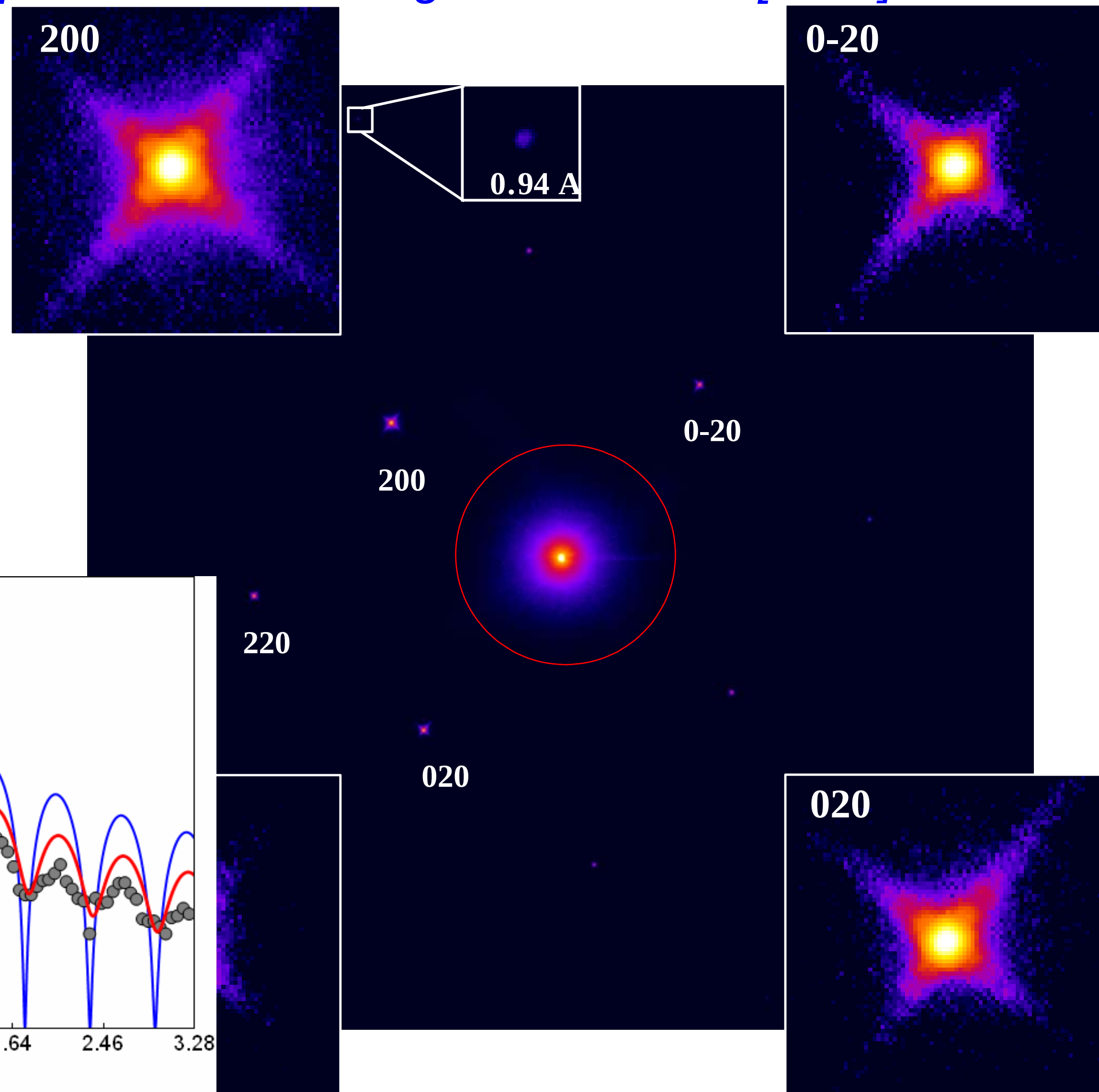

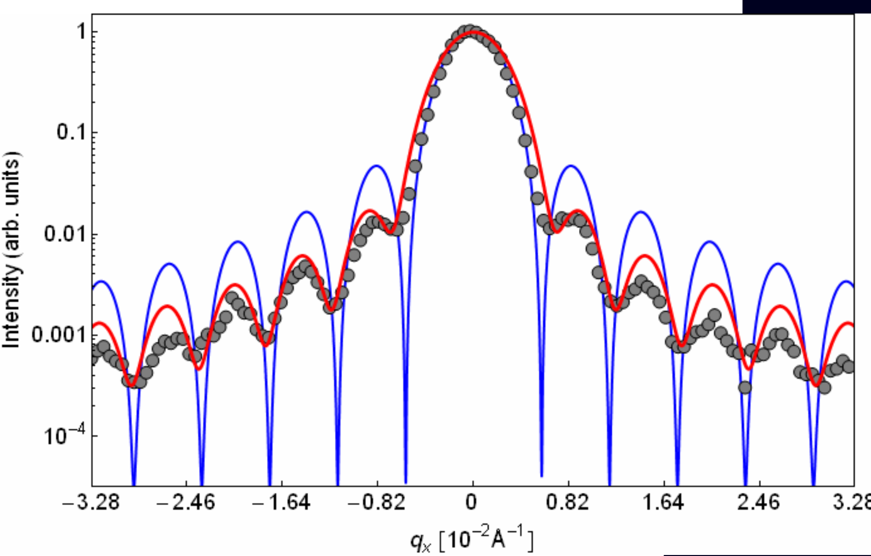

Camera length – 100 cm. Exposure time – 3 seconds.

Phase recovery at atomic resolution??

Recovered by CDI exit surface wave function of MgO nano-particle

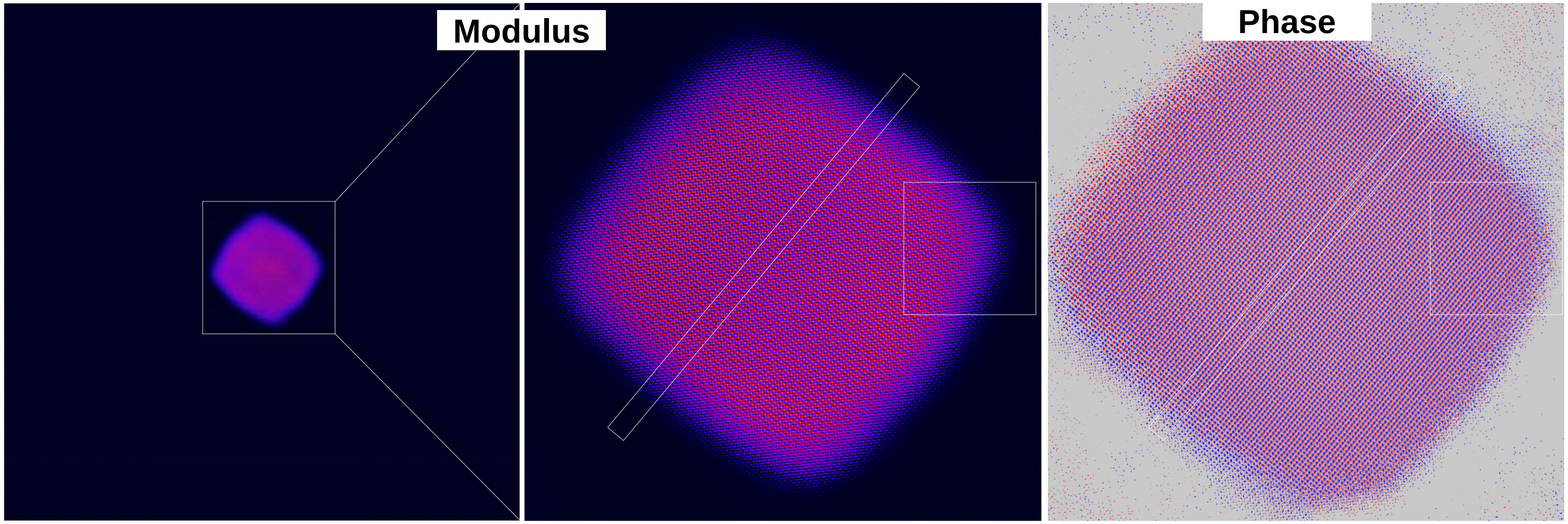

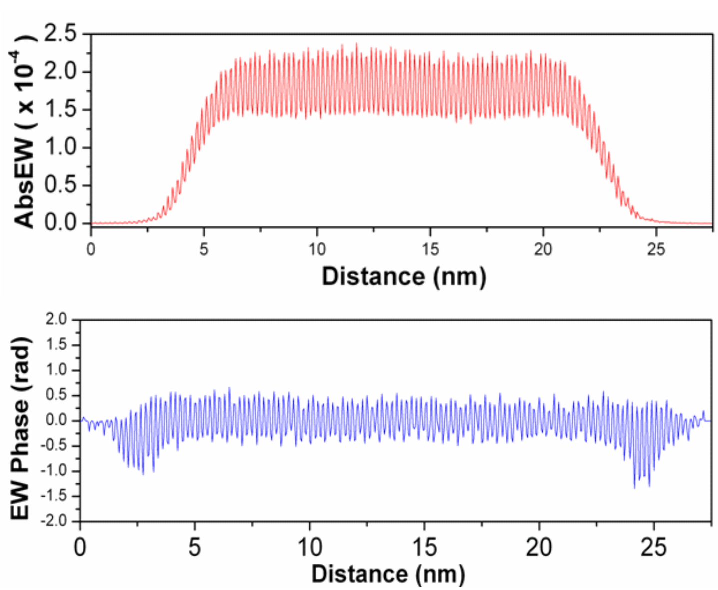

Modulus (red color) and phase (blue color) of the exit wave integrated along corresponding rectangular selection

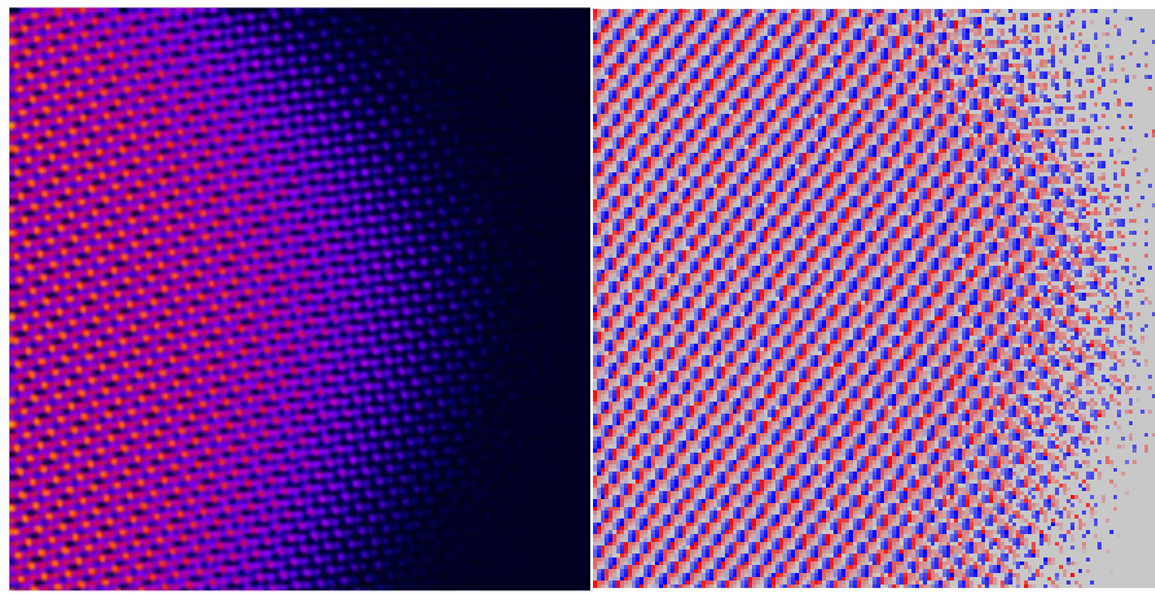

Enlarged view of the exit wave indicated by square

Surface roughness of water measured by x-ray reflectivity

A. Braslaw, et al., PRL 54 (1985)

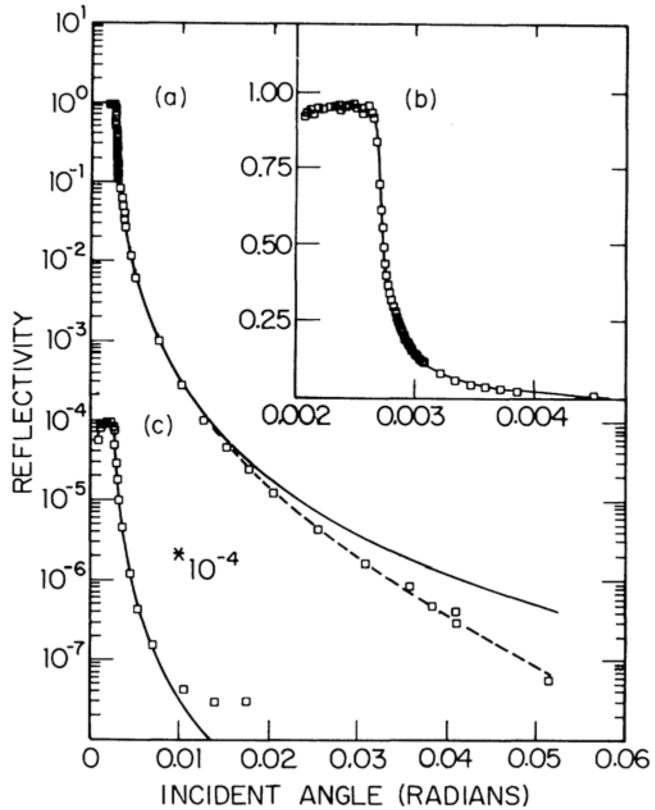

FIG. 3. (a) The measured x-ray reflectivity of water (squares) vs θ. The solid line is the convoluted Fresnel form as described in the text. The dashed line includes $|\Phi(Q)|^2$. Part (b), expanded version on a linear scale for small θ; part (c), water reflectivity measured with use of a rotating-anode x-ray source. For $\theta \gtrsim 0.01$ the signal is dominated by dark counts.

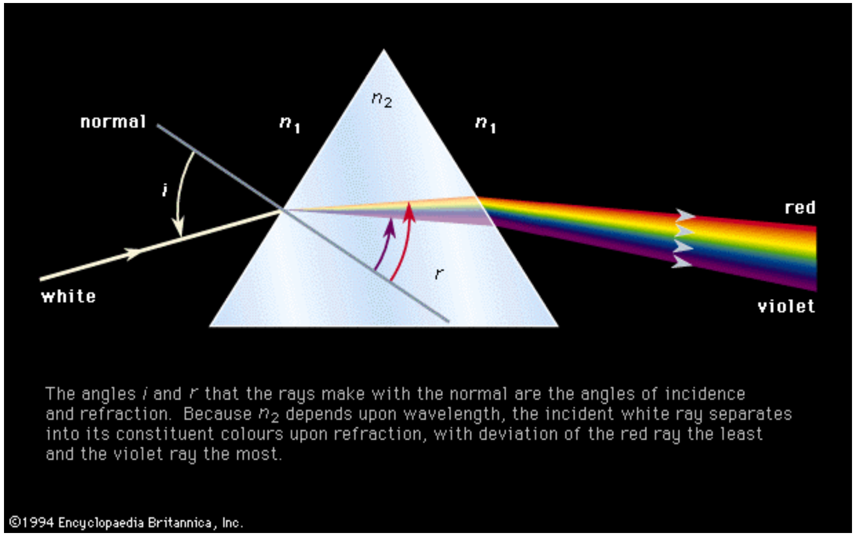

+ The prism: Energy Analyzer (energy resolution)

+ The eye: Detector (sensitivity)

- Inelastic X-ray Scattering

  an energy resolution 10^7 with 10 keV photons

Do not waste photons and have fun at experiments!

The End